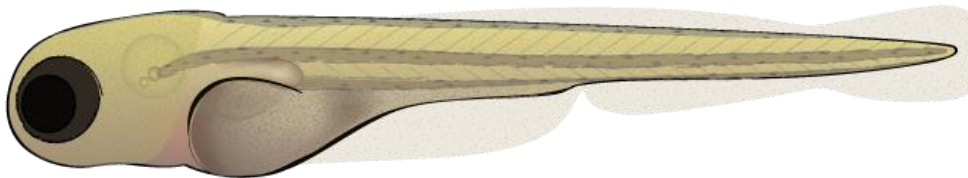




Enhanced content bio-imaging tools:
realising the potential for high-throughput
zebrafish bioassays

Submitted by **Molly Payne** to the University of Exeter as a
thesis for the degree of
Masters by Research in Biological Sciences
in May 2017



This thesis is available for Library use on the understanding that
it is copyright material and that no quotation from the thesis
may be published without proper acknowledgement.

I certify that all material in this thesis which is not my own work
has been identified and that no material has previously been
submitted and approved for the award of a degree by this or
any other University.

Signature.....

Table of Contents

Chapter 1. Estrogen Receptor Signalling and the Application of *In Vivo* Imaging Modalities for their Detection in Animal Models

1.1	The role of estrogens in vertebrates	2
1.2	Estrogen signalling in vertebrates	3
1.3	Estrogen receptor (ER) structure	4
1.4	Estrogen receptor subtypes	5
1.5	Vertebrate estrogen receptor ontogeny	7
1.6	Estrogen receptor tissue distribution	8
1.7	Estrogenic Endocrine Disrupting Chemicals (EEDCs)	11
1.8	Complexities confounding understanding of how EEDC exposure may lead to altered estrogen signaling	14
1.9	Population-level effects of EEDC exposure	16
1.10	Levels of endocrine disrupting chemicals in the aquatic environment	17
1.11	Screening and testing for EDCs	21
1.12	Small Animal Molecular Imaging (SAMI) modalities and their application for investigating the roles of estrogens	23
1.13	Small animal optical imaging	26
1.14	Optical small animal in vivo imaging of ERs and estrogenic endocrine disruption	28
1.15	Transgenic fish and their use in studies in the effects of EEDCs	29
1.16	Higher-throughput in vivo assays for the qualification and quantitation of EDC effects in transgenic models	34
1.17	Thesis Aims, Objectives and Hypotheses	36

Chapter 2. Materials and Methods

2.1	Zebrafish as a model for endocrine disruption	39
2.2	Generation of the ERE:GFP:Casper line	39
2.3	Anaesthetic preparation	40
2.4	Fish husbandry and experiments	40
2.5	Zebrafish maintenance	41

2.6 ArrayScan automated image acquisition	41
2.7 Image analysis approaches	43
2.8 Filtering approaches: mean Top-100/300/600 pixel filtering	47

Chapter 3. Realising the potential of a medium-throughput semi-automated bioimaging assay for the qualification and quantification of estrogen-induced fluorescence response in a transgenic zebrafish model

3.1 Introduction	50
3.2 Materials and Methods	53
3.2.1 Generation of embryos	53
3.2.1.1 Pair-spawned embryos	53
3.2.2.2 Group-spawned embryos	54
3.2.2 Staging of embryos and larvae	55
3.2.3 Preparation of exposure solutions	56
3.2.3.1 Stock chemical preparation	56
3.2.3.2 Working solution preparation	56
3.2.3.3 Dosing solutions in the wells	59
3.2.4 ArrayScan imaging	60
3.2.5 Zeiss imaging comparison	62
3.2.6 Comparison of laterally- vs. variably-orientated EE2-exposed larval fluorescence responses	63
3.2.7 Identification of extreme outliers	64
3.2.8 Statistical analysis	64
3.3 Results	65
3.3.1 Sensitivity vs. robustness of different semi-automated ArrayScan image analysis masking and pixel thresholding strategies	65
3.3.1.1 Whole-image/no masking approach	65
3.3.1.2 Whole-well masking approach	67
3.3.1.3 Larval-specific masking approach	69
3.3.1.4 Top-100, -300, and -600 larval-specific pixels	71
3.3.2 Comparison of pair- and group-spawned	

EE2-exposed larval responses	76
3.3.3 Comparison of laterally- vs variably-orientated EE2-exposed larval fluorescence responses	78
3.3.4 Comparison of EE2-exposed larval fluorescence responses quantified using the semi-automated ArrayScan system and manual Zeiss system	81
3.4 Discussion	82
3.5 Conclusions	88
Chapter 4. The interactive effects of water temperature and 17 α -ethynylestradiol exposure assessed in a larval estrogen-responsive transgenic zebrafish model	
4.1 Introduction	92
4.1.1 Effects of EDC exposure on teleost fish during critical life stages	92
4.1.2 Effects of temperature variation on ectothermic fish	93
4.1.3 Effects of EDCs and temperature interactions in teleost fish	97
4.1.4 Selection of experimental temperatures	99
4.2 Materials and Methods	100
4.2.1 Egg collection and sorting	100
4.2.2 Staging of embryos	100
4.2.3 Test chemicals	101
4.2.4 Experimental design	101
4.2.5 Dechoriation	102
4.2.6 ArrayScan live imaging	103
4.2.7 Larval fluorescence response analysis	104
4.2.8 Larval growth	104
4.2.9 Statistical analysis	105
4.3 Results	105
4.3.1 ArrayScan runs	105
4.3.2 Larval length over time	106
4.3.3 Mean specific growth rate	107
4.3.4 Mean larval fluorescence	111

4.3.5 Comparison of control temperature, chemically-unexposed larvae with test temperature, EE2-exposed larval fluorescence responses	114
4.4 Discussion	118
4.4.1 Effects of temperature on larval size and specific growth rate	118
4.4.2 Combined effects of temperature and EE2 on larval specific growth	120
4.4.3 Combined effects of temperature and EE2 on larval estrogenic (GFP induction) responses	122
4.5 Conclusions	125
Chapter 5. General Discussion	
5.1 Optimised parameters for a semi-automated in vivo estrogenic screening assay	128
5.2 ArrayScan analysis reveals temperature modulation effects on ERE:GFP:Casper EE2-induced responses and growth	132
Bibliography	135

List of Figures

Figure 1.1. Mechanisms of nuclear receptor action	4
Figure 1.2. Structural composition of estrogen receptors	6
Figure 1.3. Two-step mechanism of estrogenic signal amplification	31
Figure 1.4. Comparison between ERE-GFP model and ERE-GFP-Casper model	34
Figure 2.1. The Cellomics ArrayScan II	42
Figure 2.2. Up/down scanning path of the ArrayScan objective lens	42
Figure 2.3. Screenshots of the online image verification interface	48
Figure 2.4. Example of virtual Excel 96-well plate colour-coded heatmap	50
Figure 3.1. Germ-ring stage zebrafish embryo (5 $\frac{2}{3}$ hours)	55
Figure 3.2. Serial dilution and vortex-mixing of EE2 working solutions	57
Figure 3.3. Dilution of EE2 working solutions giving desired exposure concentrations in wells	58
Figure 3.4. 24-well exposure plate layout	59
Figure 3.5. Images of 4 and 5 dpf zebrafish larvae	60
Figure 3.6. Larval zebrafish digestive system anatomy	61
Figure 3.7. Larval image taken using Zeiss	62
Figure 3.8. Different larval orientations captured by ArrayScan	63
Figure 3.9. Whole image area mean pixel fluorescence intensity for ArrayScan imaged EE2-exposed larvae	66
Figure 3.10. Virtual 96-well plate heatmap of ArrayScanned EE2-dosed dataset compiled using whole-image mean fluorescence	67

Figure 3.11. Well area mean pixel fluorescence intensity for ArrayScan-imaged EE2-exposed larvae	68
Figure 3.12. Virtual 96-well plate heatmap of well-masked ArrayScan image data	69
Figure 3.13. Whole-larval area mean pixel intensity for EE2-exposed ArrayScan imaged larvae	70
Figure 3.14. Virtual 96-well plate heatmap of larval-specific area fluorescence intensity data	70
Figure 3.15. Top 100 pixel intensity threshold larval fluorescence responses	72
Figure 3.16. Top 300 pixel intensity threshold larval fluorescence responses	73
Figure 3.17. Top 600 pixel intensity threshold larval fluorescence responses	74
Figure 3.18. Virtual 96-well plate heatmaps of: a) mean Top-100 pixel; b) mean Top-300 pixel; and c) mean Top-600 pixel thresholding ArrayScan output	75
Figure 3.19. Larval-mask mean fluorescence intensity responses to EE2	76
Figure 3.20. Top-300 pixel intensity threshold fluorescence responses to EE2	77
Figure 3.21. ArrayScan raw images + Top 100 pixel intensity values for all larvae exposed to 10ng/L	79
Figure 3.22. Mean Top-300 pixel fluorescence intensities for laterally- and variably-orientated EE2-exposed ERE:GFP:Casper larvae	80
Figure 3.23. Comparison of EE2-exposed larval fluorescence responses quantified using the semi-automated ArrayScan system	81
Figure 4.1. 96-well plate layout and order of screening for semi-automated ArrayScan imaging	103
Figure 4.2. Zebrafish detection algorithm	104

Figure 4.3. Calculating larval total length from ArrayScan image	105
Figure 4.4. Mean larval length at each sampling time-point under different temperature regimes for chemically-unexposed larvae	106
Figure 4.5. Mean specific growth rates for all chemically-unexposed larvae raised under three different temperature regimes	107
Figure 4.6. Mean specific growth for chemically-unexposed and EE2-treated larvae reared at $28\pm 1^{\circ}\text{C}$	108
Figure 4.7. Mean specific growth for chemically-unexposed larvae raised at $28\pm 1^{\circ}\text{C}$ compared to 5ng/L EE2-exposed larvae raised at $32\pm 1^{\circ}\text{C}$	109
Figure 4.8. Mean specific growth for chemically-unexposed larvae raised at $28\pm 1^{\circ}\text{C}$ compared to 25ng/L EE2-exposed larvae raised at $32\pm 1^{\circ}\text{C}$	110
Figure 4.9. Larval fluorescence responses for all chemically-unexposed larvae raised under three different temperature conditions	111
Figure 4.10. Larval fluorescence responses for all 5ng/L EE2-exposed larvae raised under the three different temperature conditions	112
Figure 4.11. Larval fluorescence responses for all 25ng/L EE2-exposed larvae raised under the three different temperature conditions	113
Figure 4.12. Mean control-control larval fluorescence responses compared with 5ng/L EE2-exposed + $28\pm 1^{\circ}\text{C}$ larval responses	115
Figure 4.13. Mean control-control larval fluorescence responses compared with 5ng/L EE2-exposed + $24\pm 1^{\circ}\text{C}$ larval responses	116
Figure 4.14. Mean larval fluorescence responses for chemically-unexposed control larvae raised under $28\pm 1^{\circ}\text{C}$ temperature conditions compared to larval fluorescence responses induced in 5ng/L EE2-exposed + $32\pm 1^{\circ}\text{C}$ larvae	117

List of Tables

Table 2.1. Summary of the mask/filtering approach	43
Table 3.1. Mean and %RSD fluorescence response values at different larval-specific pixel thresholding approaches	83

Abstract

Estrogenic endocrine disrupting chemicals (EEDCs) are environmental contaminants that can alter hormone signalling in both humans and wildlife, exerting their action through estrogen receptors (ERs). A wealth of evidence has indicated that EEDCs are capable of producing a broad range of adverse outcomes by interacting with, and disrupting, the normal functioning of the estrogen system. Fish are particularly vulnerable to endocrine disruption due to EEDCs being frequently discharged into waterways. With more than 900 chemicals identified as being endocrine disruptors, of which ~200 may exert estrogenic effects, there is an urgent need for screening processes that can assess the estrogenic potential of chemicals in order to avoid human and environmental health risks. *In vivo* models capable of demonstrating the physiological effects of EEDCs hold great utility for understanding the potential health impacts of estrogens, and transgenic (TG) zebrafish (*Danio rerio*) models are particularly well-suited for the screening of EEDCs via bioimaging approaches. The pigment-free estrogen-responsive ERE:GFP:Casper model represents a promising transgenic line for qualifying and quantifying EEDC-induced fluorescence responses in larval fish and is amenable to high-throughput screening (HTS). We optimised a medium-throughput semi-automated *in vivo* bioimaging assay using the model, while simultaneously generating important data concerning estrogen-driven responses to an EEDC (EE2). Through refinement of assay parameters, including the use of various image-masking and pixel-thresholding approaches, controlled-breeding to reduce genetic variability and standardised larval orientation for image acquisition, we established the most sensitive and robust approaches for screening of the EE2-exposed model using a semi-automated imaging modality. Our optimised assay was capable of detecting a significant GFP response in 4 day old zebrafish larvae at an environmentally relevant (5ng/L) concentration of EE2. These specifications were then adopted for investigating the influence of varying incubation temperatures (24, 28 and 32°C) on EE2-exposed ERE:GFP:Casper larval growth and GFP responses. This analysis provided information concerning the potential for an EEDC to interact with temperature in a fish model, with important implications for subsequent interpretation of results. We screened the same animal over a series of timepoints generating valuable data concerning estrogen-induced fluorescence responses and specific larval growth. Incubation temperature was found to have a significant effect on GFP induction, both alone and in interaction with EE2. The findings of this thesis help to outline an improved approach for further development of higher-throughput *in vivo* estrogenic screening of a transgenic zebrafish model.

Acknowledgements

I would like to express my gratitude to Professor Charles Tyler for his valuable guidance, enthusiastic encouragement and useful critiques of this research work. I would also like to thank Dr. Malcolm Hetheridge: his willingness to give his time so generously has been very much appreciated. My grateful thanks are also extended to Dr. Stewart Owen for his kindness, patience, many lunches, and steadfast encouragement to complete this study. All of my academic supervisors have been extremely tolerant and infinitely understanding throughout this process.

This dissertation would not have been possible without the guidance and input of several individuals. I would like to thank Jon Ball for his knowledge and uncompromising perfectionism; Matt Winter for his dad jokes and unparalleled zebrafish imaging skills; Anna Tochwin for her dedication to the smooth-running of the AstraZeneca lab; Jeremy Metz for his computer wizardry (and many coffees); and Ross Brown for his uplifting enthusiasm and statistical know-how.

Assistance from members of my lab group has also been greatly appreciated: Dr. John Dowdle and Dr. Anke Lange – Lab 201 depends on you! I must also thank ARC staff members Greg, Darren, Ben, Aaron and Steve for being amazingly helpful and hardworking. Additional thanks to Sulay, Tetsu and Aya who were always happy to share their knowledge and skills whenever I asked.

A big thank you to my funders and stakeholders involved in the project: the BBSRC, AstraZeneca and the University of Exeter.

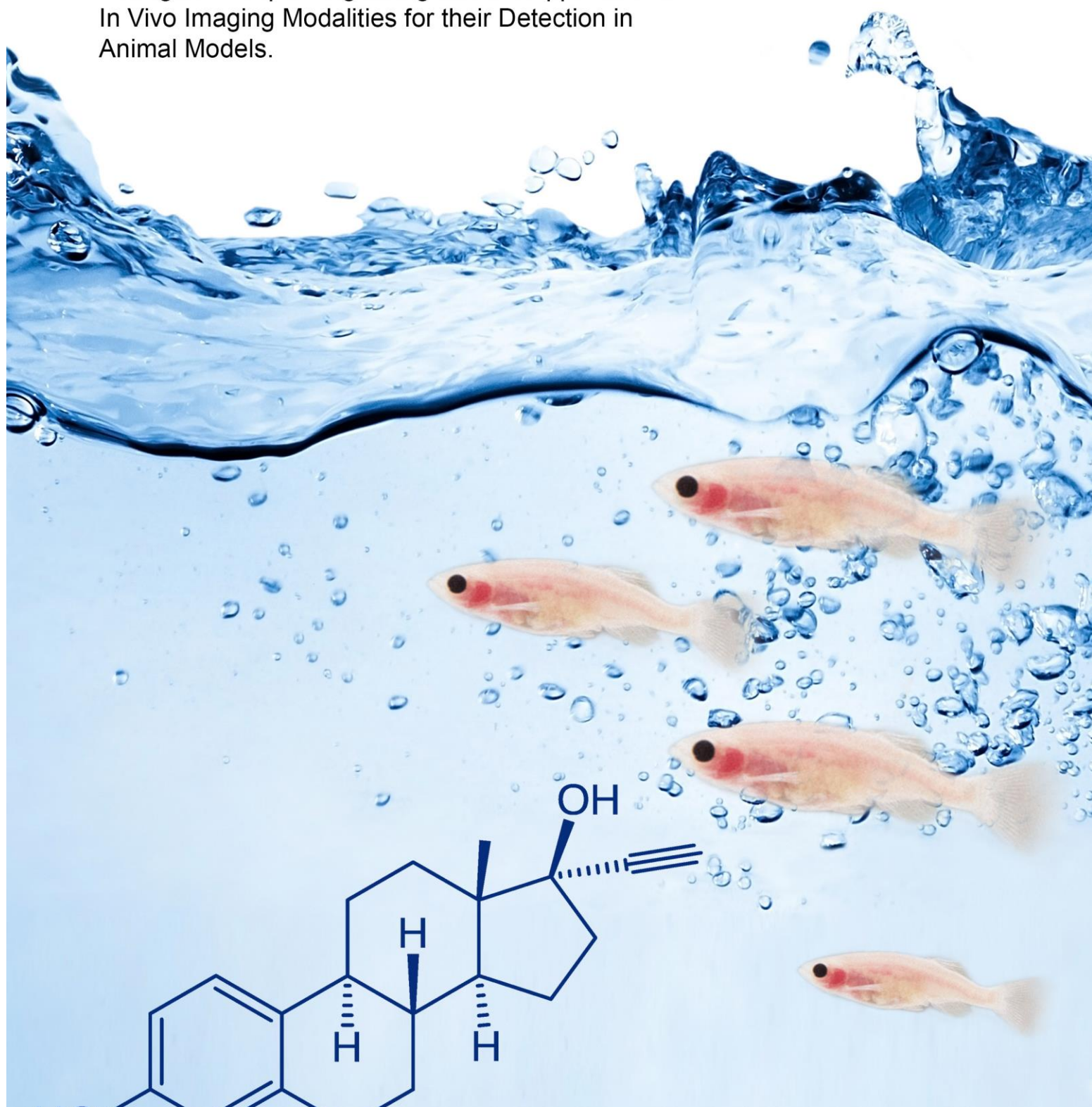
An extra special thank you to my friends: Josie Paris for being my unofficial sister and providing endless support; Kat Maltby for being fearless and incredible; Katie Mintram for her wisdom and kindness; Gaz Le Page for keeping it real; Jane Usher for always making time. Thanks too to Amy F, Rich C, Shelly, Will K, Rik, Phil H, Mark, Adam P and Guy for lovely days and dancing.

Final thanks to my amazing parents: Mum, Dad, John and Zoe. And lastly to BB – you got me to the end.

Chapter 1

General Introduction

Estrogen Receptor Signalling and the Application of In Vivo Imaging Modalities for their Detection in Animal Models.



Chapter 1.

Estrogen Receptor Signalling and the Application of *In Vivo* Imaging Modalities for their Detection in Animal Models.

This general introduction reviews the role of estrogen receptors in the normal functioning of vertebrates and investigates the mechanisms by which endogenous estrogens (and their mimics) exert their effects. Evidence for adverse effects of estrogen exposure on wildlife, principally fish, is also addressed. The review then centres on the application of imaging methods to test for altered estrogen signaling and the use of transgenic fish in studies into the effects of endocrine disrupting chemicals (EDCs). Chapter 1. then informs on the subsequent empirical thesis work that is centred on the development and application of transgenic zebrafish for screening for the effects of estrogenic chemicals. In the final section of this chapter, the thesis hypotheses are presented and a description provided on the methods adopted to address them in the experimental chapters.

1.1 The role of estrogens in vertebrates

Estrogens are a group of hormones synthesized in all vertebrates, exerting their effects via estrogen receptors (ERs). Their ubiquitous presence in vertebrates is indicative of a shared evolutionary history and important endocrine function (reviewed in Eick & Thornton, 2011). Although traditionally thought of as vertebrate-specific, the identification of a molluscan putative estrogen receptor suggested that steroidal receptors might have a more ancient history in metazoans than previously thought (Thornton et al., 2003). Homologues to the ER have also been reported in amphioxus (Schubert et al., 2006) and annelids (Keay & Thornton, 2009), although function in these organisms, if any, remains unclear.

Estrogens are known to play a role in vitellogenesis (in oviparous animals), oogenesis, testicular development and many other facets of vertebrate reproduction, as well as having multiple functions in many other organ systems and processes (Heldring et al., 2007; Matthews & Gustafsson, 2003; Nilsson et al., 2001). Non-reproductive functions of estrogens include regulation of blood lipid levels, fat deposition, water and mineral homeostasis, bone density and brain functions, including memory processes (Lange et al., 2002; Luine et al., 2003; Packard & Teather, 1997a). Estrogens are also known to exert a plethora of biological effects in the musculoskeletal, cardiovascular, immune, and central nervous systems (Gustafsson, 2003). Furthermore, deficiencies or excesses of estrogens have been linked with various disease states, such as prostate and breast cancer, and osteoporosis (reviewed in Heldring et al., 2007).

1.2 Estrogen signalling in vertebrates

Estrogens exert their action through two distinct pathways: the ('fast') non-genomic and the genomic ('classic') pathway where estrogens diffuse passively across cell membranes and bind to estrogen receptors (ERs) in the nucleus (Figure 1.1). This event induces a conformational change in the receptor, after which the receptors dimerise and bind to specific estrogen response elements (EREs) (Kimbrel & McDonnell, 2003). The EREs, located in the promoter region of target genes, will then either activate or repress gene expression (Glass, 1994; McKenna et al., 1999; Smith & O'Malley, 2004; Tsai & O'Malley, 1994). ERs are members of the nuclear receptor subfamily and share a common structure-function organisation (Duffy, 2006; Nilsson et al., 2001; Gruber et al., 2002).

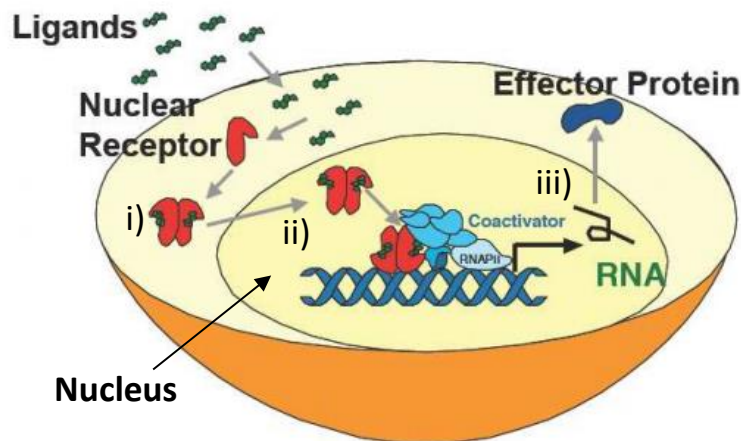


Figure 1.1. Mechanisms of nuclear receptor action (modified from Zilliacus, 2007). (i) Following ligand binding, (ii) nuclear receptors can translocate to the nucleus and (iii) directly regulate transcription.

1.3 Estrogen receptor (ER) structure

All ERs are members of the same steroid/thyroid receptor superfamily of ligand-activated transcription factors and share a modular structure. Like most nuclear receptors, they contain six distinct functional domains which are labelled A-F (Kumar et al., 1987). The N-terminal region (A/B) is the most variable between species, while the C domain - the 'DNA binding domain' (DBD), is highly conserved. Within the N-terminal region is the first 'activation function domain' (AF1) which, along with the 'second activation function domain' (AF2), is responsible for regulating the ER transcriptional activity (Zwart et al., 2010).

The C region contains two 'zinc fingers' each containing a Zn^{2+} ion, which fold together to form a compact 3-dimensional structure, enabling the ER to bind to specific EREs on the DNA (Hewitt & Korach, 2002). Within the DBD, the 'P box' at the base of the first zinc finger is involved in DNA recognition and the 'D box' on the second finger is responsible for receptor dimerization (Klug & Schwabe., 1995).

The variable D region of the ER, known also as the 'hinge region', spans between the DBD and the 'ligand binding domain' (LBD). It is poorly conserved and thought to be a potential site at which nuclear receptor co-repressor proteins interact

(Aranda & Pascual, 2001). The E region of the ER contains the LBD, consisting of 12 helices and a hydrophobic pocket where the ligand typically binds, inducing the AF2 (Brzozowski et al., 1997; Wurtz et al., 1996). The LBD is moderately conserved in sequence but highly conserved in structure, and additionally functions to enable dimerization, as well as the binding of coactivator and corepressor proteins.

The F region represents the end of the AF2 and culminates in the C-terminus of the receptor. The F domain regulates gene transcription in a ligand-specific manner (Montano et al., 1995) with tissue-specific modulation capabilities (Koide et al., 2007). It has also been demonstrated that the domain impacts receptor dimerization (Yang et al., 2008).

Different ER ligands may act as agonists or antagonists depending upon the conformational change they induce in the 12 helices of the LBD. Agonistic compounds activate a change in the conformation of the ligand binding pocket, enabling helix 12 to adopt the correct position in which the coactivator can bind, activating transcription. The conformational alteration caused by antagonist binding results in helix 12 blocking the coactivator pocket, thereby inhibiting transcription (Kimbrel & McDonnell, 2003).

The way in which estrogen receptor activity is controlled is far more complex than simply a ligand-induced change in binding site conformation switching transcription 'on' or 'off'. Both ERE-promoter context and ER subtype need to be taken into account, as well as the fact that some ligands, such as selective estrogen receptor modulators (SERMs) like tamoxifen, can induce tissue-specific agonistic/antagonistic responses (Gruber et al., 2002; Watanabe et al., 1997).

1.4 Estrogen receptor subtypes

In the vertebrate lineage, classical estrogen signalling occurs via the binding of estradiol to the ERs, which are encoded for by different *esr* genes. Due to a duplication event occurring early in the vertebrate line (Thornton, 2001), the mammalian genome contains two major ER isoforms – ER α (Green et al., 1986) and ER β (Kuiper et al., 1996) (Figure 1.2.). ER α mediates most of the known

estrogenic actions in mammals, and is expressed primarily in the ovaries, uterus, testes, bladder, prostate, lung and brain (Speirs et al., 2002).

ER β is expressed in a diversity of normal and malignant tissues, several of which also express ER α (Koehler et al., 2005). As well as acting as an important hormone receptor for maintaining the normal functioning of vital organs, ER β is also involved in regulating apoptosis and controlling antioxidant gene expression, modulating immune responses, and has been related to the risk of heart failure (Koehler et al., 2005).

The ER α and ER β subtypes have small differences in the AF1 region, and the ligand binding domain of ER β has a smaller volume compared to that of ER α . The DNA binding domain, however, is structurally identical (see Figure 1.2.) and both receptors bind ligands with similar affinity (Nilsson et al., 2001). ER α has been reported to stimulate transcription with superior efficiency compared with ER β (McDonnell & Norris, 2002).

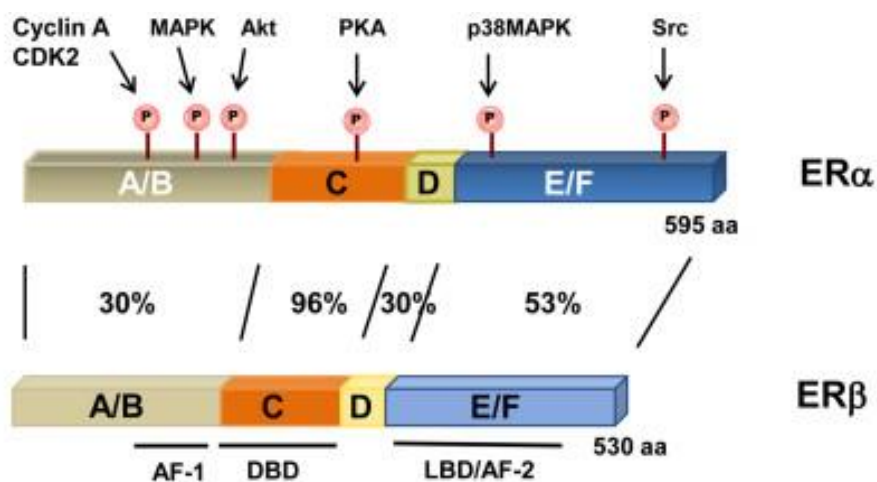


Figure 1.2. Structural composition of estrogen receptor (ER) α and ER β (from Roman-Blas et al., 2009).

Using knock-out mice, unique but overlapping roles have been established for the ER subtypes (Matthews & Gustafsson, 2003). Both ERs are co-expressed in a range of tissues and are capable of forming functional heterodimers. However, ER α and ER β have differential transactivation activities within certain cell-type, ligand and promoter contexts. As an example, in the presence of estradiol, the

two ER subtypes oppose each other's function in the regulation of the cyclin D1 promoter (Hall & McDonnell, 1999; Liu et al., 2002).

ER α and ER β are capable of exerting different effects on the growth and differentiation of a variety of tissues including bone, liver, uterus, colon, mammary gland and brain (Clark & Peck, 1979; Helguero et al., 2005; Somjen et al., 2011; Wada-Hiraike et al., 2006). Illustrating this, a microarray analysis of ER β -inactivated (BERKO) mice found that 95% of the estrogen-regulated genes increased in the bone of wild-type mice were also up-regulated in the ER β -inactivated mice, but at a much higher rate (Lindberg et al., 2003). The data indicated that ER β reduced ER α -regulated gene transcription in the bone of wild-type mice, supporting the notion that ER β antagonizes the activities of ER α . With ER β knocked-out, estrogen-regulated gene transcription increased dramatically. The ability of ER β to modulate ER α -mediated gene transcription was described as a "Ying Yang" relationship between the two ER subtypes in mice (Lindberg et al., 2003).

Further investigation found an estrogen-induced stimulatory effect on estrogen-regulated genes in the liver of the ER β -inactivated mice (184% of the effect observed in wild-type). It would appear that the relative tissue distributions of the ER subtypes have a major deterministic effect on the biological impact of their respective ligands (Lindberg et al., 2003). However, precisely which genes were transcriptionally regulated directly (by a 3-week treatment of estradiol), and which may have been regulated as a secondary response by genes themselves regulated by estradiol, was not established.

1.5 Vertebrate estrogen receptor ontogeny

Estrogen receptors are not required for all stages of life and the ontogeny of estrogen-responsiveness during development can provide information concerning the sequence of physiological events leading to the competence of target organs. In mammals, very low concentrations of estrogen receptors have been reported in the pituitary and uterus of mice at birth (Clark & Gorski, 1970). It was observed that estrogen receptor concentrations then rise in these tissues

until ~10-15 days of age, after which time the concentrations of estrogen receptors remain fairly constant.

Highly-specific probes have been used to establish the differential expression of ER β in comparison with ER α mRNA in both reproductive and non-reproductive tissues during mouse embryogenesis (Lemmen et al., 1999). The earliest expression, detected at embryonic day 9.5 (E9.5), was for ER α in the wall of the heart atria, which continued to be expressed until E12.5 in both males and females. Among a wide array of tissues, ER α was found to be expressed in the midgut at E10.5, and both receptors were detected in the renal cortex of both sexes from E14.5 onwards. Only ER β was detected in the brain of males and females from E10.5 until E16.5, with ER α eventually being expressed at E16.5 alone (Lemmen et al., 1999). The time- and tissue-specific expression patterns of ER α and ER β through exogenous estrogen binding indicated that each subtype had a specific function during development.

1.6 Estrogen receptor tissue distribution

Both ER subtypes α and β are expressed in the reproductive and non-reproductive tissues of adult rats (Walker & Korach, 2004). In the brain, ER α is more highly expressed in regions affiliated with reproductive behaviours, such as the hypothalamus (McEwen & Alves, 1999), while lower levels of expression have been detected in the hippocampus (Walker & Korach, 2004). These observations were corroborated by observed infertility and an absence of sexual behaviour in male and female ER α knock-out mice (Bodo & Rissman, 2006).

Within the mammalian brain ER β has been detected predominantly in the hippocampus, cerebellum, cerebral cortex and olfactory bulbs (Gustafsson, 1999). ER β expression was reported in subpopulations of neurons known to be important in endocrine and nervous system interaction, indicating a role for ER β beyond the hormonal-hypothalamic regulation of reproduction (Bodo & Rissman, 2006). These findings are substantiated by reports of fewer neurons in the cortex and a smaller overall brain size in ER β knock-out mice, despite normal reproductive behaviour and competency being maintained (Wang et al., 2001).

Evidence showing that the ER β knock-out mice suffered a degeneration of neural bodies across the brain (Wang et al., 2001), combined with the reduced ability to learn while normal reproductive capabilities was generally maintained (Bodo & Rissman, 2006), supported the suggestion that ER β moderates the non-reproductive effects of estrogens and may have a crucial role in developmental diseases of the CNS (Gustafsson, 1999).

ER β has also been observed to have a ligand-dependent protective role in the auditory system, insulating it from auditory trauma (Meltser et al., 2008). ER β was found to be localised in the nuclei of inner and outer ear hair cells (sensory receptors of the vertebrate auditory system and vestibular system), as well as the spiral ganglion nuclei. ER β and aromatase knock-out mice were shown to have an increased sensitivity to acoustic trauma following an acoustic challenge, resulting in hearing loss (Hultcrantz et al., 2006; Meltser et al., 2008).

The above research, taken along with the characterisation of double knock-out, or alpha beta ER knock-out mice, has shown that life is possible without either or both ER subtypes but reproductive function is severely impaired. Perhaps the most remarkable findings from the knock-out mouse data were those that indicated the role of estrogen as a morphogen, evident from the structure of the ovary (Course & Korach, 1999), mammary gland (Förster et al., 2002), uterus (Course & Korach, 1999), lung (Morani et al., 2006), prostate (Weihua et al., 2001), and brain (Wang et al., 2001).

Estrogen-induced morphogenesis requires a complex interplay of co-regulatory proteins, with cross-talk between estrogen signalling and growth factors crucial for understanding both normal and malignant growth (reviewed in Heldring et al., 2007). As an example, acute morphogenesis occurs in the ventral prostate as a result of ER β knock-out in rodents (Heldring et al., 2007; Imamov et al., 2004; Prins, 1992; Prins & Birch, 1995; Prins et al., 1998; Weihua et al.; Woodham et al., 2003). Researchers attempted to extricate the processes by which a loss of ER β led to such abnormalities. In that work, it was found that expression of transforming growth factor beta (TGF- β), an estrogen-stimulated growth repressor (Itoh et al., 1998) was limiting the rate of prostate growth (Adam et al., 1999), and as ER β is the only subtype expressed in the adult prostate epithelium, it was considered likely that estrogen regulation of TGF- β was mediated by ER β .

Thus, the ER β was found to have a role in limiting alveolar growth in the prostate (Heldring et al., 2007).

Teleost fish are unique among the vertebrates in possessing ER α and two ER β s (ER β 1 and ER β 2) as a result of an ancient duplication following the divergence of ray- and lobe-finned fish (Ma et al., 2000; Menuet et al., 2002). The additional ER subtype was first established in the Atlantic Croaker (*Micropogonias undulates*) (Hawkins et al., 2000) and has since been identified in the zebrafish (*Danio rerio*) (Menuet et al., 2002). It is now established that ray-finned fish species (Actinopterygii) possess at least three different subtypes generated from three distinct genes. These ER forms have been shown to bind estradiol with high affinity and subsequently activate a reporter gene under the regulation of a consensus ERE, demonstrating that the two ER β s act as functional ligand-dependent transcription factors (Bardet et al., 2002; Lassiter et al., 2002; Menuet et al., 2002).

The two ER β subtypes identified in fish share a higher degree of amino acid homology with the ER α isoform. The rainbow trout (*Oncorhynchus mykiss*) is the only species in which a duplication of the ER α has also been identified (Nagler et al., 2007). Zebrafish have been found to express all three of the ER mRNA forms in both reproductive and non-reproductive tissues, including the brain, gonads, pituitary, liver and intestines (Menuet et al., 2002), though all are present at differing levels and exhibit considerable overlap, particularly within the preoptic nucleus. Zebrafish express as many as three ER forms within the same cell, which has been shown to occur within the preoptic area, bed nucleus of the stria terminalis, and amygdala (Shughrue et al., 1997; Shughrue et al., 1998), and this co-occurrence of ERs makes identifying the potential modes of action of estrogenic target genes difficult.

In mammals, it has been shown that ER α and ER β preferentially form heterodimers and the transcription activity of these is similar to that of the ER α homodimer (Cowley et al., 1997; Pettersson et al., 1997; Tremblay et al., 1999). Thus, in zebrafish it seems likely that *in vivo* estrogenic actions might be dependent on the ratio of ER subtypes within a specific cell. It has been suggested that the specific functions and mechanisms of the respective ERs in

teleosts are more complex than those seen in mammals and may prove difficult to analyse in the adult and developing zebrafish (Menuet et al., 2002).

Studies of early developmental expression of ERs in the zebrafish revealed that as early as 3 hours post-fertilization (hpf) there is a high degree of ER β 2 transcript expression (Bardet et al., 2002; Lassiter et al., 2002; Tingaud-Sequeira et al., 2004). In addition, ER β 1 was also found to be highly expressed. The abundance of both ER β subtypes suggests the presence of transcripts of maternal origin. ER α transcripts, however, were not detected in zebrafish before 12 hpf, but subsequently demonstrated a significant increase in abundance at 72 hpf (Bardet et al., 2002).

The overall distribution pattern of estrogen receptor genes in zebrafish embryos has been investigated using whole-mount *in situ* hybridisation (Tingaud-Sequeira et al., 2004). High levels of ER β 1 and ER β 2, and low levels of ER α mRNA, were detected in the epidermis, pectoral fin buds, hatching gland and, at lower levels, in the developing brain of 24 hpf embryos. By 60 hpf, ER β 1 mRNA was detected at high levels in mature primary neuromasts of the lateral line system and by 3 days post-fertilization (dpf), all mature primary neuromasts throughout the lateral line expressed an abundance of both ER β subtype transcripts. ER β 1 transcripts were still detected in the lateral line after the mechanoreceptive hair cells that cover it had been obliterated by neomycin - an ototoxin that induces hair cell death. This finding is consistent with ER β 1 transcripts being present in supporting cells, which have been demonstrated as being the progenitors of newly regenerated sensory hair cells (Balak et al., 1990).

1.7 Estrogenic Endocrine Disrupting Chemicals (EEDCs)

There is increasing concern, both within the scientific community and amongst the public, about the presence of EEDCs in the environment. EEDCs can be grouped into natural compounds and those that are synthetically derived. Natural EEDCs include phytoestrogens (derived from plants) and mycoestrogens (produced by fungi). Synthetic estrogens include ubiquitous industrial compounds such as bisphenol A (BPA) and its analogues, polychlorinated biphenyls (PCBs) and phthalates, but also encompass pharmacological estrogens, such as the

drug 17 α -ethinylestradiol (EE2) used in the contraceptive pill. Like natural ligands, EEDCs are capable of activating ERs, leading to potentially adverse endocrine disruptive effects in wildlife and humans.

Estrogen mimicking represents just one of a range of mechanisms by which EEDCs can disrupt the normal functioning of the endocrine system: they have been defined as substances that 'interfere with the synthesis, secretion, transport, binding, action, or elimination of natural hormones in the body that are responsible for development, behavior, fertility, and maintenance of homeostasis (normal cell metabolism)' (Crisp et al., 1998). EEDCs have also been shown to influence sex-specific behaviour and physiology, as well as normal reproductive function (De Coster & Larebeke, 2012; Zoeller et al., 2012). Exposing wild roach (*Rutilus rutilus*) to environmentally relevant concentrations of the synthetic estrogen EE2 for up to 2 years resulted in complete male sex-reversal and an all-female population (Lange et al., 2009). An estrogen-sensitization effect in female roach exposed to environmentally relevant levels of EE2 in early life was also observed, indicated by increased levels of the mRNAs for estrogen-sensitive genes 398 days after original exposure.

EEDCs have challenged the long-held concept in toxicology that 'the dose makes the poison', as they have been found to be capable of having effects at low doses that cannot necessarily be predicted by effects at higher doses. They are able to disrupt physiological pathways of endogenous estrogen actions in vertebrates and invertebrates alike, producing effects in both reproductive and non-reproductive systems (Rempel & Schlenke, 2008).

Humans and wildlife appear especially susceptible to the adverse effects of EEDCs during the early developmental stages, particularly during periods of urogenital tract and nervous system development. A review has indicated that many EDCs, including those with estrogenic properties, cause detrimental health outcomes from the neonatal period through to adult life (reviewed by Vaiserman, 2014). This review focused particularly on epigenetic mechanisms linking adverse early-life exposures to long-term health outcomes. Evidence from both animal and human studies suggested that there may be a 'sensitive period' during development (usually perinatal) where the first encounter between a hormone and its developing target cell receptor will influence that hormone-receptor

interaction for life (Csaba, 2011; Kundakovic & Champagne, 2011). For example, low-dose exposure of neonatal rats to BPA during development was found to result in an increase in prostate gland susceptibility to adult-onset hormonal carcinogenesis and precancerous lesions (Ho et al., 2006).

Further evidence from animal studies into in-utero and/or neonatal BPA exposure has indicated that the EEDC produces a broad range of adverse adult outcomes including impaired reproductive function, altered sexual behavior, and dysregulation of the immune system (Abi Salloum et al., 2013; Doherty et al., 2010). Owing to these potential health concerns, the use of BPA in polycarbonate infant feeding bottles was prohibited in Canada (2009), USA (2010), and the European Union (2011), and in 2015 France banned its use in all food and beverage packaging. However, these restrictions have led manufacturers to adopt alternative bisphenols, namely bisphenol AF (BPAF), bisphenol F (BPF), and bisphenol S (BPS) (Liu et al., 2012) and these analogues are already being widely used, with BPS being found in canned foods and soft drinks (Gallart-Ayala et al., 2011; Viñas et al., 2010) as well as thermal receipt paper (Becerra & Odermatt, 2012; Liao et al., 2012) and BPAF being incorporated extensively in the manufacture of electronic devices and optical fibres (Yang et al., 2012). Initial studies have indicated that, like BPA, at least some of these analogues have the ability to perturb the normal functioning of the endocrine system in a range of organisms (Eladak et al., 2015; Feng et al., 2012; Ji et al., 2014; Naderi et al., 2014; Yang et al., 2014).

Recently published research into the short-term effects of the phytoestrogen genistein on the reproductive characteristics of male gibel carp (*Carassius auratus gibelio*) showed a range of disruptions in reproductive capacity (Nezafatian et al., 2017). These included an observed reduction in fertilization rate and offspring viability in addition to impaired spermatogenesis – all factors that might contribute to reduced reproductive success.

Zearalenone is a potent mycoestrogen found worldwide in a number of cereal crops (Kuiper-Goodman et al., 1987). Entering the food chain via contaminated cereals, it can rapidly infiltrate sewage effluent and the aquatic environment, posing potential threat to both wildlife and humans. Toxicological assessment was carried out on zebrafish into the developmental toxicity of zearalenone in

larvae and adults (Bakos et al., 2013). Defects in the heart and eye development and an upward curvature of the body axis were observed at high exposure concentrations of 500 µg/L and above, with disturbances in the development of the adult tail fin primordium seen at 72 hpf in fish exposed to 250 µg/L zearalenone.

1.8 Complexities confounding understanding of how EEDC exposure may lead to altered estrogen signaling

The endocrine system has evolved to respond to low levels of endogenous hormones (Eick & Thornton, 2011), and therefore EEDCs that mimic these natural hormones are likely to elicit estrogen-response mechanisms at similarly low doses (Sheehan, 2000; Welshons et al., 2003). Furthermore, EEDCs that influence the uptake, metabolism, production or release of hormones in the body may also have an impact at low doses (Welshons et al., 2003).

Further uncertainty confounding the predictability of EEDC actions derives from the complex set of mechanisms by which EEDCs can exert their effects, making it difficult to establish effective doses and all possible associated risks. The most widely studied mechanism via which EEDCs bring about their effects is through the binding and activation of ERs α and β : however, the ability of EEDCs to affect more than one hormone at once (potentially in antagonistic ways), as well as different components of the same pathway, convolute generating predictions concerning their effects. It is these complexities which add unpredictability to the outcome and manner by which EEDC exposure may alter estrogen signaling.

An endocrine disruption testing protocol - The Tiered Protocol for Endocrine Disruption (TiPED) – was proposed for identifying hazard in the design of new chemicals (Schug et al., 2013). The complexity of the potential effect of a chemical on the endocrine system was highlighted, with factors including life stage at exposure, route of exposure and duration of exposure all to be taken into account. On the basis of this complexity, the need for a range of assays and approaches to identify chemicals with endocrine-disrupting properties was established and it was proposed that a combination of approaches was required, including computational methods, as well as both *in vitro* and *in vivo* testing.

A wealth of research has been dedicated to deciphering which EEDCs bind which ERs, to what extent these responses occur for environmentally relevant concentrations, and how this expression compares to that induced by endogenous estrogens. Various species of fish model have been widely used as sentinels for impacts of endocrine disruption at a population level and also for study into the effects of EEDCs on individual fish (Andersen et al., 1999; Metcalfe et al., 2001; Mills & Chichester, 2005; Scholz & Kluver, 2009; Yokota et al., 2001), but how these findings extrapolate more widely is less well established.

One study of the sensitivities to environmental estrogens in a range of fish species (species that included those extensively used in laboratory, and for studies on wild populations) found differences in the responsiveness of the ER (Tohyama et al., 2015). ERs of carp (*Cyprinus carpio*) and roach (*Rutilus rutilus*) appeared to be relatively less sensitive to a range of EEDCs than those of the zebrafish, three spined stickleback (*Gasterosteus aculeatus*) and medaka (*Oryzias latipes*). The zebrafish ER β 2 showed the highest relative sensitivity. One of the implications of this study was the risk (uncertainty) associated with making predictions about endocrine disruption based on the receptor activation of a few fish model species, which may not necessarily translate well to all fish species.

Due to the fact that most EEDCs will readily enter into the aquatic environment and likely impact wildlife living there (Taylor & Harrison, 1999; Tyler et al., 1998; Vos et al., 2000), it is imperative that predictions can be made about how estrogen signaling is affected in exposed organisms. Fish are particularly at risk of EEDC exposure and provide useful sentinels for their effects. Some adverse consequences have been proven as a consequence of exposure to estrogens in fish, including unbalanced sex ratios, reduction in gonadal growth and presence of gonadal deformities, postponed sexual maturation, decreased egg production, lowered sperm count, repressed spermatogenesis and the pervasive occurrence of intersex (Andersen et al., 1999; Metcalfe et al., 2001; Mills & Chichester, 2005; Scholz & Kluver, 2009; Yokota et al., 2001). Through building greater understanding of the functional divergence in ERs across different species and identifying those that are more or less sensitive, it should be possible to make better predictions as to whether altered estrogen signaling in a particular animal is likely to have functional consequences.

1.9 Population-level effects of EEDC exposure

Advancing our understanding of estrogen signaling and its functioning throughout the lifetime of an organism could greatly help in informing on EEDC exposure risk to human and environmental health. Following the COMPRENDO project (Comparative Research on Endocrine Disruption) workshop a monograph was compiled highlighting the need for study into the wider ecological relevance of endocrine disruption in wildlife populations which will inform on how the impacts of EEDCs need to be placed within a context with other environmental pressures faced by organisms (Jobling & Tyler, 2006).

Studies elucidating the impacts of EDCs on wildlife populations are relatively scarce, due largely to their time-consuming and challenging nature. Recent research into endocrine disruption in frog populations by Lambert et al. (2015) provided support for the wider ecological influence of EEDCs by showing that sex ratios of metamorphosing frogs became increasingly female-dominated along a suburban gradient, which correlated with the increased distribution of surface water phytoestrogens associated with human-modified environments (Hayes et al., 2003; Skelly et al., 2010; Smits et al., 2014).

Blanchfield et al. (2015) reported on a 7-year whole-lake study of a fathead minnow (*Pimephales promelas*) population, to which EE2 had been applied for three consecutive summers, resulting in a dramatic population collapse. At 3 years post-treatment, however, male fish exhibited no gonadal abnormalities ($n=14$) in contrast with 100% of those ($n=10$) sampled 7 months after EE2 treatment. Additionally, the initial elevation in blood levels of vitellogenin (VTG, a bioindicator of estrogen) in the male fathead minnows also fell to similar values as those reported for males in a reference lake, indicating a full recovery at the biochemical level within 3 years.

Disruption of wildlife population sex ratios in response to EEDCs have been reported in the broad snouted caiman (*Caiman latirostris*) exposed to environmentally relevant levels of BPA (Stoker et al., 2003); in common frogs (*Rana temporaria*) dosed with EE2 (Brande-Lavridsen et al., 2008) and also prochloraz - a fungicide known to interact with ERs (Vinggaard et al., 2002), and in wild mussels (*Elliptio complanata*) living in waters contaminated with EEDCs from an upstream municipal effluent outfall (Gagné et al., 2011). Modification of

sex ratios such as these have been shown to correlate with the increasing prevalence of synthetic xenoestrogens in surface water: a 10% complete feminization was observed in male African clawed frogs (*Xenopus laevis*) exposed to environmentally relevant concentrations of atrazine, a widely-used pesticide with estrogenic properties (Hayes et al., 2010).

Knowledge of the potential of various xenoestrogens to mimic, block or alter endogenous estrogenic signaling systems across different populations can aid in pinpointing, predicting, and ultimately preventing adverse health effects occurring at different cell, tissue and organ levels throughout diverse life stages. Small animal models provide a complex and holistic system that cannot yet be duplicated in cell culture or nonliving systems. Knowledge of estrogenic potential can advise researchers on the outcome of substances introduced to a live organism, including processes concerning entry to the system, how the liver and other organs can alter it, and the manner in which it is taken up, and subsequently interacts with, various tissues.

1.10 Levels of endocrine disrupting chemicals in the aquatic environment

Natural and synthetic hormones are both frequently detected in sewage treatment work (STW) effluent and their receiving surface waters at concentrations ranging from pg/L to ng/L (Baronti, 2000; Belfroid, 1999; Kuch & Ballschmiter, 2001). Alkylphenols, a family of organic compounds, many of which exert endocrine disrupting effects, are usually found in the environment at the µg/L level (Bolz et al. 2001; Jin et al. 2004; Stachel et al. 2003). Due to the low-level nature of individual EDCs, taken in conjunction with their unpredictable metabolic behaviour, their removal from STWs is often incomplete (Daughton & Ternes, 1999).

Estrogenic hormones represent the class of EDCs of most concern for the aquatic environment due to their potency, persistence and high degree of potential for causing endocrine disruption in wildlife (Jobling et al., 1998). Estrogens commonly found in the environment include 17β-estradiol (E2), estrone (E1), estriol (E3), EE2 and mestranol (MeEE2). They all exert their effects by passing through the plasma membrane of the cell and binding to intracellular receptors.

Concentrations of E2 as low as 1 ng/L have been observed to induce vitellogenin in male trout and EE2 exposures as low as 0.1 ng/L may provoke feminization in some species of wild male fish (Hansen et al., 1998; Purdom et al., 1994). The hormones E2 and E1 are naturally excreted by humans and animals, particularly females. It has been estimated that human males excrete an average of 3.9 µg/day of E1, 1.6 µg/day of E, and 1.5 µg/day of E3 in their urine. Menstruating women excrete an estimated 8 µg/day of E1, 3.5 µg/day of E2, and 4.8 µg/day of E3, while pregnant females are thought to release 600 µg/day of E1, 259 µg/day of E2, and 600 µg/day of E3 in their urine. Women taking the oral contraceptive pill have been estimated to excrete EE2 at a rate of 35 µg/day. These estimations of daily excretion considered in conjunction with previous measurements and data concerning estrogenic dilution factors have led to predictions of ng/L levels of estrogens in English rivers (Johnson et al., 2000).

STW effluents and influents worldwide have been found to contain varying concentrations of estrogenic EDCs. Influent of six Italian sludge STWs were analysed for the presence of estrogenic steroids and were found to contain average levels of 52 ng/L E1, 12 ng/L E2, 80ng/L E3 and 3 ng/L EE2 (Baronti et al., 2000). The raw sewage of a Brazilian STW was examined for the occurrence of estrogenic compounds and was found to contain E1, E2 and EE2 at concentrations of 40, 21, and 6 ng/L, respectively (Ternes et al., 1999a). An analysis of steroid estrogen presence in the influents of Japanese STWs reported E2 concentrations ranging from 20 – 94 ng/L in the summer and 30 – 90 ng/L in the autumn (Nasu et al., 2000). Estrogenic EDCs were detected in three Dutch STWs at levels ranging from below the limit of detection (< LOD) - 64ng/L, 11–140 ng/L, and < 0.2–8.8 ng/L for E2, E1 and EE2, respectively (Johnson et al., 2000).

Concentrations of estrogens in STW effluents varied widely across different sampling locations. Levels of EE2 varied from < LOD at many sites to as high as 7, 7.5, 15, and 42 ng/L in the UK, Netherlands, Germany and Canada, respectively (Belfroid et al., 1999; Desbrow et al., 1998; Ternes et al., 1999a). More recent studies into environmental EE2 levels have reported concentrations as high as 78.15 ng/L in the St Clair River, Canada (Al-Ansari et al., 2010), 41 ng/L in the Venice lagoon (Pojana et al., 2007), 24 ng/L in Jiaozhou Bay, China (Zhou et al., 2012), and 27.4 ng/L in the Dan-Shui River, Taiwan (Chen et al.,

2007). The high ER affinity of EE2 contributes to its potency, with *in vitro* testing in fish showing it to be 11-30 times more potent than E2, while E2 is 2.3-3.2 times more potent than E1 (Colman et al., 2009; De Mes et al., 2005).

It has been suggested that hydrophobic sediments may act as a sink for EE2 compounds in estuarine, riverine and marine environments, with concentrations predicted to be up to 1000 times higher than that of the overlying water column (Lai et al., 2000). EE2 and other estrogenic compounds were reported at levels ranging from < 0.05–2.52 ng/g in estuaries, from < 0.12–22.80 ng/g in rivers, and from < 0.05–3.6 ng/g in coastal marine areas (Labadie & Hill, 2007). EE2 has also been reported to bioaccumulate and biomagnify in aquatic organisms, with significant accumulation occurring in benthic invertebrate *Chironomus tentans* (Dussault et al., 2009). It is predicted that consumption of invertebrate food items may represent an additional source of EE2 exposure for vertebrate predators.

Livestock wastewater represents a further source of EE2 in the aquatic environment. EE2 is widely used to improve productivity and treat various diseases in farm animals (Gadd et al., 2010). Levels of estrogens excreted by livestock have been shown to be of the same (or even exceed) those produced by humans (Briciu et al., 2009; Liu et al., 2012b). Total daily levels of estrogens excreted by individual swine have been reported to range from 120–2300 µg – an order of magnitude higher than that of a typical human (Liu et al., 2012b). The combined farm population is thought to generate approximately four times more estrogenic output than the UK human population (Johnson et al., 2006). Annual levels of estrogen excretion are reported to have reached around 33 tons in the EU and 49 tons in the USA (Tang et al., 2013).

The potential toxicity of EE2 has been extensively studied and it is well-established that levels as low as 1 ng/L can affect the endocrine systems of exposed organisms (Robinson & Hellou, 2009). The embryonic and juvenile stages of aquatic organisms, particularly fish, are particularly sensitive windows to the effects of EE2 (Liu et al., 2012c). Female medaka (*Oryzias latipes*) were reported to exhibit a reduction in gonadal weight and subsequent decreased egg production at EE2 exposure levels of 10 ng/L (Scholz & Gutzeit, 2000). At the same concentration of EE2, elevated levels of aromatase were detected in the

testis of exposed male medaka, suggesting that a degree of feminisation had occurred (Peters et al., 2010).

At 1 ng/L EE2 significant female-biased changes in sex ratios were observed in zebrafish, with 100% sex reversal at levels of 2 ng/L (Örn et al., 2003). Three week exposures of 1, 5 and 25 ng/L EE2 were shown to suppress testicular *esr1* mRNA expression in male *Paramisgurnus dabryanus*, whereas exposed females were found to exhibit a significant upregulation of ovarian *esr2a* mRNA expression at 1 ng/L EE2 (Zhang et al., 2012). Juvenile male rainbow trout were shown to express high levels of vitellogenin plasma when exposed to 4.5 ng/L EE2 (Larsson et al., 1999). Similarly, increased vitellogenin production was reported in juvenile zebrafish after exposure to 2 ng/L EE2 (Pawlowski et al., 2004). Testis-ova was induced in adult male medaka after a six-week exposure to 20 ng/L EE2 (Hirakawa et al., 2012).

At the behavioural level, the frequency of courtship-specific behaviour performed by dominant male zebrafish was found to be decreased in animals exposed to 0.5 ng/L EE2 for 6 days (Colman et al., 2009). EE2 was also shown to affect anxiety and shoaling behaviour in adult male zebrafish exposed to 0.5 ng/L or 25 ng/L over a 14-day period (Reyhanian et al., 2011). Swimming activities were found to be significantly reduced in fish exposed to 25 ng/L EE2, while those exposed to 5 ng/L were recorded to spend significantly less time away from the shoal compared to control fish. Further research into behavioural alteration in zebrafish exposed to 5 ng/L EE2 supported these findings (Larsen et al., 2008).

Common effluent treatment procedures have been reported to be insufficient for the removal of estrogenic contamination: EE2 is especially persistent and tends to remain unchanged during its passage through the ecosystem. Studies employing various species of microbe and bacteria in an effort to degrade estrogens, however, have shown that almost 100% of E2 and EE2 can be removed from water using mixed cultures of specific microbes (*A. xylosoxidans* and *Ralstonia pickettii*) (Weber et al., 2005). Bacteria such as *Sphingomonas* strain KC8 and *Bacteroidetes* have also been shown to be effective in the microbial degradation of many estrogenic compounds (Fujii et al., 2002; Roh & Chu, 2010; Yoshimoto et al., 2004; Yu et al., 2011). Nitrifying microorganisms

(i.e. *Nitrosomonas sp.*) have additionally been found to be effective at removing EE2 compounds (Shi et al., 2007; Vader et al., 2000).

1.11 Screening and testing for EDCs

In acknowledgement of the risks posed by exposure to endocrine disrupting chemicals, the European Union imposed testing of all current and novel chemicals suspected of possessing endocrine disrupting properties that are produced in quantities greater than 1 ton/year (REACH legislation). Such regulations ultimately mean that all potential EDCs will need to be screened at least in a medium-throughput capacity in order to ascertain risks posed by the large number of chemicals in current and future use.

Extensive chemical monitoring is required to assess the potential environmental impact of estrogens and other EDCs in the aquatic environment. A battery of *in vivo* and *in vitro* ecotoxicological tests form the current strategy for detecting and measuring levels of EEDCs (Baker et al., 1999; Isidori et al., 2010; Palermo et al., 2008; Reel et al., 1996; Shelby et al., 1996). *In vitro* tests are often used as a primary screening step, before moving onto *in vivo* approaches (OECD, 2003). Such tests include ligand-binding assays (where the competitive binding of estrogens in a water sample to hormone receptors are measured), cell-free assays (studying steroidogenesis and hormone metabolism), transgenic yeast, cell lines, primary cell cultures and organ cultures.

In vitro assays have the benefit of being relatively inexpensive, are often quick to perform, and can be conducted at high-throughput. In addition, since these approaches are simplified biological systems, they are often highly sensitive and specific to the detection and characterization of individual compounds. *In vitro* methods also circumnavigate the ethical issues associated with *in vivo* methodologies. A major drawback of *in vitro* assays is that knowledge concerning the mechanism of action of a chemical must be obtained prior to its analysis. This is because the ability to make predictions about how a measured response might manifest *in vivo* depends on the mechanism that the assay is based on. Because *in vitro* assays are mechanism-specific, they do not take into account the many factors that may affect the mechanism of the compound *in vivo*.

In vivo assays have a different set of benefits and limitations. Some major drawbacks include the fact that they are often expensive, cannot easily accommodate high-throughput screening, and are unable to characterize compounds in isolation. Furthermore, they can be subject to a high degree of variability due to seasonal, inter-individual, and temporal deviations, making the repeatability of assays difficult. *In vivo* methods are also subject to ethical and socio-political concerns and limitations.

However, *in vivo* screening approaches have the major benefit of accounting for the wide range of biological factors that may affect the mechanism of a chemical. These include cross-talk between different biological pathways, simultaneous environmental influences (such as temperature and light), and the integration of different mechanisms exerted by different cell types, tissues and organs – all of which will influence the action of a compound. Unlike *in vitro* assays, *in vivo* screening methods also take bioaccumulation, metabolic transformations, and homeostatic controls into account – factors that can all influence the potency and efficacy of chemicals in living systems.

An integrated assessment of EDCs in agricultural runoff highlighted the integrated value of combining *in vitro* and *in vivo* approaches (Cavallin et al., 2014). Surface stream water was assessed for relative estrogenic and androgenic activity using *in vitro* cell assays, and tested for endocrine-disrupting effects in exposed fathead minnows using an *in vivo* approach. *In vitro* estrogenic activity was detected in samples from all of the six sampled sites. However, the *in vivo* exposures showed no significant dose-dependent effects for any of the biological endpoints measured, with the exception of elevated male testosterone production observed in one of the exposure groups. This study emphasised the need for a combination of techniques to be used in obtaining a complete characterization of EDCs in environmental samples.

The large-scale screening of chemicals imposed by the European Union will inevitably increase the numbers of animals needed to be used for *in vivo* chemical testing, and this consequently counters the drive to reduce the quantity of animals required by implementing more efficient screening. The three R's (replacement, refinement, reduction) - principles now widely accepted internationally as underpinning the humane use of animals in research – will require that non-

regulated, early life-stage, pre-feeding fish larvae or tadpoles be more widely used in place of mammals. Ideally, these animals will provide a robust enough signal in response to chemicals such as EEDCs, so that their screening may eventually be robotized.

1.12 Small Animal Molecular Imaging (SAMI) modalities and their application for investigating the roles of estrogens

Small animal *in vivo* imaging is a technique being widely-used by investigators to address biological questioning, spanning the investigation of circadian rhythms in the murine brain (Abraham et al., 2005), to visualizing immune cell activation and infiltration at sites of infection (Davies et al, 2005). *In vivo* imaging modalities can largely be divided into primarily morphological/anatomical and primarily molecular systems (Willmann et al., 2008), the latter of which will be the focus of this review.

The term 'molecular imaging' has been defined as being 'the visual representation, characterization, and quantification of biological processes at the cellular and subcellular levels within intact living organisms' (Massoud & Gambhir, 2003). Molecular imaging has the major benefit of replacing single-time-point animal dissection and thus creates the opportunity for repeat study of the same individual for the expression of specific genes over time.

Molecular imaging emerged in the 21st century and united the disciplines of molecular biology and *in vivo* imaging. Rather than relying on nonspecific macroscopic alterations in the physiology or metabolism of tissues, molecular imaging typically exploits specific molecular probes in order to observe precise molecular events responsible for disease or to evaluate treatments.

By employing imaging biomarkers (detectable biological image features) to visualize targets or pathways, molecular imaging allows researchers to identify and differentiate normal biological processes from pathogenesis or pharmacological responses to a therapeutic treatment. Imaging biomarkers include anatomical, physiological or molecular variables detectable by one or more imaging modality.

Strong ties exist between nuclear medicine and molecular imaging: since its emergence, the aim of nuclear medicine has been to facilitate non-invasive diagnosis in living subjects (Williams, 2008). Nuclear imaging originally relied on hand-held Geiger Counters to measure the biodistribution of radioactive substances throughout the body without generating an image. By 1950, the rectilinear scanner, the first system that allowed images of organs to be formed, was developed (Cassen et al., 1951). This device was later superseded by the Photoscanner in 1956 which incorporated a photographic component, resulting in improved resolution and sensitivity but also a lengthy image-acquisition time and motion artifacts.

By 1965, the Gamma Camera had been developed to address many of the drawbacks of the Photoscanner (Zum Winkel et al., 1965): the improved design had the advantage of being capable of dynamic images in addition to being able to image large areas at a time. Later modification of the Gamma Camera to use computers and reconstruction algorithms resulted in the development of the first single photon emission computed tomography (SPECT) system (Keyes et al., 1978). SPECT works by measuring the emission of photons after a radioactive tracer has been administered to the subject and has the benefit of being extensively validated and relatively sensitive. The limitations of SPECT, however, include its high cost and risks associated with radiation.

Nuclear medicine was later subject to a revolution with the advent of additional highly sensitive *in vivo* imaging modalities, such as positron emission tomography (PET), and the development of novel radiolabelled molecules that targeted specific molecular processes. Like SPECT, PET makes use of radiotracers to produce images with high spatial resolution and good specificity, but also imposes the same disadvantages of high cost and risks caused by radioactive components. Newer strategies, not restricted to radioactive signaling, have since emerged such as magnetic resonance imaging (MRI), computer tomography (CT), ultrasound (US) and optical signaling methods.

Briefly, MRI uses non-ionising radiation to generate three dimensional detailed anatomical images. It has the advantage of imaging without the need for ionising x-rays, can obtain images without the use of contrast agents, and allows for precise tissue characterisation. The limitations of MRI include its expense, long

image acquisition time, and its tendency to introduce unique artefacts. CT scanners employ a narrow beam of x-rays to generate cross-sectional images of the subject. One of the principle advantages of CT includes its rapid acquisition of clear and specific images. One of the main limitations of CT scanning is the relatively high dose of radiation it necessitates. CT scans often require the use of contrast agents which can produce allergic responses in the subject. US scans use high frequency sound waves to generate images of organs, tissues or vessels. US scans are safer than modalities that use radiation or cause ionisation and can provide images of soft tissues, but the images they produce are of relatively poor resolution compared to CT and MRI and can be difficult to interpret.

Both pharmaceutical companies and academia alike are becoming increasingly interested in small animal molecular imaging (SAMI). Recent technical advances in the fields of molecular and cell biology, including the availability of various transgenic animals, highly specific new drugs and imaging probes, plus the development of novel specialised equipment for small animal imaging, has resulted in a convergence between established cell culture, *in vitro* assays and *in vivo* animal imaging.

This union of technologies and techniques within the field of live molecular small animal imaging has led to the possibility of several important research targets being realised. These include: 1) the possibility of developing noninvasive *in vivo* methods for reflecting specific and complex molecular and cellular processes such as protein-protein interactions; 2) simultaneous monitoring of multiple molecular events; 3) tracking and observation of cell trafficking and targeting; 4) optimisation of gene and drug therapy; 5) the ability to image the effects of compounds at a cellular and molecular level; 6) to assess the progression of disease at a molecular level of pathology; and 7) to achieve all of these imaging goals in a fast, quantitative and reproducible way, allowing for any potential responses to be monitored within the same animal, ultimately reducing the numbers of animals required (Massoud & Ghambir, 2003).

Four prerequisites that should be met for successful imaging at the molecular level were outlined as follows: a) the availability of high-affinity probes with good pharmacodynamics; b) the ability of these probes to overcome biological barriers such as cell membranes; c) the use of chemical or biological amplification

strategies; and d) the availability of rapid, sensitive and high-resolution imaging techniques (Weissleder & Mahmood, 2011). With small animals being increasingly used in research, imaging methods must incorporate sufficiently high spatial resolution as well as adequate specificity and sensitivity in order to provide the most accurate possible illustration of molecular concentration and distribution.

While *in vitro* techniques have provided invaluable insight into the mechanics of the cell and disease states, *in vivo* imaging has allowed researchers to overcome the inability of *in vitro* to provide analyses over time and in intact organisms, i.e. the 'full picture' of biochemical processes. *In vivo* techniques have also negated the necessity to dissect organs, tissues and cells from their natural microenvironment (introducing artificial conditions), as well as the incapacity to analyse samples more than once due to the destructive nature of many *in vitro* techniques. As mentioned earlier, the costly and ethically-compromising requirement to euthanase animals, preventing repeated/longitudinal study of the same organism, can also be avoided (James & Ghambir, 2012).

1.13 Small animal optical imaging

Optical imaging can be divided into fluorescence and bioluminescence imaging, and their respective modalities are relatively inexpensive, faster, simpler, more convenient and more user-friendly than other imaging modalities (Kang & Chung, 2008). Since the development of the first light microscope in 1674, the field of optical imaging has progressed rapidly, with the addition of useful techniques such as dark field, bright field and differential interference contrast.

Fluorescence microscopy has allowed for substantial advances to be made in cellular biology and has become an essential tool in biomedical sciences. It provides direct insight into the processes of living cells at sub-cellular resolutions and enables the visualisation of a diverse range of processes including protein transport, metabolism, location and the associations of ions. Thus, the effects of chemicals can be characterised in the intact context of the dynamic and complex living system. Advances in the field of optical imaging have included the synthesis of fluorescent proteins (reviewed in Shaner et al., 2005) and the availability of numerous new fluorophores (reviewed in Suzuki et al., 2007).

During fluorescence microscopy, the sample of interest is typically labelled with a fluorophore (a fluorescent chemical compound), which is excited by one wavelength of light, subsequently emitting light of a longer, lower energy wavelength after a short interval (fluorescence lifetime). This emitted fluorescent light can then be isolated from the surrounding radiation using filters designed for that discrete wavelength, allowing for the microscope user to see only the fluorescing elements of the specimen.

Fluorescent microscopes work in much the same way as conventional light microscopes except that they use a much higher intensity light source to excite the fluorescent species of interest within a specimen (Bradbury & Evennette, 1996). The fluorescent microscope radiates the specimen with excitation light before filtering out the weaker emitted fluorescence. The development of more powerful light sources, such as lasers, has led to the construction of more sophisticated microscopes such as the confocal and total internal reflection fluorescence (TIRF) systems. Fluorescent confocal microscopy uses a high intensity light source to focus on a pinpoint and image through layers of a specimen ('Z-stacks'), allowing 3D reconstructions of the target sample to be generated.

The field of fluorescence microscopy can be divided into several major categories: 'autofluorescence' (or primary fluorescence) is the ability of some specimens to fluoresce naturally if excited by light of the appropriate wavelength. Fluorescent stains (first used by Haitinger, 1933) can typically be used to selectively dye tissue components of interest, generating fluorescence upon appropriate excitation known as 'secondary fluorescence'. An additional technique (first used by Coons & Kaplan, 1950) is 'immunofluorescence', which involves the binding of a fluorescent dye to an antibody allowing for its subsequent localisation within samples. Further fluorescent materials include fluorescent proteins (such as green fluorescent protein - GFP), and small organic dyes that can be used to label antibodies. Quantum dots, semiconductor nanocrystals (<100 nm) that absorb and then re-emit photons of light, can also be utilised for bioimaging when coupled to proteins and other small molecules, allowing them to bind to targets of interest.

Fluorescence and bioluminescence imaging both require the same basic infrastructure consisting of a charge-coupled device (CCD) camera and a filtered light source. This set-up has the advantage of being relatively cheap and easy to assemble, and the use of low-energy photons for generating images rather than, for example, gamma rays, renders the system relatively safe. However, it is the nature of this emission light coupled with the light-scattering effect of most biological tissues that limit the imaging depth and resolution of traditional fluorescence microscopy (Helmchen & Denk, 2005). Nevertheless, for the purpose of small animal imaging, the depth of penetration achieved using a conventional fluorescence microscope is usually sufficient, making the technique highly suitable for preclinical research (Debbage & Jaschke, 2008).

1.14 Optical small animal *in vivo* imaging of ERs and estrogenic endocrine disruption

Acridine orange (AO) is a cell-permeable fluorescent dye found to be highly-selective for apoptotic cells, which it highlights with a reduced green fluorescence and enhanced orange fluorescence compared to normal cells (Tucker & Lardelli, 2007). This change in emission is thought to result from the breakdown of DNA into fragments during apoptosis, which denature and then bind to AO, giving an orange fluorescence (Darzynkiewicz, et al., 1992). It has been established that exposure of zebrafish embryos to genistein (a plant-derived phytoestrogen) elicited cell death in a dose-dependent manner *in vivo*, and this apoptosis was localised mainly in the hindbrain and anterior spinal cord (Sassi-Messai, 2009). Detectable responses in live embryos were seen at genistein concentrations as low as 2.5µM. Genistein induced the majority of cell death during a precise developmental window around 12hpf. This reported use of fluorescent staining to elucidate the deleterious effects of an EEDC demonstrated its utility as an optical approach for qualifying, quantifying and identifying temporal points of chemical sensitivity during development.

The EEDC tributyltin chloride (TBT) is known to activate estrogen receptors (Penza et al., 2011) including those in fat cells, via which it can induce a dramatic increase in adiposity (an excess of body fat). Live zebrafish larvae, exposed to environmentally relevant concentrations of TBT (Zhang et al., 2011), were

stained with the lipophilic fluorescent dye Nile Red (NR) before being imaged using a fluorescent microscope (Tingaud-Sequeira et al., 2011). NR staining was carried out before and after the one-day TBT exposure period in order to quantify adipose tissue fluorescence area. TBT was shown to cause a significant increase in adiposity at the environmentally relevant concentration of 0.05 μM regardless of the lipid composition of the background diet. This *in vivo* assay effectively demonstrated the use of a vital dye in characterizing the potential obesogenic impact of an EEDC.

A variety of transgenic (TG) animal models have been developed that are capable of visually responding to EEDCs via the expression of fluorescent proteins that can be usefully quantified. These novel TG models have made it possible to visualise both the interaction and biological effects of estrogens occurring within intact live organisms. Extracted from the jellyfish *Aequorea victoria* (Tsien et al., 1998), green fluorescent protein (GFP) has enabled a revolution in noninvasive imaging in living cells and organisms (Vonesch et al., 2006). Genes of interest can be fused to the gene for GFP, allowing a wide range of cellular proteins to be made fluorescent without the requirement for additional cofactors (Rittscher, 2010).

1.15 Transgenic fish and their use in studies into the effects of EEDCs

An example of a novel imaging tool in the investigation of EEDC effects upon animal models is a TG estrogen-responsive zebrafish: the ERE:GFP line that expresses GFP driven by estrogen response elements in accordance with developmental estrogen signaling, and upon exposure to exogenous ER ligands (Gorelick & Halpern, 2011; Lee et al., 2012a).

ERE:GFP zebrafish models have provided valuable information concerning the tissue-specificity of ER expression in the developing embryo in real-time, highlighting potential areas of concern for EEDC-exposed fish. Gorelick and Halpern (2011) reported strong GFP responses in the developing liver and pancreas of estradiol (E2) exposed fish embryos from 2dpf onwards, while lower level GFP could be detected in the brain and heart valves at 4dpf. At 5 and 6dpf,

the GFP expression can be clearly observed throughout the embryo in the liver, pancreas, kidneys, brain, heart valves and hair cells.

Lee et al.'s (2012a) similar TG line (incorporating multiple tandem EREs and a Gal4ff-UAS system for enhanced response sensitivity, Figure 1.3.) also expressed GFP in tissues shown previously to be responsive (Gorelick & Halpern, 2011), as well as in the somite and skeletal muscles, otic vesicles and neuromasts in response to exogenous estrogens. While the earlier model was shown to be capable of inducing a GFP response only at very high exposure concentrations (E2 at 1–100 µg/L; Gorelick & Halpern, 2011), Lee et al. demonstrated a detectable response in their TG model from EE2 concentrations as low as 1ng/L in the heart and liver. The sensitivity of this model also facilitated investigation of stage-dependent responses to EE2 (100ng/L) from 1hpf to 96hpf. Expression of GFP was observed in the heart, liver and muscle from as early as 24hpf, where it progressively increased until a maximal expression level was reached at 96hpf. Life-stage-dependent GFP responses were also observed in the otic vesicle after 48hpf, and eye and forebrain after 72hpf, demonstrating the effectiveness of this ERE-TG model for investigating time-related effects of estrogens *in vivo*.

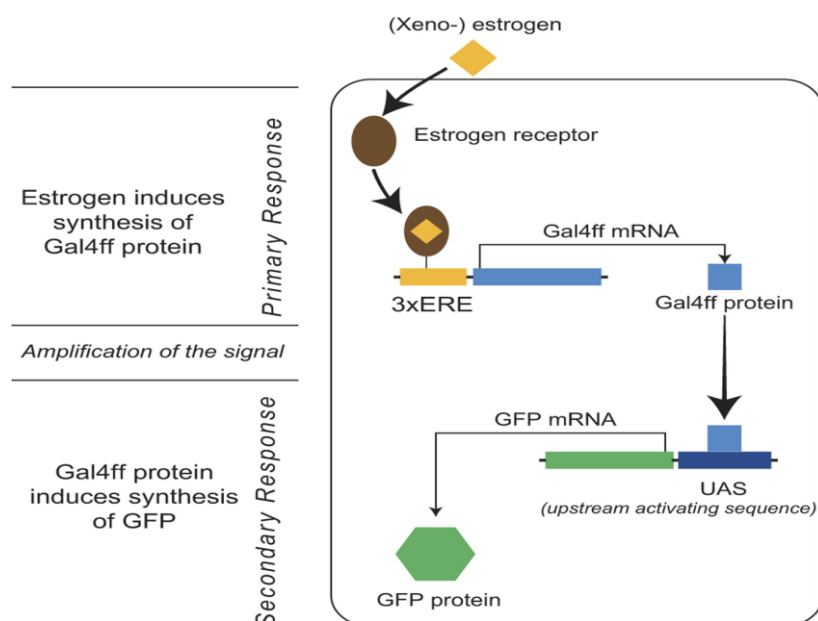


Figure 1.3. Two-step mechanism of estrogenic signal amplification in the Gal4ff-UAS transgenic system. EREs respond to the estrogenic signal, driving the initial reporter, Gal4ff, which binds to the upstream activating sequence (UAS), which subsequently drives the expression of GFP (from Lee et al., 2015).

The discovery of many estrogenic biomarker genes led to the development of a range of animal models that allow for responses to estrogens to be visualised. In addition to Gorelick and Halpern (2011) and Lee et al.'s (2012a) exploitation of the estrogen response elements to drive GFP expression in zebrafish target cells, Brion et al. (2012) utilised the *cyp19a1b* gene, which encodes a brain form of aromatase (aromatase B), modified to drive GFP expression in radial glial progenitors in response to estrogen exposure. Several systems have involved GFP-tagging the *choriogenin h* (*chgh*) gene and vitellogenin1 (*mvtg1*) promoter (genes related to egg production) in transgenic medaka in order to drive GFP expression and visualize responses to EEDCs in the liver (Kurauchi et al., 2008; Salam et al., 2008; Zeng et al., 2005). These systems varied in their sensitivity and response time to EEDCs, but shared the ability to quantify the GFP response via optical bioimaging methods. However, Gorelick and Halpern (2011) and Lee et al.'s (2012a) models had the dual benefit of expressing a detectable level of GFP in EE2 concentrations as low as 0.1ng/L, in addition to allowing ER response visualisation in a wide range of estrogenic tissues rather than being limited to liver or radial glial cell.

In addition to the several estrogen-responsive TG zebrafish lines described (Brion et al., 2012; Gorelick & Halpern, 2011; Lee et al., 2012a), which are capable of generating ER-driven GFP signals quantifiable by fluorescence microscopy, there are also a number of transgenic models effective in elucidating EEDC-induced developmental perturbations detectable using optical imaging methods. For example, the *Tg(nkx2.2a:mEGFP)* transgenic zebrafish expresses GFP under the *nkx2.2a* promoter specifically in the central nervous system (CNS) and pancreas (Pauls et al., 2007): when exposed to atrazine (an EEDC which induces aromatase, leading to an excess synthesis of estrogen) a neurotoxic effect was revealed, indicated by a reduction in GFP-labelled ventral axon lengths (Zhang & Gong, 2013). The insecticide methoxychlor has been shown to exert estrogenic effects in humans and zebrafish (Lemaire et al., 2006; Versonnen et al., 2004): using the huORFZ transgenic zebrafish line, stress-related cellular processes were detected via GFP induction and it was established that this EEDC was capable of inducing stress in both the brain and spinal cord (Lee et al., 2014).

Fluorescent imaging, used in conjunction with transgenic animals, can provide a wealth of information regarding the impact of EEDC perturbation across a range of biological systems *in vivo*. The zebrafish Fli-EGFP reporter line expresses EGFP (enhanced green fluorescent protein) in all blood vessels throughout embryogenesis and exposing this model to diclofenac, an anti-inflammatory drug with estrogenic properties, revealed it to exert a broad deleterious impact on the whole cardiovascular development of zebrafish (Li et al., 2016).

A study undertaken using the *cyp19a1b*-GFP transgenic zebrafish found significantly increased fluorescence intensity in the brain for BPA exposure (by 16-fold compared to the DMSO control) and for exposure to BPAF and BPF, 14- and 13-fold GFP inductions respectively, indicating that they had endocrine disrupting potential nearly equivalent to BPA (Cano-Nicolau et al., 2016). As there is growing evidence suggesting that BPA has a negative impact on neural development (reviewed in Kajta & Wojtowicz, 2013; Negri-Cesi, 2015), this *in vivo* bioimaging assay usefully highlighted bisphenol analogues for further investigation into their potential as EEDCs.

The *cyp19a1b*-GFP transgenic zebrafish model has also been applied in investigating the effects of estrogenic compounds in combination using *in vivo* via optical imaging. As aquatic wildlife is likely to be exposed to a mixture of EEDCs rather than just one in isolation, it is crucial that the potential endocrine-disrupting effects of combinations are studied. It was observed that binary mixtures of EE2 and Levonorgestrel (LNG, used in emergency contraceptives and birth control pills) had an additive effect on the expression of 96hpf zebrafish radial glial cell GFP *in vivo*, which was more potent than the EC50 concentrations of the two chemicals alone (Hinfrey et al., 2016). Interestingly, it is known that LNG does not bind with zebrafish ERs (Cano-Nicolau et al., 2016), indicating that its conversion into estrogenic metabolites is resulting in its interaction with the zebrafish estrogenic pathway and generating an exaggerated fluorescence response in the *cyp19a1b*-GFP model.

The ERE:GFP line has been further improved for *in vivo* imaging of EEDC affects by crossing it with a pigment-free “Casper” zebrafish strain (White et al., 2008), generating a highly-translucent ERE:GFP:Casper model for detecting estrogen-induced GFP responses (Green et al., 2016). The model demonstrated a consistent and improved fluorescence signal (at 5dpf) compared to the original TG line (see Figure 1.4.) due to its lack of pigmentation, making it highly suitable for the screening of EEDCs. The sensitive estrogen-responsive ERE:GFP:Casper held great potential for utilisation in higher-throughput screening approaches and we subsequently adopted it for the optimisation of a medium-throughput, semi-automated bioimaging assay.

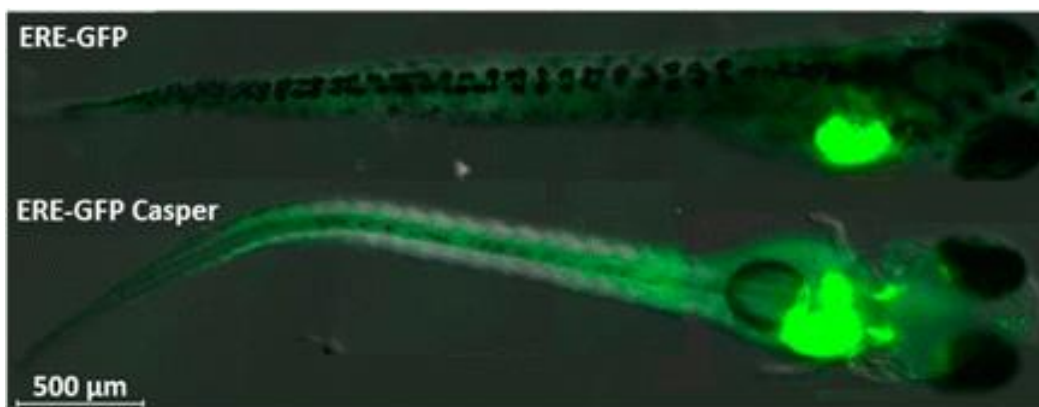


Figure 1.4. Comparison between ERE-GFP model and ERE-GFP-Casper model (demonstrating enhanced fluorescence response) exposed to 50ng/L EE2, imaged using Zeiss Axio Observer at 10x magnification under consistent GFP excitation (from Green et al., 2016).

1.16 Higher-throughput *in vivo* assays for the qualification and quantitation of EDC effects in transgenic models

In vivo whole-animal screening holds great promise for bypassing many of the bottlenecks that currently impede both the discovery of new drugs and potential for identifying existing chemicals that pose an environmental threat. However, *in vivo* screening systems are still largely subject to optimisation, with the future aim of matching the high-throughput screening (HTS) capacities of *in vitro* assays. Zebrafish studies are typically hampered by the need for low-throughput, manual techniques such as orientation for imaging, and manual pipetting of the animal. Several imaging platforms have thus emerged in recent years that improve the throughput of live whole-organism screening. Higher-throughput zebrafish assays allow for much larger numbers of animals to be analysed than is possible with mammalian studies, potentially improving statistical variability.

A number of systems have been developed using commercially available plate readers to quantify fluorescence expressed by TG zebrafish embryos and larvae arrayed in multiwell plates. For example, a semi-automated system was developed for higher-throughput screening of the ERE:GFP:Casper model using an ArrayScan II (Cellomics Inc., Pittsburgh PA) plate reader (Green et al., 2016). This platform was capable of automatically acquiring GFP images of each well of a 96-well plate of 5dpf EEDC-exposed animals in 1.5 hours before a custom

image-processing algorithm was applied for semi-automated data-extraction. The system reliably identified fluorescent responses to a range of different environmental estrogens, with EEDC-induced GFP found to be significantly elevated above chemically-unexposed larval responses in ERE:GFP:Caspers exposed to 5ng/L EE2.

The Automated Reporter Quantification *in vivo* (ARQiv) system is an example of a purpose-built whole-organism high-throughput screening modality which, like the ArrayScan, utilises a fluorescence plate reader for robust quantification of reporter signals *in vivo* (Walker et al., 2012). Designed to provide a first-tier HTS drug discovery platform, the ARQiv system is outfitted with specific detection functions that allow for changes in individual TG zebrafish models to be monitored over time. In theory, the system is capable of screening more than 200,000 animals per day for a single time-point assay, but this assumes HTS automated handling of embryos for arraying in a multiwell format – necessitating the use of an additional commercially-available system such as a Complex Object Parametric Analysis and Sorting (COPAS™, Union Biometrica, USA) instrument.

An example of a HTS platform that circumvents manual handling of zebrafish larvae is vertebrate automated screening technology (VAST, Pardo-Martin, 2010). The VAST microfluidics system extracts larvae from a multiwell plate or reservoir before automatically orientating, imaging and returning them to the dosing media. VAST is capable of positioning larvae for subsequent high-speed confocal imaging, and allows for *in vivo* optical manipulations such as localised activation of fluorescent reporters.

With technology advancing in the field of automated handling and microfluidics systems, the emerging bottleneck of concern is now rapid image-processing and data extraction. Fortunately, a wealth of open-source bioimaging software has been developed in recent years, including FIJI (Schindelin et al., 2012), ICY (De Chaumont et al., 2012), and CellProfiler (Carpenter et al., 2006), that have allowed analysis to keep pace with image acquisition.

Integrated approaches that combine microfluidics with microscopy and automated image-processing are essential for the progression of high-throughput bioimaging assays. The systems will also need to be user-friendly and as simplistic as possible, in order that the automation software required to

accompany them can be similarly accessible and generalisable. Once such integrated systems have been developed, the emphasis will fall on cost-reduction so that such analytical toolkits may become widely available.

1.17 Thesis Aims, Objectives and Hypotheses

The overall aim of this thesis is to establish the most sensitive and robust approach for screening an EEDC-exposed estrogen-responsive zebrafish model using a semi-automated imaging modality through refinement of assay parameters. Various image-masking and pixel-thresholding approaches will be applied to generate fluorescence data from pair-wise and group-spawned zebrafish larvae arrayed according to either standardised or random orientation approaches for image acquisition. The sensitivity and specificity of each approach will be assessed for its relative contribution to an optimised screening assay, the objective being to then use these parameters to pursue a further line of investigation into the effect of larval incubation temperature on subsequent interpretation of estrogen-induced fluorescence results.

It is hypothesised that the development of image-masking and pixel-thresholding approaches will improve the sensitivity and robustness of GFP response detection in the transgenic model, and that the detection of the fluorescence response at environmentally-relevant concentrations of EE2 will be possible using a medium-throughput, semi-automated approach to screen the ERE:GFP:Casper zebrafish. Uniform orientation of the larval model during image acquisition is also expected to reduce variability of the detected fluorescence response between animals.

Comparison between a manual imaging approach using a higher-resolution imaging modality with mounted samples is predicted to generate more sensitive and robust data than the semi-automated approach, but at a cost of greater time effort. The application of pair-wise breeding and careful developmental staging of the embryos is expected to significantly improve the reproducibility of the transgenic fluorescent response following exposure to a range of EE2 concentrations.

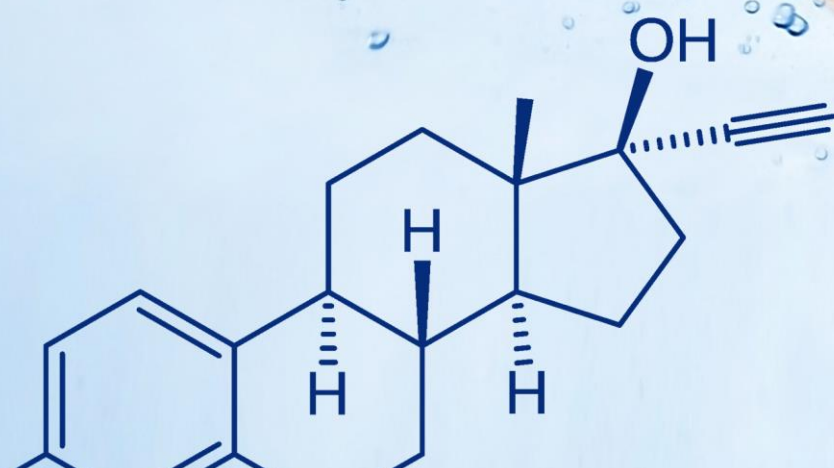
After establishing the most sensitive and robust approaches for the screening of the EE2-exposed model using a semi-automated imaging modality, the optimised specifications will be used to investigate the potential of an EEDC to interact with estrogen receptors under varying larval incubation temperatures. The aim of this analysis being to establish the potential for variations in temperature regimes to influence EE2-induced fluorescence responses in the model, and to generate information concerning the potential impacts of an EEDC and thermal regimes on the specific growth of the early-life stage model as a further endpoint for potential estrogen-induced perturbation.

It is expected that a greater estrogen-driven mean GFP response will be observed at a higher incubation/water temperature regime as a consequence of more rapid larval development resulting in higher levels of estrogen receptor activity. Specific growth rate is predicted to be accelerated compared to unexposed larvae raised under optimal temperature conditions. At the lower exposure temperature, mean larval GFP responses are expected to be lower compared to control responses for EE2-treated animals as a consequence of restricted growth. Specific growth rate is predicted to be reduced compared to unexposed larvae raised under optimal temperature conditions.

It is the intention that these findings presented in this thesis will outline an improved approach for further development of higher-throughput *in vivo* estrogenic screening of a transgenic zebrafish model.

Chapter 2

Materials and Methods



Chapter 2.

Materials and Methods

2.1 Zebrafish as a model for endocrine disruption

Fish are commonly used as models for evaluating endocrine disruption, particularly as their hypothalamic-pituitary-gonadal (HPG) axis is highly conserved across all vertebrates. They are used both in their own right for predicting and protecting against endocrine perturbation in fish, and as a model for mapping findings with effects in mammals. Thus, responses to EEDCs observed in fish can be usefully extrapolated for the prediction of modes of action in other species, including humans (Ankley & Johnson, 2004). The zebrafish, transgenic model for studying estrogens is a tropical freshwater species belonging to the minnow family (Cyprinidae) and is a model regularly used in ecotoxicological studies. They are group-spawners, with females that oviposit in carefully selected territories defended by the successful male. Zebrafish are capable of breeding all year round, with females spawning clutches of up to several hundred eggs every 2-3 days (Kimmel et al., 1995). The zebrafish is the model adopted throughout this thesis work.

2.2 Generation of the ERE:GFP:Casper line

The ERE:GFP:Casper zebrafish was developed by colleagues at the University of Exeter (Green et al., 2016) by crossing the estrogen-responsive ERE:GFP line (Lee et al., 2012) with a Casper line supplied by University College London. The original ERE:GFP model incorporated a 3 x tandem ERE and a *To/2*-mediated GAL4FF – UAS system and was shown to be responsive to a range of estrogenic chemicals in a wide variety of tissues including brain, heart, liver, skeletal muscle and neuromasts (Lee et al., 2012).

The Casper line has translucent skin due to silencing of the *roy* (dark) and *nacre* (silver) pigmentation genes. Larvae generated by crossing ERE:GFP:Caspers from the F2 and F3 generations were used to generate the larvae for the following studies. These animals were reared to sexual maturity after initial estrogenic screening of larvae (50ng/L EE2 exposure from 0-5 dpf) ensured that they were homozygous for the ERE/Casper genotype when fluorescent responses were examined using an inverted compound microscope (Zeiss Axio Observer) under consistent GFP excitation (180 ms using filter set 38 HE: BP 470/40, FT 495, BP 525/50).

2.3 Anaesthetic preparation

Tricaine (3-amino benzoic acid ethylester) comes in a powdered form from Sigma (Cat.# A-5040) and was made up in 10ml aliquots before the start of experiments. 400mg tricaine powder was added to 97.9ml rig water with ~2.1ml of 1M Tris (pH9) to adjust pH to ~7. Aliquots were then stored at -20°C and, once thawed, were used within 2 weeks and refrigerated during this time at 2-8°C. On the day it was needed, tricaine was brought up to room temperature (28±1°C) and 50µL diluted in 350µL rig water in wells of a 24-well plate (Greiner CELLSTAR® 24 Well Cell Culture Plate). Larvae were manually pipetted into this solution in 100µL of their original exposure media, giving a final tricaine concentration in the well of 0.04%.

2.4 Fish husbandry and experiments

All experimental procedures conducted in this research with fish followed U.K. Home Office regulations regarding the use of animals in scientific procedures and followed local ethical review guidelines ensuring their humane treatment. Fish were maintained in the Aquatic Resources Centre (ARC); a custom-built aquarium facility at the University of Exeter with dedicated rooms for maintaining zebrafish. Rig water supply was prepared from mains tap water filtered by reverse osmosis (Environmental Water Systems (UK) Ltd) and then reconstituted with Analar-grade mineral salts to standardise synthetic freshwater (final concentrations to give a conductivity of 300mS: 117mg/L CaCl₂·2H₂O, 25.0 mg/L

NaHCO₃, 50mg/L MgSO₄·7H₂O, 2.3mg/L KCl, 1.25mg/L Tropic Marin Sea Salt), aerated and heated to 28°C, before being supplied to individual zebrafish tanks on a flow through system. Water was routinely monitored for temperature, pH, conductivity, ammonia, nitrite and nitrate - all of which were maintained within the acceptable limits for zebrafish (U.S. EPA Guidelines). Photoperiod was set at 12:12 hour light:dark (08:30-20:30 light), with an artificial dawn to dusk transition of 30 minutes.

2.5 Zebrafish maintenance

Adult ERE:GFP:Casper zebrafish were maintained at a controlled temperature (28±1°C) and photoperiod (12:12 phased light:dark cycle). The adult fish were fed live brine shrimp twice daily (Brine Shrimp Cysts Premium 260 Grade enriched with NEW HUFA Artemia Enrichment, ZM Fish Food) and dry pellet (GEMMA Micro 300, Skretting) or frozen brineshrimp (Tropical Marine Centre aquarium products) feed once a day.

2.6 ArrayScan automated image acquisition

The 96-well plate was loaded onto the Cellomics ArrayScan II HCS/High Content Screening System plate reader (Figure 2.1.) for automated image acquisition. The system had been previously customised by the installation of a x1.25 magnification objective (Olympus) which enabled acquisition of the whole larval body in one 512 x 512-pixel image. The objective had been programmed to centre above each well of the 96-well plate before autofocussing to obtain fluorescent images of the larval GFP responses using 16 seconds of fluorescent light (488 nm) exposure. The images were captured using an up/down scanning option (Figure 2.2.) so that animals were imaged column by column alternately across all dosing concentrations.



Figure 2.1. The Cellomics ArrayScan II HCS/High Content Screening System.

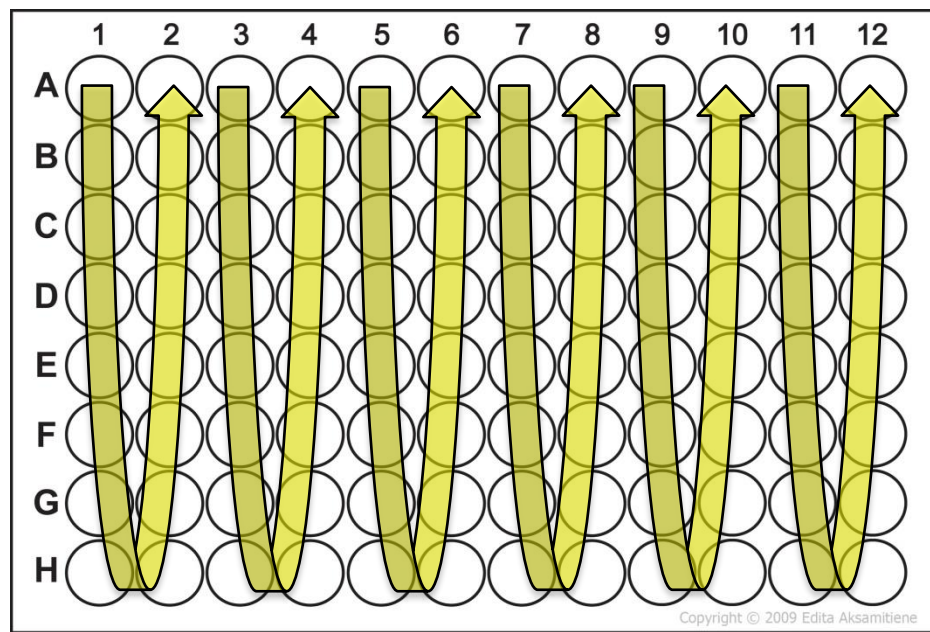


Figure 2.2. Up/down scanning path of the ArrayScan objective lens across the 96-well optiplate.

2.7 Image analysis approaches

Table 2.1. Summary of mask/filtering approach, area identified by respective approach, and (approximate in some cases) number of pixels that mean pixel fluorescence intensity averaged across.

Masking/pixel filtering approach:	Area identified:	Number of pixels fluorescence intensity averaged across:
Whole image mean fluorescence	None	262144
Whole well area mean fluorescence	Circular well area	86969
Whole larval-specific mean fluorescence	Larval body area	Approx. 11600
Top 600 larval-specific pixel mean fluorescence	Top 600 brightest pixels within larval-specific area	600
Top 300 larval-specific pixel mean fluorescence	Top 300 brightest pixels within larval-specific area	300
Top 100 larval-specific pixel mean fluorescence	Top 100 brightest pixels within larval-specific area	100

After automated image acquisition of the estrogen-exposed ERE:GFP:Casper model using the ArrayScan II, a series of custom Python masking and pixel thresholding strategies were applied to quantify larval-specific fluorescence from the automatically-generated ArrayScan images (summarised in Table 2.1).

6 custom Python masking strategies were applied to the GFP-channel ArrayScan images and their output pixel information compared to assess relative dose-response sensitivities and the fluorescence intensity variability for larval-specific intensity data quantification of each approach.

Before any fluorescence data was collated and output for analysis, all images were manually 'accepted' or 'rejected' via the online interface (<http://pubs.acs.org/doi/abs/10.1021/acs.est.6b01243>) (Figure 2.3.). Images rejected at the verification stage were not used for fluorescence intensity data extraction, whereas images accepted at the verification stage were used for subsequent fluorescence intensity data quantification at the 6 levels of fluorescence data extraction (listed in Table 2.1.).

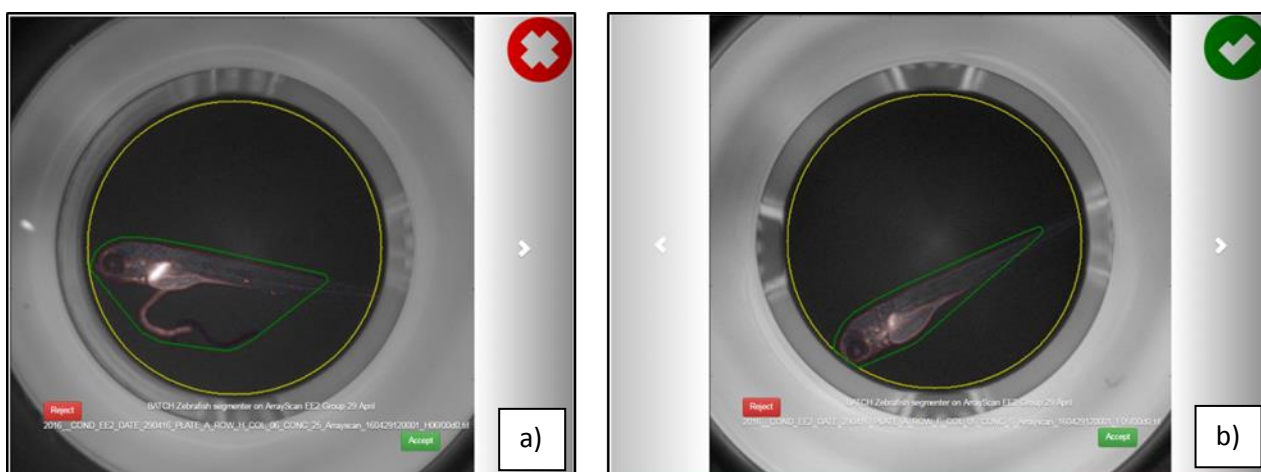
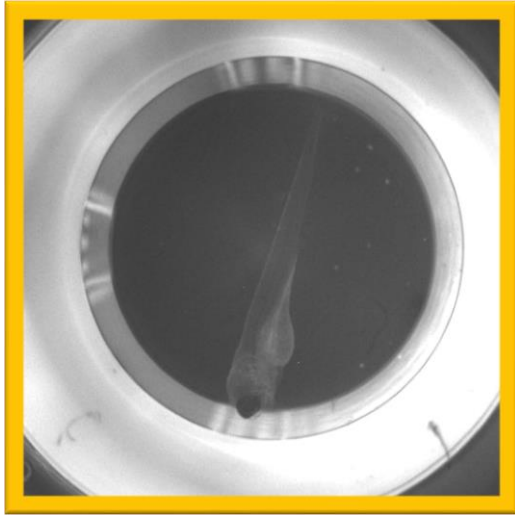


Figure 2.3. Screenshots of the online image verification interface, demonstrating examples of: a) larval outline incorrectly identified (green line) due to presence of autofluorescent artefact; b) correctly identified larval outline (larval body tightly delineated by green line).

After uploading the ArrayScan images to the online interface, a custom-designed Python algorithm was run which first extracted the average pixel value of the entire image (see Masking approach 1.). Next, the algorithm searched for and identified the circular outline of the well edge, using a series of circular Hough transforms to detect the location and size of the well. Once the circular perimeter of the well had been identified (see Masking approach 2.), the image was filtered using a median filter and the background subtracted (this reduced noise and background gradients, respectively).

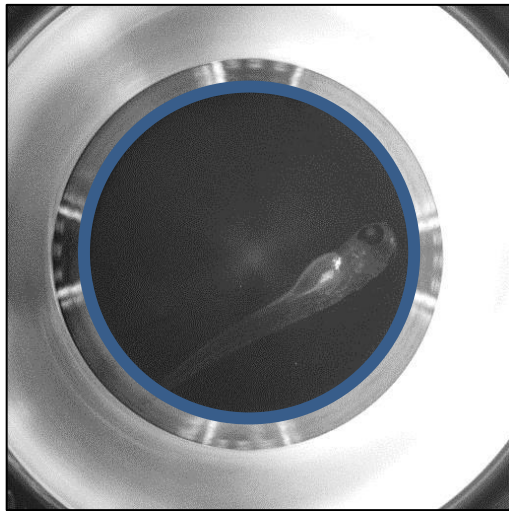
The resulting filtered image was next passed through a Sobel edge detection algorithm and median-absolute-deviation thresholding applied to pick out the image edges. A distance transform was subsequently used to grow the edges (closing any small gaps in the outline), after which, the largest contiguous region was selected as representing the larval outline. The full larval mask was then calculated as the convex hull of the outline image and the average pixel intensity contained within this larval-specific area was output (see Masking approach 3.).

The next three approaches involved the algorithm isolating and ranking the brightest 600, 300 and 100 pixels contained within the delineated larval-specific outline, before averaging and outputting the respective mean intensity values at each level of thresholding (see Filtering approaches: 1, 2, 3).



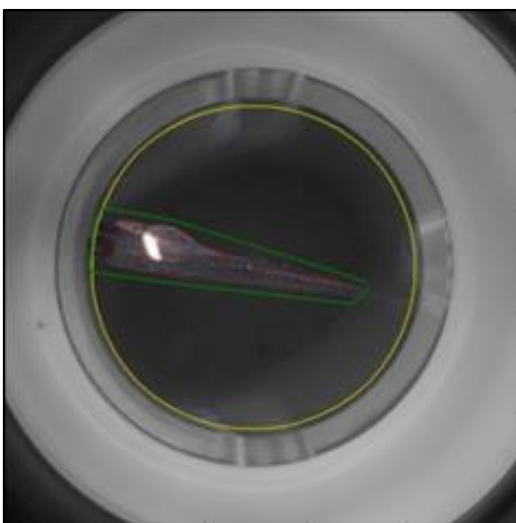
Masking approach 1: Whole-image mean fluorescence

Without any masking protocol, the algorithm averaged the fluorescence intensity value across all image pixels - outlined within yellow box.





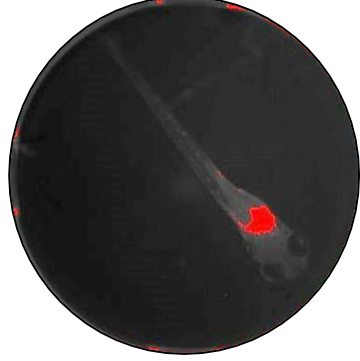
Masking approach 2: Whole-well area mean fluorescence

The crudest masking procedure carried-out by the algorithm identified the circular edge of the well and averaged pixel intensity across the whole imaged well-area (outlined by blue circle). This contained both the larva and its background/bottom of the well.



Masking approach 3: Whole larval-specific mean fluorescence

The next level of masking located the larva within the well and applied a mask around its outline (green outline) before averaging fluorescence intensity across the pixels contained within this area.

Filter 1: Top-100 Pixel Filter	Filter 2: Top-300 Pixel Filter	Filter 3: Top-600 Pixel Filter
		

2.8 Filtering approaches: mean Top-100/300/600 pixel filtering

After the application of the larval-specific outline, the final levels of image processing isolated, extracted and output the mean intensity values of the Top-100, -300 and -600 pixels within the larval body area (pixels highlighted in red). The Top-600 pixels (see Filter 3.) were chosen as the upper thresholding limit as sensitivity of the extracted fluorescence data became significantly limited at this level, with pixel filtering representing the limiting factor. The mean Top-100 pixels (see Filter 1.) were used as the lower thresholding limit as further decreasing the pixel number from which intensity data was extracted made no significant improvement to sensitivity.

The output ArrayScan fluorescence value image data was collated in Microsoft Excel, with each larval response mapped into a well of a virtual well plate corresponding with the 96-well optiplate in which the animal was imaged (Figure 3.4.). A separate heatmap was generated for each level of data extraction for every data set. The virtual well plate was a colour-coded heatmap ascending from green-yellow-red according to pixel values. This conditional formatting feature allowed for quick visual identification of potential extreme outliers (i.e., unresponsive larvae lacking the estrogen-responsive element), maximum and minimum larval responses (highlighted in red and yellow, respectively) and trends in responses across the dosing range and plate itself. The virtual plate heatmap provided a second level of verification, during which within-plate extreme outliers

(i.e. any major pipetting errors or EE2-exposed unresponsive animals with GFP responses at the same level of the control animals) could be discarded from data collation.

96 Well Optical Plate:														
	1	2	3	4	5	6	7	8	9	10	11	12		
A													Blank	Means/conc.
B	0	1	1	1	1	1	1	1	1	1	1	1	Iso Water	0.92
C	2	2	2	2	2	2	2	2	2	2	2	2	DMSO	2.00
D	3	3	3	3	3	3	3	3	3	3	3	3	1ng/l EE2	3.00
E	4	4	4	4	4	4	4	4	4	4	4	4	2.5ng/l EE2	4.00
F	5	5	5	5	5	5	5	5	5	5	5	5	5ng/l EE2	5.00
G	6	6	6	6	6	6	6	6	6	6	6	6	10ng/l EE2	6.00
H	7	7	7	7	7	7	7	7	7	7	7	8	25ng/l EE2	7.08
Key:	Min.												Max.	
	1	2	3	4	5	6	7	8	9	10	11	12		
	0	Lowest ranked pixel value												
	8	Highest ranked pixel value												

Figure 2.4. Example of virtual Excel 96-well plate colour-coded heatmap with values mapped directly from corresponding wells of the ArrayScanned optiplate for quick visual identification of outliers, trends and anomalies. Highest and lowest ranked pixel value cells highlighted for rapid visual confirmation of dose-response orientation.

Chapter 3

Realising the Potential of a Medium-Throughput Semi-Automated Bioimaging Assay for the Qualification and Quantification of Estrogen-Induced Fluorescence Response in a Transgenic Zebrafish Model.



Chapter 3.

Realising the potential of a medium-throughput semi-automated bioimaging assay for the qualification and quantification of estrogen-induced fluorescence response in a transgenic zebrafish model

3.1 Introduction

There is a need to generate models capable of visualising receptor responses across multiple organs, in real-time, at exposure concentrations that are consistent with environmentally measured levels and known to produce adverse effects (i.e., at the low ng/L). Furthermore, such tools need to be amenable to high-throughput screening in order to provide the numbers allowing the generation of statistically meaningful data (high number of replicates), for dose-dependent assessments and to study temporal change.

Such requirements have led to the development of several transgenic zebrafish models for the quantification of responses to estrogenic endocrine disrupting chemicals (EEDCs) and identification of potential adverse effects, as discussed in Chapter 1. (Brion et al., 2012; Chen et al., 2010; Gorelick & Halpern, 2011; Lee et al., 2012). Estrogen-responsive transgenic zebrafish models offer greater insight into which EEDCs might be capable of inducing responses within animals and humans, to what extent, at which concentrations, and within which specific target organs.

Green et al. (2016) further enhanced the sensitivity of the ERE:EGFP zebrafish model (developed by Lee et al., 2012) by crossing it with a pigment-free Casper line, generating an estrogen-responsive and highly-translucent ERE:EGFP:Casper model. The model was subject to high-content target tissue analysis to ascertain the lowest concentrations at which GFP responses could be detected for a range of EEDCs. Expression of GFP was reported in individual liver cells at EE2 exposure concentrations as low as 1ng/L using confocal imaging (Nikon AIR) at 4x magnification under consistent “GFP” laser excitation. The authors also used a customised plate-reader ArrayScan system (Cellomics, Inc., Pittsburgh, PA) at x1.25 magnification (Olympus) to carry out semi-automated higher-throughput

screening for the quantification of GFP responses to a range of known EEDCs, including EE2, using 5 days post-fertilization (dpf) ERE:EGFP:Casper larvae. Here, the observed lowest significant response (LSR: lowest exposure concentrations that elicited a fluorescence response significantly higher than that of controls) in the larval fish was found for an EE2 concentration of 5ng/L and 10 ng/L. The semi-automated ArrayScan system was effectively 5-10 times less sensitive than the low-throughput confocal approach.

The authors suggested improved sensitivity could be partly achieved by uniformly orientating the larvae and improving image masking for the qualification and quantification at the specific tissue level. The aim of these proposed improvements was to remove interfering autofluorescence and establish organ-specific GFP expression patterns in response to various EEDCs in a rapid, higher-throughput and semi-automated way. In this study, we investigated a range of image masking algorithms and pixel filters to establish the image acquisition approach which would generate the most sensitive data whilst also minimising fluorescence intensity variation between images that might be introduced by non-uniform larval orientation.

Improving receptor-GFP signal-to-noise ratio at the larval individual-level is one approach to increasing sensitivity, but there is also a need to improve inter- and intra-assay variability. This would allow statistically significant responses to be detected at lower exposure concentrations, and potentially using fewer animals, which is also beneficial from both practical and ethical perspectives. Consistency can be improved in a number of ways including the use of a more standardised experimental protocol and by staging embryos so that they are at the same developmental point at the time of initial exposure, in addition to using eggs from a single brood pair to (in principle) minimise genetic variation. These approaches have been adopted within the study described in this chapter.

Substantial research has indicated that genetic variation has a significant effect on many phenotypic endpoints (Barata et al., 2000; Nowak et al., 2007). Genetic variation of laboratory strains of zebrafish and wild fish were compared, with considerably less variability being found in samples of commonly used laboratory fish (Coe et al., 2008). This reduced genetic variation may affect responses to

chemical exposures seen in laboratory zebrafish studies and could potentially improve the sensitivity of the ArrayScan approach. We compared responses to EE2 in the ERE:GFP Casper for both pair- and group-spawned embryos, the former of which we predicted would limit genetic variation and hence provide a less variable EE2 dose-response. This chapter investigates the above, considering the variation in responses to estrogen for fish derived from group-spawning fish and pair-spawning fish (the former having the likelihood of greater genetic variation than the latter in the embryos collected for analysis).

The estrogen chosen for this work was the synthetic estrogenic compound 17 α -ethynylestradiol (EE2). EE2 has received much attention in recent years. Found in nearly all formulations of the oral contraceptive pill, EE2 has a binding affinity for the human estrogen receptor (ER) of one to two times higher than its natural analogue, 17 β -estradiol (E2) (Shyu et al., 2011). In some species of fish, this receptor affinity has been shown to be up to five times higher, meaning that EE2 can elicit estrogenic responses at very low (ng/L) concentrations (Laganà et al., 2000; Lima et al., 2012; Mazellier et al., 2008; Saaristo et al., 2009; Tomšíková et al., 2012). It is also clear that many estrogenic effects are observed in the low to sub-ng/L concentration range (reviewed in Aris et al., 2014).

A range of adverse outcomes in response to low-level EE2 exposure have been established in zebrafish (*Danio rerio*). For example, significant female-biased alterations have been reported in juvenile zebrafish sex ratios at 1ng/L, with a complete sex reversal at 2ng/L EE2 (Orn et al., 2003); and significantly abnormal testicular morphology, plus the presence of oocytes in the gonads of male zebrafish, have been observed at exposure levels of 2ng/L EE2 (Xu et al., 2008). At the behavioural level, dominant male zebrafish exposed to 0.5ng/L EE2 for either 6 days or 48 hours at varying concentrations (0.5, 5, and 50ng/L EE2) exhibited a decreased frequency of courtship-specific behaviour towards females and aggressiveness towards rival males (Colman et al., 2009).

Additional observed deleterious effects in fish species elicited by EE2 exposures of 5ng/L or less include: a high incidence of deformities and significant reduction in the body length and weight of the Chinese rare minnow (*Gobiocypris rarus*) at 4ng/L EE2 (Zha et al., 2008); modulation of hormone receptors and signalling

pathways in juvenile Atlantic salmon (*Salmo salar*) at 5ng/L (Mortensen & Arukwe, 2007); and a 650-fold increase in vitellogenin gene expression in Gilthead seabream (*Sparus aurata*) at 5ng/L (Cabas et al., 2012). Suppressed testicular *esr1* mRNA expression has been reported in two-month-old male *Paramisgurnus dabryanus* at EE2 exposures of 1, 5 and 25ng/L, while ovarian *esr2a* mRNA expression was significantly elevated in the brains of females at 1ng/L EE2 (Zhang et al., 2013). At concentrations as low as 1ng/L EE2, a negative impact on the complex and lengthy mating behaviour of Gulf pipefish (*Syngnathus scovelli*) was observed, caused by a reduction in the perceived attractiveness of male fish to females (Partridge et al., 2010).

In terms of the environment, EE2 has been measured at concentrations as high as: 42ng/L in a Canadian sewage affluent (Ternes et al., 1999); 831ng/L in an investigation of US streams (Kolpin et al., 2002); and 25ng/L in a study of Brazilian surface waters (Sodré et al., 2010). However, throughout Europe the reported EE2 levels have generally been lower: typically ranging from 0.5ng/L up to 15ng/L (Belfroid et al., 1999; Desbrow et al., 1998; Johnson et al., 2000; Svenson et al., 2003; Ternes et al., 1999) in both effluents and surface waters.

In this chapter, responses to EE2 in the ERE:GFP:Casper for both pair- and group-spawned embryos were compared. We predicted that embryos derived from pair-breeding fish (i.e. the embryos derived from a single female) would provide less variable responses as an experimental cohort (exposed to EE2) compared with embryos derived from a group of spawning females.

3.2 Materials and Methods

3.2.1 Generation of embryos

3.2.1.1 Pair-spawned embryos

Pair-spawned embryos were generated by selecting 10-12 crosses of randomly paired male and female adults (sexed by eye) and netting them directly from stock tanks into clean transparent 1-litre plastic spawning chambers (Techniplast) filled with rig water to within a half-inch of the top of the tanks. This procedure was

carried out ~45 minutes after the final feeding of the day, ensuring that all fish had had an opportunity to feed. The screened insert of the spawning chambers were half-covered in a layer of marbles that prevented the adult fish from predated on their eggs, and have also been shown to mimic the gravel preferred spawning substrate of females (Spence et al., 2007). Lids were placed on the spawning chambers and they were labelled in accordance with local and Home Office regulations.

Spawning chambers were kept in a temperature controlled room at $28\pm 1^{\circ}\text{C}$, overnight on a 12:12 hour light:dark 30 minute phased-change light cycle. Approximately 1 hour after the lights came on the following day, and prior to morning feeding, adult fish were transferred back to their original tanks. The screened insert of the spawning chamber was removed and water siphoned through an embryo-collecting screen to retain any eggs. Eggs were then carefully rinsed using rig water to remove any scales, faeces or other debris, and transferred to clean, labelled Petri dishes (Greiner 94 x 16 mm, with vents) filled with fresh rig water. Eggs were subsequently examined under a dissecting microscope to sort fertilised from unviable embryos, before being pipetted into fresh rig water and inspected regularly for normal development.

3.2.1.2 Group-spawned embryos

Group-spawned embryos were generated by putting small (DuraCross™, dimensions: 8"L x 4"W x 3"H) spawning chambers into the stock tanks of 50-80 sexually mature fish at least 45 minutes after the final feed. The removable perforated insert of the chambers were partially covered with a layer of marbles, and imitation plastic plants were placed in the traps to provide artificial spawning sites. The following morning, spawning chambers were removed from stock tanks, the perforated screen removed, and water in the collection tank siphoned through an embryo-collecting screen. Eggs were rinsed with rig water and then pooled (with at least two other batches of random size) in a labelled Petri dish. This approach ensured that a randomised assortment of eggs from a variety of spawning events by different parent fish had been obtained. Eggs were inspected regularly for mortality or fungal infection using a dissection microscope, and viable eggs pipetted out into fresh rig water in readiness for staging and chemical exposure.

Minimally, 72 viable embryos were required per pool of group-spawned eggs, and per pair-spawning event, to ensure sufficient numbers survived until dosing stage – ideally, sufficient numbers of embryos would survive until the imaging stage (providing 12 animals per concentration).

3.2.2 Staging of embryos and larvae

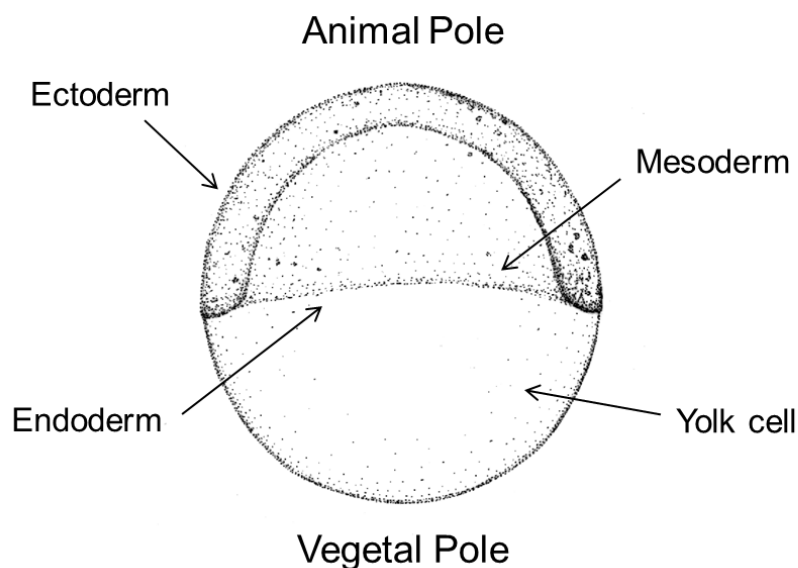


Figure 3.1. Germ-ring stage (5²/₃ hours)

(Source: modified from https://zfin.org/zf_info/zfbook/stages/figs/fig1.html [accessed 2016])

Following collection and sorting, embryos were stored in rig water at 28±1°C and checked regularly under a dissection microscope until the majority (>80%) had reached the clearly-definable 5²/₃ hour germ-ring development stage (described by Kimmel et al., 1995; see Figure 3.1.). This was done to ensure optimal developmental synchronicity and to minimise the influence of natural variation between animal exposure responses. The germ-ring stage can be distinguished as the point at which the germ-ring forms as a thickened annulus at the blastoderm margin when viewed from the animal-polar angle. Embryos remain at this stage for ~20 minutes before entering the shield stage at ~6 hours. The germ-

ring stage therefore represented a convenient, easily-identifiable developmental stage and time-window for simultaneously staged exposure. Embryos were arrayed via manual pipetting in labelled 24-well plates (Greiner CELLSTAR® 24 Well Cell Culture Plate), with one embryo per well transferred in 200µL rig water, and exposed to 800µL of test or control solutions up until 4dpf.

3.2.3 Preparation of exposure solutions

3.2.3.1 Stock chemical preparation

17 α -ethinylestradiol (EE2, CAS no. 57-63-6, Sigma-Aldrich Chemical Co. ($\geq 98\%$)) was selected as the chemical for standardising and validating this assay due to its environmental relevance and its high binding affinity for all piscine ER subtypes (Shyu et al., 2011). The primary EE2 stock solution was prepared by dissolving 2.09mg in 1.672ml of dimethyl sulfoxide (DMSO, molecular biology grade), to give a 1250000µg/L stock solution (kept refrigerated at 2-8°C between experiments).

3.2.3.2 Working solution preparation

A working solution of EE2 was prepared by dilution of 100µl of stock into 900µl DMSO in a microcentrifuge tube (Eppendorf, 2ml) to give 1ml x 125000µg/L dilution. Further working solutions of EE2 were prepared by serial dilution of 100µl into 900µl DMSO in 4 x 2ml microcentrifuge tubes until a concentration of 12.5µg/L EE2/DMSO was obtained. Solutions were kept refrigerated at 2-8 °C until needed, when they were thawed at room temperature (28 \pm 1°C) before use.

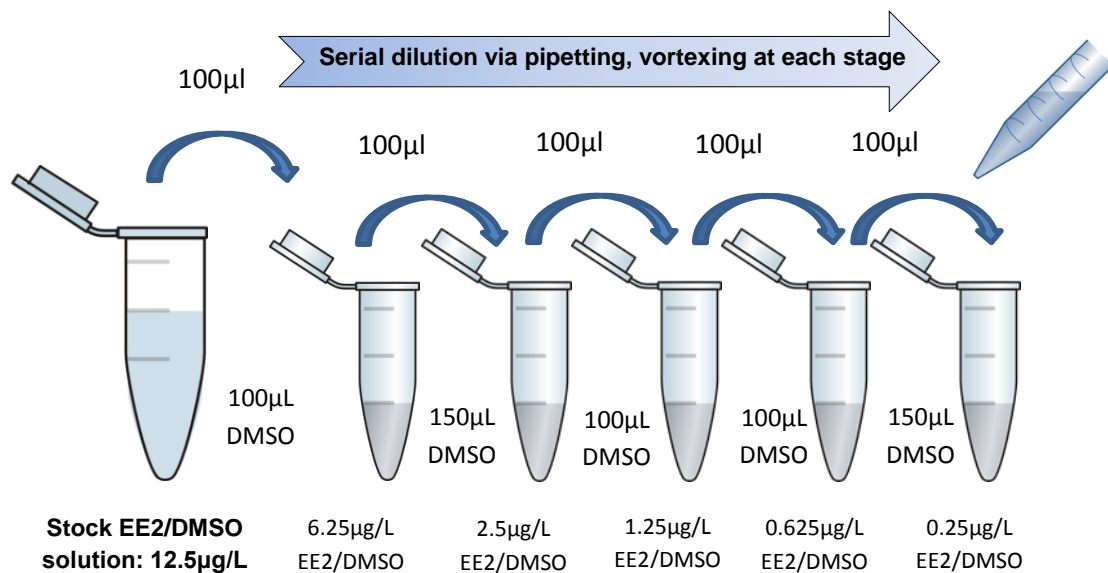


Figure 3.2. Serial dilution and vortex-mixing of the 1.25g/L stock EE2/DMSO solution in DMSO to give progressively more dilute working solutions.

The 12.5 µg/L concentrated EE2/DMSO solution was then further serially diluted (after thawing at room temperature $28 \pm 1^\circ\text{C}$) on the day of each assay (see Figure 3.2. for volumes) to give final working solutions of 6.25, 2.5, 1.25, 0.625 and 0.25 µg/L EE2/DMSO. Each new solution was vortex-mixed for ~ 10s after each stage of pipetting to ensure thorough dilution.

3.2.3.3 Dosing solution preparation

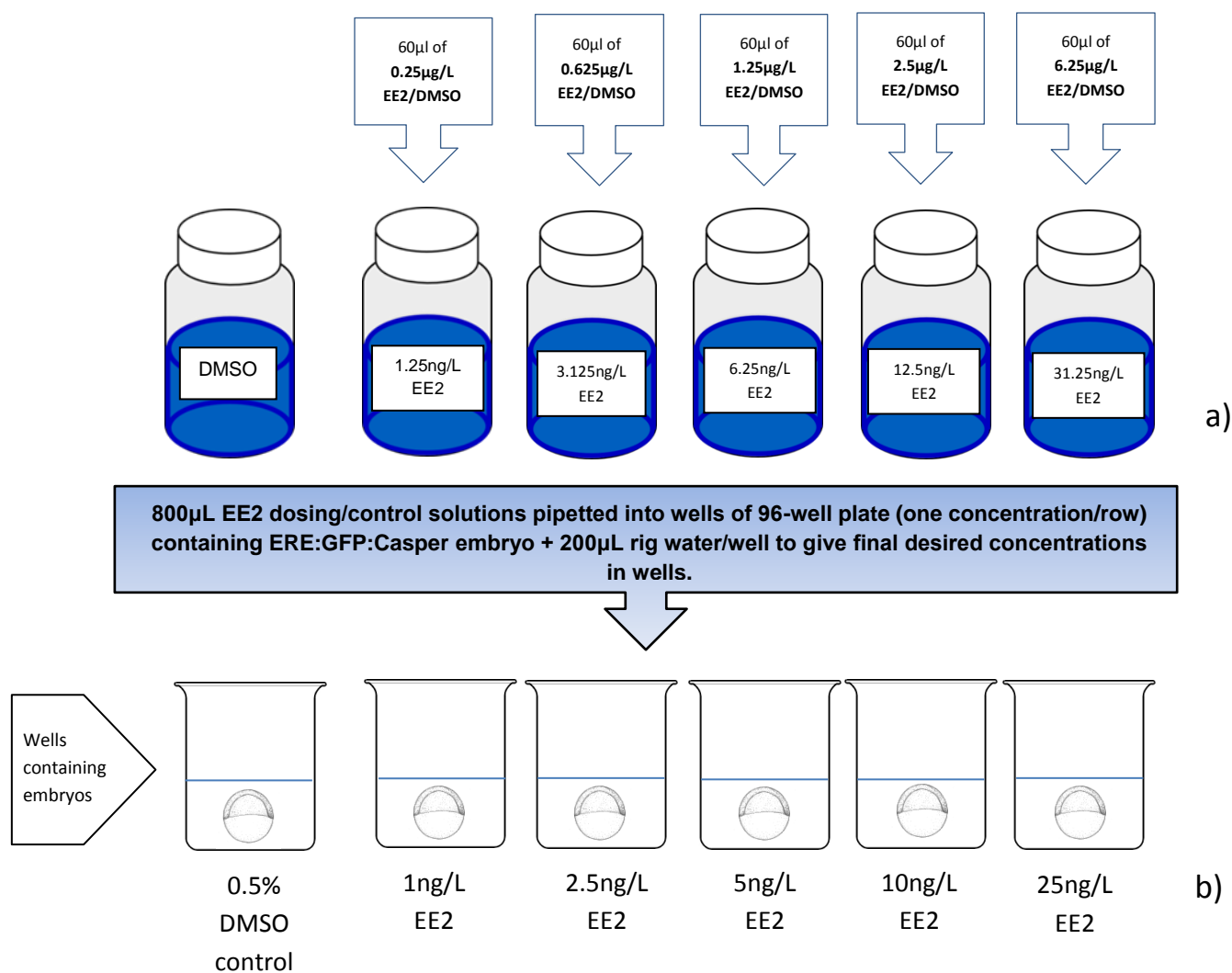


Figure 3.3. a) Dilution of 60 µL working EE2 solutions into glass vials of 10 ml rig water to give 1.25x dosing solutions; b) Final stage dilution of 800 µL of the 125% dosing solutions in plate wells containing 200 µL rig water to give final 1, 2.5, 5, 10 and 25 ng/L EE2/DMSO concentrations. 0.5% DMSO vehicle control in wells diluted down from 0.625% DMSO in rig water.

Dosing solutions were prepared from each working solution by pipetting 60 µL of each solution into 10 ml fresh rig water in 5 x 28 ml glass vials, which were subsequently mixed thoroughly on a magnetic stirrer for ≥ 10 minutes. These solutions were freshly prepared on each day of exposure to provide working solutions which were 125% of the final desired well concentration: 1.25, 3.125, 6.25, 12.5, and 31.25 ng/L (Figure 3.3.).

3.2.3.3 Dosing solutions in the wells

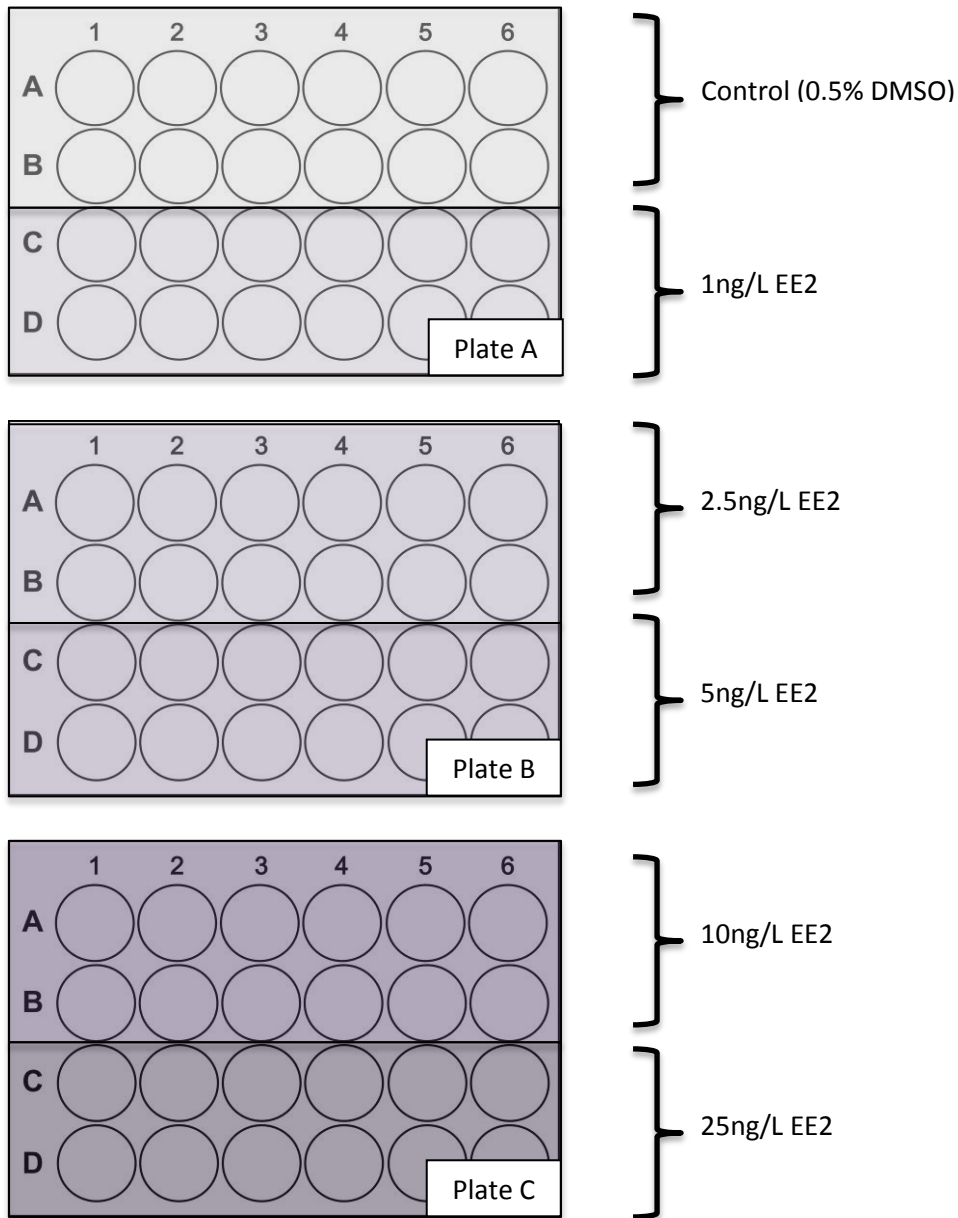


Figure 3.4. 24-well exposure plate layout consisting of one embryo per plate well in EE2 and vehicle control solutions. Plates containing embryos were stored at $28\pm 1^\circ\text{C}$ for an exposure period of 4 days prior to imaging.

800 μL of each dosing solution was then pipetted into each well of three labelled 24-well plates (2 concentrations per plate, see Figure 3.4. for plate layout) in which embryos had been pre-arrayed in 200 μL rig water/well. This resulted in 1ml of the final nominal desired EE2 concentrations in rig water per well. Stock solutions of vehicle control/DMSO media were diluted with rig water to give a final 0.5% DMSO concentration in the well for the vehicle control dosing solution. The

embryos were exposed from 5.7 to 96 hpf, being maintained at a constant temperature of $28\pm 1^\circ\text{C}$ under a 12:12 hour light:dark 30 minute phased-change light cycle with no media changes.

3.2.4 ArrayScan imaging

Following the 4-day exposure, at 96 hpf, all larvae were transferred in $100\mu\text{L}$ well-solution (using a manual pipette and wide bore tips) from the 24-well dosing plates into corresponding wells of fresh 24-well plates containing tricaine solution (0.04% in rig water). Each larva was anaesthetised for ≥ 5 minutes at $28\pm 1^\circ\text{C}$. The 12 larvae allocated to each concentration were then transferred by manual pipette in $50\mu\text{L}$ of anaesthetic solution (to ensure they remained immobile during image acquisition) into the wells of a 96-well optiplate (Corning® 96 well plates, half-area clear polystyrene wells flat bottom), 12 larvae per concentration, per row. The top row (wells A1-A12) of the 96-well plate were blank, rig water-only controls ($50\mu\text{L}/\text{well}$), imaged to check that fluorescent imaging settings remained consistent between ArrayScan runs.

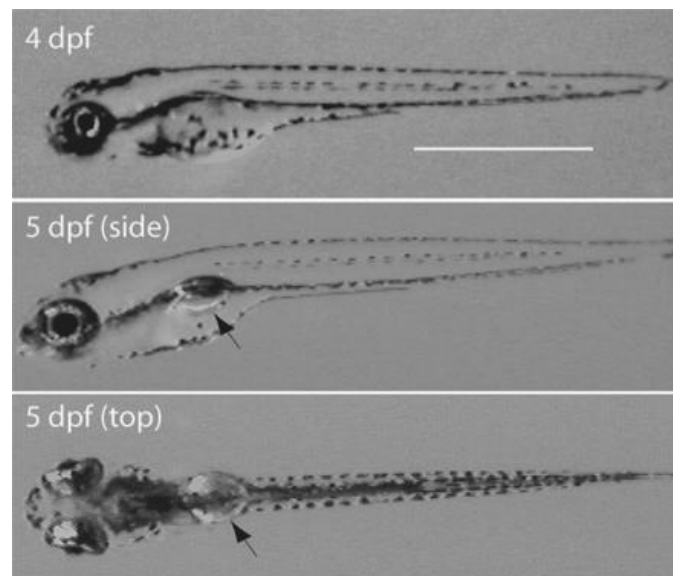


Figure 3.5. Images of 4 and 5 dpf zebrafish larvae. The swimbladder has inflated and is visible in 5 dpf larva (arrows), but not in the 4 dpf larva. Scale bar, 1 mm. (Source: Zeddies & Fay, 2005)

Larvae were imaged at 4 dpf (Figure 3.5.) as this was the point at which most of the major internal organs – including the heart, kidney, liver and intestine – were fully developed (Westerfield, 1995). This stage of development is comparable to that of three months of development in the human embryo (Parng et al., 2004). The inflation of the swim bladder (Figure 4.5.) at 96-120 hpf via air-gulping (Goolish & Okutake, 1999; Winata et al., 2009) may also have obstructed and increased variation of detected fluorescence.

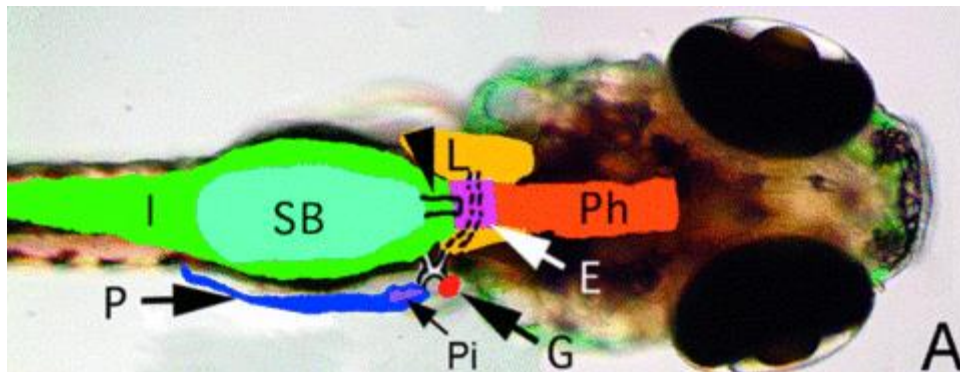


Figure 3.6. Larval zebrafish digestive system anatomy. Overlay outlines the liver (L) in yellow. (Source: <https://zfin.org/action/figure/all-figure-view/ZDB-PUB-030312-8> accessed: 2017)

Previous research has shown the liver to be the most sensitive organ in the ERE:GFP model in response to EE2: using confocal microscopy, a dose of 1ng/L EE2 was reported to induce a GFP response in larval liver cells of the ERE:GFP:Casper (Lee et al., 2012). The teleost fish liver consists of two lobes, the left of which is bigger and spreads through most of the corporeal cavity (Vicentini et al., 2005) (Figure 3.6.). Therefore, it seemed likely that consistently imaging larvae laterally, orientated left-side facing the objective, would generate more sensitive and robust fluorescence data in response to EE2. We compared a selection of uniformly-orientated EE2-exposed larval responses with the same number of randomly-orientated larvae to assess whether orientation had any influence on the sensitivity and reproducibility of the fluorescence intensity data.

3.2.5 Zeiss imaging comparison

A direct comparison of acquisition time, sensitivity and variation in quantified fluorescence was made between the automated ArrayScan system and a manual inverted compound microscope (Zeiss Axio Observer) using the same x1.25 level of magnification and consistent GFP excitation (180 ms using filter set 38 HE: BP 470/40, FT 495, BP 525/50). Anaesthetised larvae were taken off the ArrayScan and uniformly embedded individually on their left sides in 0.7% low melting agarose (Sigma-Aldrich, CAS: 39346-81-1) plus rig water on glass slides within circular silicon isolators (to mimic the circular 96-well plate well walls that the image analysis algorithm identified, see Figure 3.7.). The objective was then manually focussed on each larva, and a GFP and brightfield image acquired for each individual animal. The images were later uploaded to the interface and accepted or rejected based on the accuracy of the automated larval masking algorithm in the same manner as the ArrayScan images.

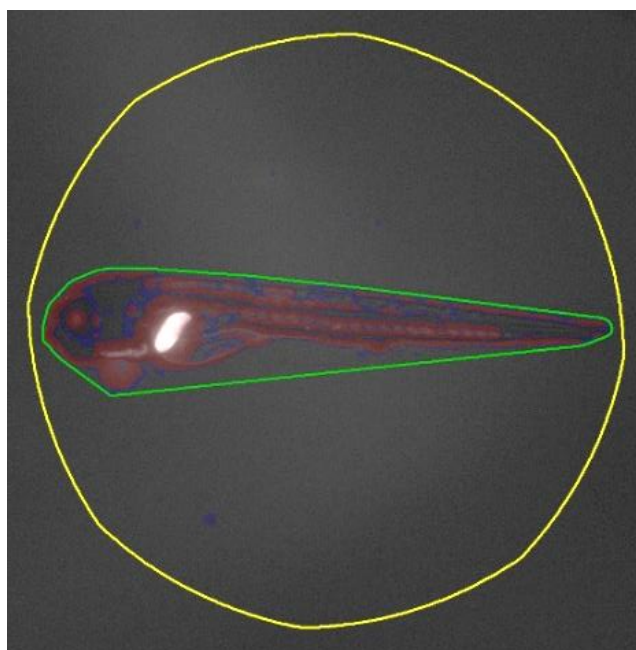


Figure 3.7. Manually embedded and laterally-orientated EE2-exposed larvae captured using the Zeiss inverted compound microscope and identified using the online image analysis interface.

3.2.6 Comparison of laterally- vs. variably-orientated EE2-exposed larval fluorescence responses

The larval masking algorithm outlines and extracts fluorescence intensity data from larvae of varying orientations across a singular run (Figure 3.8.), incorporating a wide range of fluorescence variation between individual larvae, even within a single dose condition. Previous research has shown the liver to be the most sensitive organ in the ERE:GFP model in response to EE2 (Green et al., 2016). Taking the left-side biased positioning of the fish liver into consideration, it was assumed that uniform lateral orientation of the larvae would generate more robust and sensitive fluorescence data, as this perspective provided the most unobstructed view of the EE2-responsive organ.

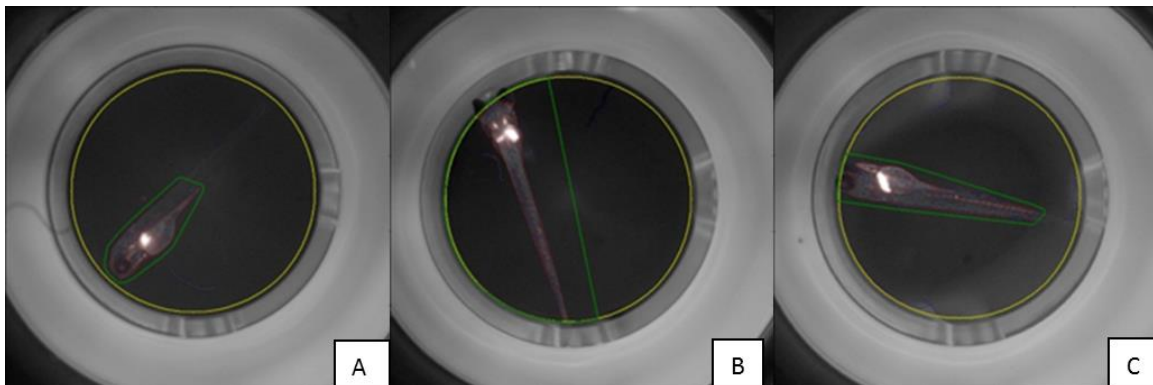


Figure 3.8. Different larval orientations captured by ArrayScan across a single run (10ng/L EE2).

ArrayScan images of laterally-orientated, left side-down, pair-spawned EE2-exposed larvae from 4 datasets (~55 larvae/orientation) were hand-selected from the online interface and compared with randomly-selected, variably-orientated larvae from the same exposure plates in order to compare sensitivity and variability.

3.2.7 Identification of extreme outliers

Virtual Excel 96-well plate colour-coded heatmaps with values mapped directly from corresponding wells of the ArrayScanned optiplate were used to allow quick visual identification of extreme outliers within and between 96-well plates. Image data was then re-examined on a case-by-case basis and individual images discarded from data if an obvious anomaly could be detected before being included in statistical analysis. Criteria for image exclusion comprised of artefacts within the well, larvae which had failed to develop or abnormal larvae damaged by manual pipetting. Only images with visually apparent anomalies were excluded.

3.2.8 Statistical analysis

Fluorescence intensity values were averaged across EE2 concentrations for eight repeated ArrayScan runs per clutch-type (pair- and group-spawned). Group-spawned larval responses alone were used to compare the sensitivity and robustness of the six different levels of masking. Pair-spawned larval responses were quantified to establish whether the sensitivity of the assay could be further improved by reducing the influence of genetic diversity. All values were presented as mean \pm SEM with statistical significance indicated at the $p < 0.05$ (*) or < 0.01 (**) level using ANOVA and the Games-Howell post-hoc test to calculate LSMs and the Mann-Whitney U test to compare differences between two groups as a third level of between-group verification. Fluorescence response robustness at a given dose concentration was calculated using relative standard deviation (%RSD) and stated as \pm 'x' % about the mean.

3.3 Results

3.3.1 Sensitivity vs. robustness of different semi-automated ArrayScan image analysis masking and pixel thresholding strategies

It took approximately 1.5 hours for the ArrayScan system to automatically acquire one fluorescent image/well of a full 96-well plate containing EE2-exposed larvae. The automated algorithm correctly identified the larval outline in ~80-90% of the ArrayScan images, meaning that they could be 'accepted' using the manual verification interface. Poorly orientated larvae, or images containing artefacts (such as dust), were often incorrectly masked by the automated system and were manually 'rejected' at the verification stage. Each level of masking was analysed according to its LSR (the lowest concentration at which an EE2 dose was found to elicit a fluorescence response significantly higher than control) and robustness – calculated as relative standard deviation percentage (%RSD). Verified ArrayScan images taken from 8 pooled datasets of group-spawned EE2-exposed larvae were collated before being processed using the 6 different intensity data extraction approaches to assess sensitivity and robustness of each output.

3.3.1.1 Whole-image/no masking approach

For the whole-image/no mask approach, mean pixel intensity was plotted against the standardised EE2 concentration range (Figure 3.9.). Lack of any significant difference observed between the dosing conditions and their respective fluorescence responses indicated that the bright fluorescence reflected by the surface of the plate itself was attenuating the larval-specific EE2-induced GFP signal.

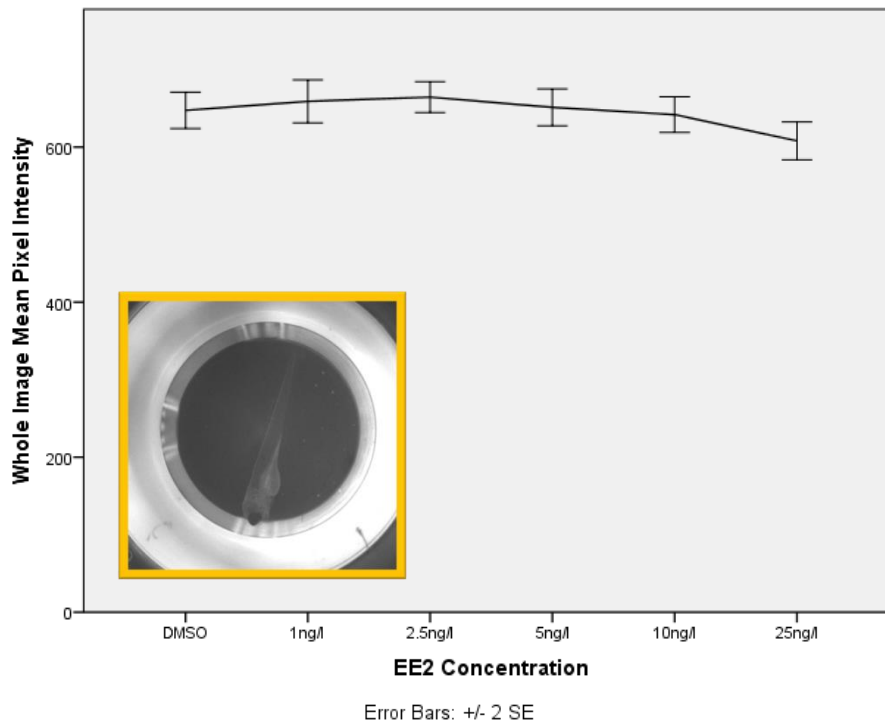


Figure 3.9. Whole image area mean pixel fluorescence intensity for ArrayScan imaged EE2-exposed larvae ($N=369$) reported as mean \pm 2SEM. Inset image demonstrating image area from which pixel intensity values extracted and subsequently averaged across (inset image, yellow box).

The Excel heatmapped virtual plate of whole-image fluorescence data (Figure 3.10.) also indicated the contribution of fluorescence interference from neighbouring larval GFP responses through the transparent well walls: wells with fewer neighbours at the plate extremities had lower pixel values regardless of EE2 concentration and larval response. Larval-specific responses were completely obscured by plate surface fluorescence reflection in addition to the large area across which the pixels were averaged.

96 Well Optical Plate:														
	1	2	3	4	5	6	7	8	9	10	11	12		
A													Blank	Means/conc.
B	620.1252	X	685.3265	675.0396	681.7267	659.9782	662.2116	657.5856	665.9619	646.9819	X	627.0664	Iso Water	658.20
C	631.0088	681.7856	690.7272	712.0012	693.8381	707.2599	643.6559	X	X	667.3518	638.0767	611.8998	DMSO	667.76
D	X	680.9387	688.5884	697.346	684.701	X	658.9464	652.598	671.7507	661.0219	X	617.1023	1ng/l EE2	668.11
E	X	X	X	X	688.9608	664.7981	686.6145	644.9685	643.3262	654.1688	648.7089	605.8679	2.5ng/l EE2	654.68
F	630.5236	688.5042	702.6284	692.6176	684.7244	654.3798	X	655.8225	663.4311	692.6443	650.9322	X	5ng/l EE2	671.62
G	619.3556	668.6145	690.2514	708.0433	706.4146	656.7756	669.7429	X	668.095	663.0036	651.3102	618.8912	10ng/l EE2	665.50
H	600.0939	640.1003	656.7766	663.0508	678.0211	638.262	639.1618	636.9797	643.5752	636.0612	X	591.4846	25ng/l EE2	638.51

Figure 3.10. Example of a virtual 96-well plate heatmap of ArrayScanned EE2-dosed dataset compiled using whole-image mean fluorescence values and demonstrating fluorescence interference effects influencing pixel values at the extreme edges of the plate.

3.3.1.2 Whole-well masking approach

The well-masked mean fluorescence value extraction approach also failed to generate a dose-response curve (Figure 3.11.), but did negate the reflective influence of the well plate surface. However, larval-specific fluorescence responses were still strongly attenuated by the large pixelated area (relative to the larval mass) that pixel values were averaged across. In addition, the inclusion of any potentially autofluorescent artefacts within the well contributed to the overall dissimulation of the larval-specific GFP responses although, at the highest EE2 concentration, a slight but insignificant upward trend in the mean fluorescence intensity could be seen. Lack of any significant difference between dosing condition fluorescence responses indicated that background noise within the well, combined with the large area over which the mean pixel intensity was averaged, was attenuating the larval-specific EE2-induced GFP signal.

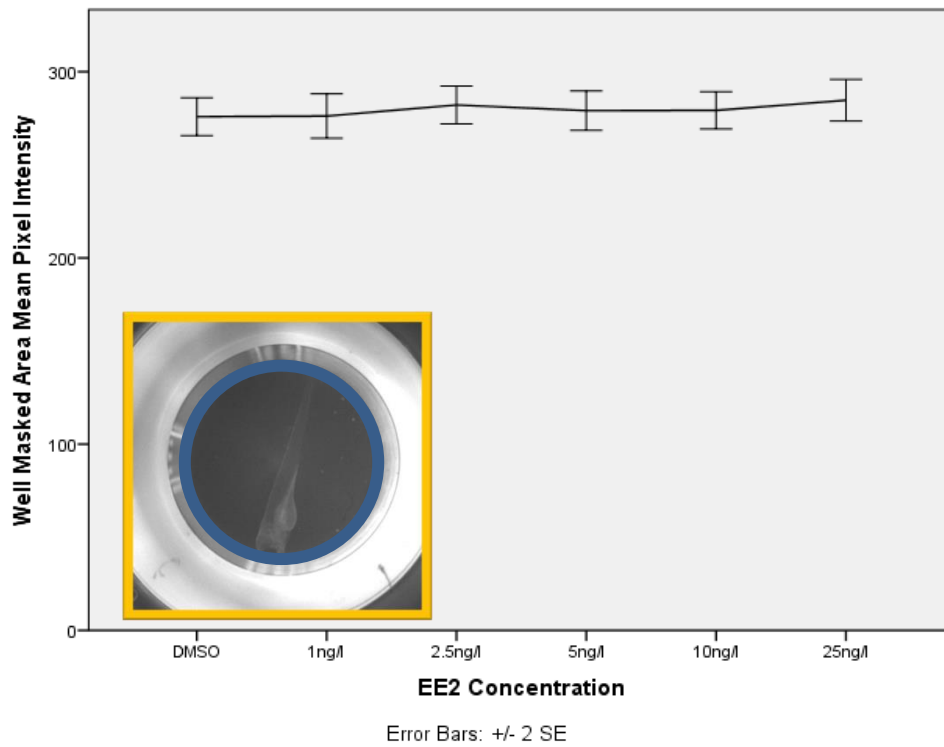


Figure 3.11. Well area mean pixel fluorescence intensity for ArrayScan-imaged EE2-exposed larvae ($N=369$) reported as mean \pm 2SEM. Inset image demonstrating masked image area from which pixel intensity values extracted and averaged across (inset image, blue circle).

The Excel heatmapped virtual plate of well-area responses (Figure 3.12.) suggested the possible inclusion of autofluorescent artefacts generating fluorescent peaks unrelated to the larvae (indicated by high fluorescence values extracted at control and low-dose exposure conditions). Low mean fluorescence intensities across the EE2 dosing range suggested attenuation of the larval-specific fluorescence being averaged across the comparatively large pixelated well area.

96 Well Optical Plate:														
	1	2	3	4	5	6	7	8	9	10	11	12		
A													Blank	Means/conc.
B	287.7367	X	298.4761	294.6936	333.2448	288.9746	285.6273	282.6536	296.1922	285.8391	X	319.1123	Iso Water	297.26
C	290.8154	299.2881	299.106	324.672	293.9942	290.551	285.4139	X	X	289.3671	290.0197	294.6799	DMSO	295.79
D	X	299.5045	295.3735	296.0811	288.6626	X	278.0453	278.2888	292.5223	289.7241	X	285.1241	1ng/l EE2	289.26
E	X	X	X	X	291.4062	280.949	277.7002	278.6671	302.1528	288.1741	281.9856	285.0463	2.5ng/l EE2	285.76
F	268.3166	293.3498	300.6836	299.1867	291.1851	284.8793	X	279.2905	293.267	339.2415	284.4719	X	5ng/l EE2	293.39
G	256.8717	287.1449	305.709	297.3204	293.5895	290.7649	292.6693	X	295.1694	292.665	292.596	295.8582	10ng/l EE2	290.94
H	282.7267	297.0815	308.7114	308.8794	348.7753	294.4859	284.6623	291.2504	302.8628	309.9327	X	284.8399	25ng/l EE2	301.29

Figure 3.12. Virtual 96-well plate heatmap of well-masked ArrayScan image data demonstrating obscured dose-dependent larval-specific fluorescent responses at all dose conditions except 25ng/L EE2.

3.3.1.3 Larval-specific masking approach

The larval-mask mean pixel value approach generated data with a fluorescent dose-response which differed significantly to the control response at the higher EE2 dose concentrations (Figure 3.13.). This elevated larval fluorescence was discernible at the 10ng/L and 25ng/L EE2 exposure conditions. The identification of the larval outline and application of a mask by the algorithm ensured that larval-specific fluorescence response data alone was extracted from the ArrayScan images. The verification stage made certain that pixel values were derived from the larval-masked area exclusively. The signal-to-noise ratio (SNR) of the mean larval-area fluorescence data was, however, attenuated by the large pixelated field used for pixel-averaging, as most of the larval body did not strongly express GFP and was thus comprised mostly of low-intensity pixels. No extreme outliers were detected in the data at this level of thresholding.

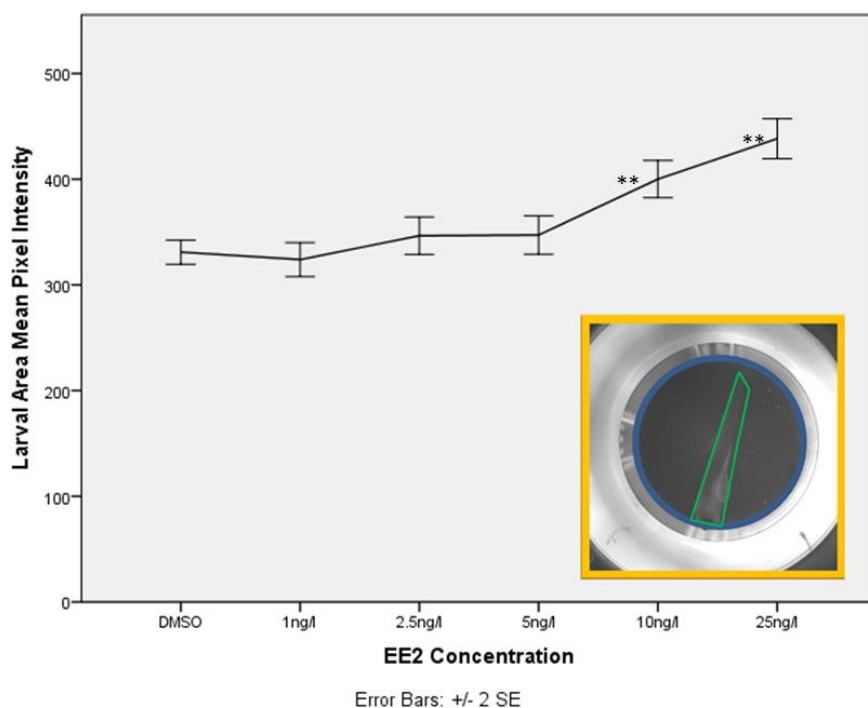


Figure 3.13. Whole-larval area mean pixel intensity for EE2-exposed ArrayScan imaged larvae (N=369), reported as mean ± 2SEM (asterisks indicate significant difference compared with DMSO control, ** p < 0.01). Inset image demonstrates larval area identified and outlined by algorithm (inset image, green line), across which pixel intensity values were extracted and averaged across.

The fluorescence/concentration averages column at the far right of the Excel heatmapped virtual plate (Figure 3.14.) showed an inflection in whole-larval fluorescence intensity responses at the higher EE2 doses (indicated by the orange and red highlighted cells). The most highly-fluorescent larvae (highlighted in red) had been exposed to the highest EE2 concentration and the least fluorescent larvae (highlighted in yellow) had been exposed to the media control.

96 Well Optical Plate:														
	1	2	3	4	5	6	7	8	9	10	11	12		Means/conc.
A													Blank	
B	341.9484	X	336.7392	350.7314	345.4066	353.6423	335.6711	341.4937	388.011	302.4398	X	320.2993	Iso Water	341.64
C	347.1419	353.2775	360.333	352.4769	338.4578	377.4638	336.6565	X	X	324.7364	338.9228	364.8398	DMSO	349.43
D	X	359.0295	368.8852	335.4923	343.0745	X	351.1419	338.459	317.8489	326.6426	X	337.4326	1ng/l EE2	342.00
E	X	X	X	X	339.8201	321.4233	336.2576	305.88	361.3922	342.4372	317.7842	390.7222	2.5ng/l EE2	339.46
F	353.1801	404.2365	352.7849	379.7295	355.2652	338.1922	X	312.169	353.9408	363.2539	329.2043	X	5ng/l EE2	354.20
G	379.4102	412.7277	409.8044	387.9794	382.6945	315.1722	370.0837	X	384.5726	424.2768	388.7766	415.3328	10ng/l EE2	388.26
H	390.3122	522.0724	461.5392	423.099	539.5434	426.7046	450.3602	415.9973	419.2929	439.6546	X	390.0286	25ng/l EE2	443.51

Figure 3.14. Virtual 96-well plate heatmap of larval-specific area fluorescence intensity data.

3.3.1.4 Top-100, -300, and -600 larval-specific pixels

The Top-100, -300 and -600 mean pixel value thresholding approaches greatly improved the SNR ratio of the fluorescence data extraction, with mean EE2-exposed larval fluorescence responses indicating significant differences to the control response at all EE2 dosing conditions above 2.5ng/L. By isolating and ranking the Top-100, -300 and -600 pixels contained within the larval-specific outline, the brightest selection of pixels were averaged across smaller respective pixelated areas, improving the SNR of the extracted fluorescence responses.

The Top-100 pixel thresholding approach culminated in a degree of pixel saturation at the higher EE2 concentrations, resulting in some loss of information regarding larval GFP response variation and the plateauing of pixel values at the highest (25ng/L) EE2 dosing condition (Figure 3.15.). Focussing on a very small pixelated area at the Top-100 thresholding level also resulted in a high degree of variation between captured larval responses, which was improved upon by averaging pixel values across a larger area (Figures 3.16. and 3.17.), thus decreasing standard error. The Top-600 pixel thresholding approach further reduced variation and improved data robustness, but began to limit the LSR point at which a significant difference between EE2-dosed larval responses and the control could be distinguished.

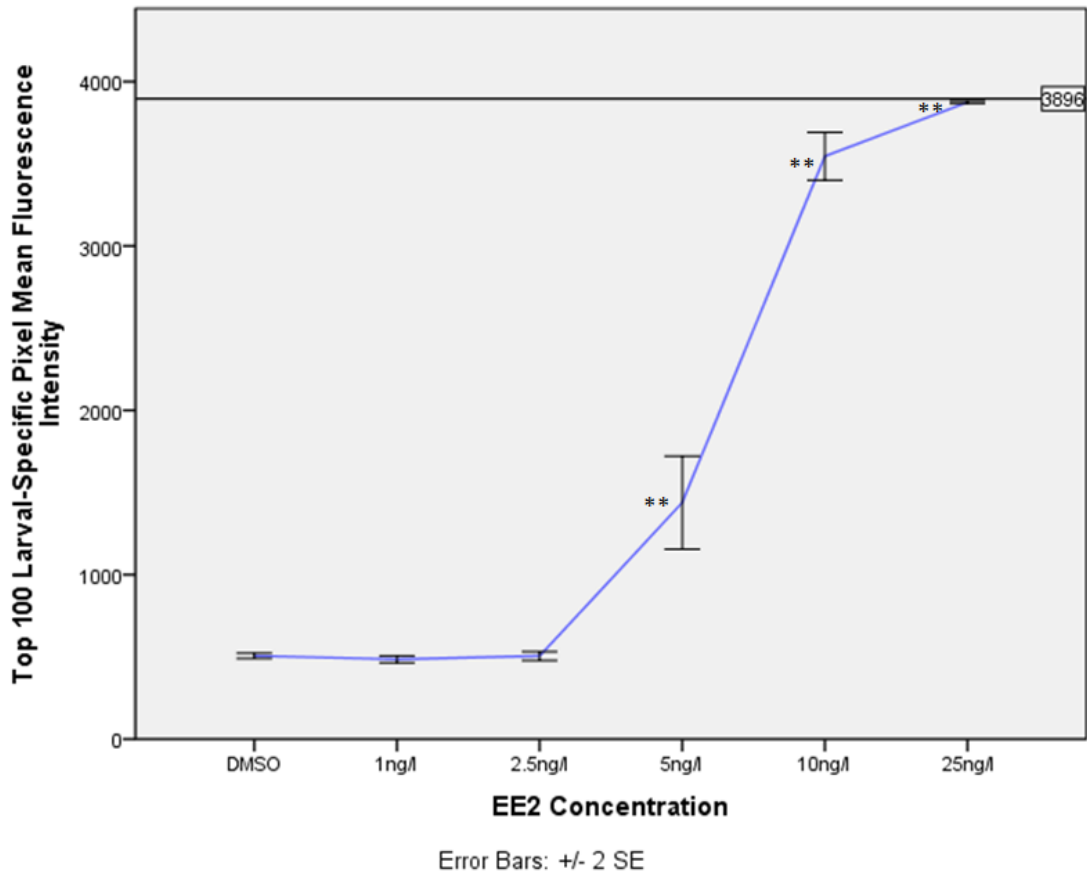


Figure 3.15. Top 100 pixel intensity threshold larval fluorescence responses (extracted from group-spawned data) to EE2 reported as mean \pm 2SEM (asterisks indicate significant difference compared with DMSO control, ** $p < 0.01$). Data points were plotted and statistical analyses carried out following removal of extreme outliers ($N=327$). Y axis reference line represents 3896 pixel value saturation point.

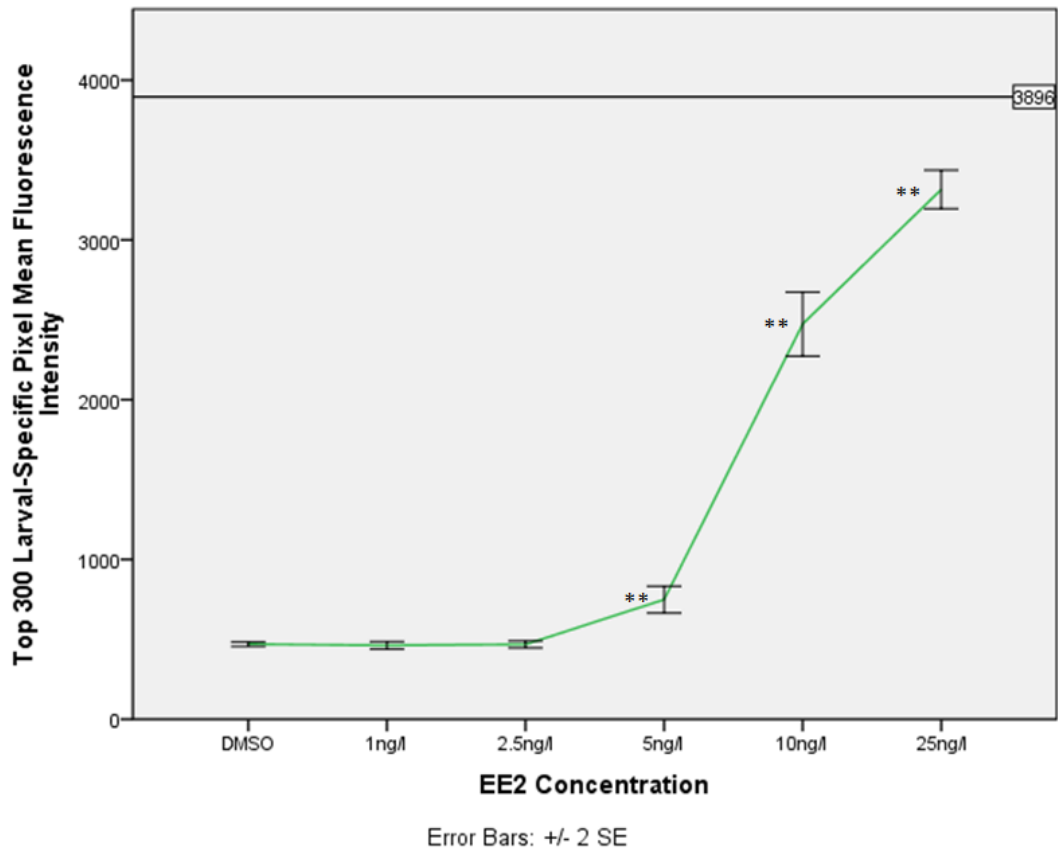


Figure 3.16. Top 300 pixel intensity threshold larval fluorescence responses (extracted from group-spawned data) to EE2 reported as mean \pm 2SEM (asterisks indicate significant difference compared with DMSO control, ** $p < 0.01$). Data points were plotted and statistical analyses carried out following removal of extreme outliers ($N=347$). Y axis reference line represents 3896 pixel value saturation point.

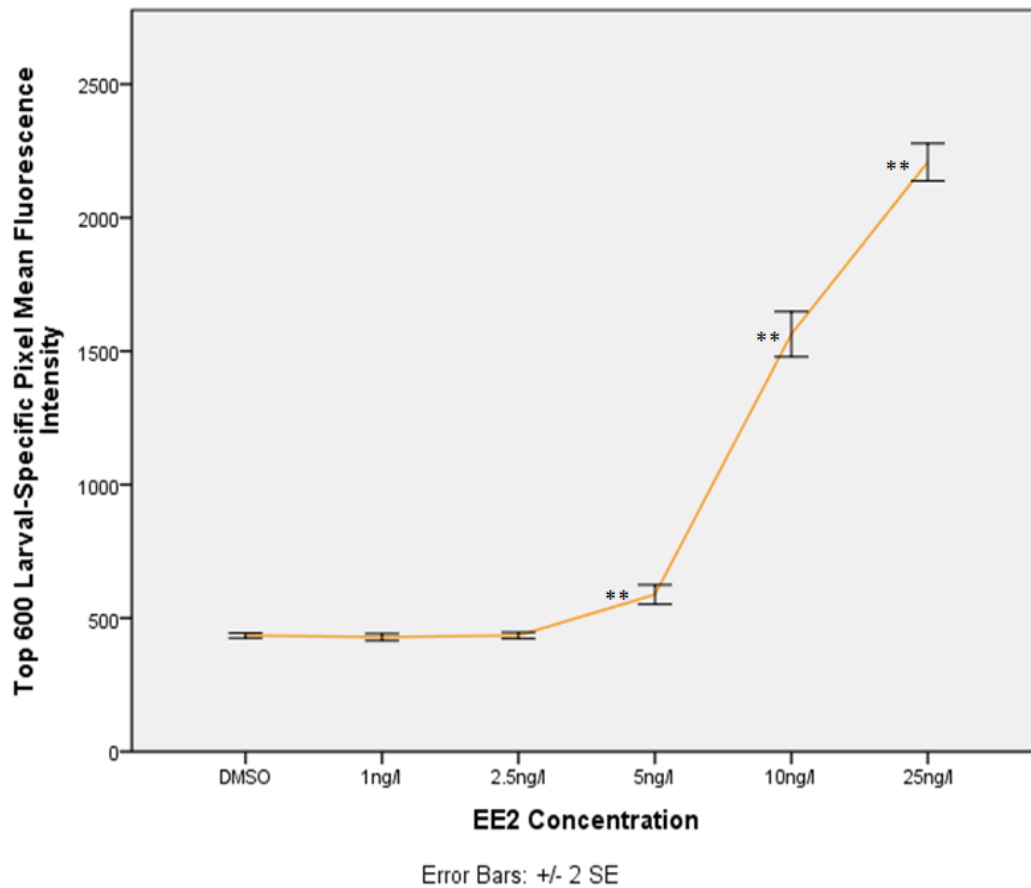


Figure 3.17. Top 600 pixel intensity threshold larval fluorescence responses (extracted from group-spawned data) to EE2 reported as mean \pm 2SEM (asterisks indicate significant difference compared with DMSO control, ** $p < 0.01$). Data points were plotted and statistical analyses carried out following removal of extreme outliers ($N=323$).

The Excel heat-mapped virtual plates showing fluorescence intensity values for the mean Top-100, -300 and -600 pixel thresholding approaches illustrated the high degree of saturation for the 25ng/L EE2-dosed larvae at the 100-Pixel thresholding level (Figure 3.18a.).

a) Top 100 pixel threshold ArrayScan output

96 Well Optical Plate:														
	1	2	3	4	5	6	7	8	9	10	11	12		
A													Blank	Means/conc.
B	581.19	X	473.17	520.57	453.5	510.29	460.72	469.5	510.21	433.63	X	422.38	Iso Water	483.52
C	465.82	531.38	517.03	494.98	500.54	484.95	546.42	X	X	437.4	428.1	556.2	DMSO	496.28
D	X	517.22	527.12	462.27	445.61	X	516.26	498.7	413.38	435.06	X	479.58	1ng/l EE2	477.24
E	X	X	X	X	463.32	425.04	502.34	398.03	568.86	431.55	448.51	555.05	2.5ng/l EE2	474.09
F	790.53	1911.7	1202.93	793.41	660.79	439.55	X	421.02	499.89	583.56	505.35	X	5ng/l EE2	780.87
G	2193.43	2642.19	3451.5	1878.16	2438.83	1101.75	3895.5	X	2585.95	3749.69	3737.08	3635.44	10ng/l EE2	2846.32
H	3896	3896	3896	3896	3896	3896	3895.53	3896	3896	3895.45	X	3896	25ng/l EE2	3895.91

b) Top 300 pixel threshold ArrayScan output

96 Well Optical Plate:														
	1	2	3	4	5	6	7	8	9	10	11	12		
A													Blank	Means/conc.
B	509.82	X	447.55	475.27	431.67	482.52	446.02	451.35	488.88	407.43	X	406.51	Iso Water	454.70
C	441.13	478.00	482.64	470.09	483.91	471.60	469.77	X	X	418.49	416.20	499.34	DMSO	463.12
D	X	482.92	491.06	445.77	428.84	X	477.94	465.90	399.69	417.74	X	457.59	1ng/l EE2	451.94
E	X	X	X	X	441.45	407.45	456.23	383.88	519.95	419.05	420.75	523.31	2.5ng/l EE2	446.51
F	604.84	1116.43	773.95	607.62	549.07	420.92	X	401.87	460.96	538.92	467.68	X	5ng/l EE2	594.22
G	1203.42	1575.68	2130.90	1074.83	1345.42	851.09	2452.13	X	1378.65	2148.80	2305.86	2317.65	10ng/l EE2	1707.68
H	2699.30	3399.27	3697.04	3507.95	3866.58	3147.30	3237.10	3326.94	3492.30	3383.36	X	3030.23	25ng/l EE2	3344.31

c) Top 600 pixel threshold ArrayScan output

96 Well Optical Plate:														
	1	2	3	4	5	6	7	8	9	10	11	12		
A													Blank	Means/conc.
B	467.88	X	433.07	453.38	417.22	461.30	432.46	438.67	472.34	393.57	X	394.94	Iso Water	436.48
C	427.19	454.88	462.79	457.30	473.57	460.09	441.57	X	X	404.71	406.76	477.00	DMSO	446.58
D	X	464.12	467.39	433.77	415.88	X	459.48	446.93	390.72	406.06	X	443.80	1ng/l EE2	436.46
E	X	X	X	X	427.30	396.07	435.18	373.41	498.07	410.03	404.53	502.50	2.5ng/l EE2	430.89
F	531.22	824.81	635.65	538.77	500.85	408.54	X	388.04	443.62	509.56	449.16	X	5ng/l EE2	523.02
G	824.13	1093.09	1401.54	759.06	887.27	673.16	1480.14	X	924.65	1344.86	1511.13	1525.48	10ng/l EE2	1129.50
H	1668.14	2074.26	2362.30	2157.20	2613.09	2017.87	2020.03	2066.45	2359.67	2060.52	X	1818.08	25ng/l EE2	2110.69

Figure 3.18. Virtual 96-well plate heatmaps of: a) mean Top-100 pixel; b) mean Top-300 pixel; and c) mean Top-600 pixel thresholding ArrayScan output for the same dataset.

3.3.2 Comparison of pair- and group-spawned EE2-exposed larval responses

Eight plates of EE2-exposed pair-spawned and seven of group-spawned larvae were ArrayScan imaged, initially generating ~410 correctly-masked images per spawning type (verified via the online interface). Using the whole-larval masking approach, an LSR at 10ng/L EE2 was observed for both spawning types at the $p < 0.01$ significance level (Figure 3.19). RSD around the 10ng/L EE2-induced mean fluorescent inflection point was $377.65 \pm 16.32\%$ and $400.08 \pm 17.43\%$ for pair- and group-spawned larvae, respectively.

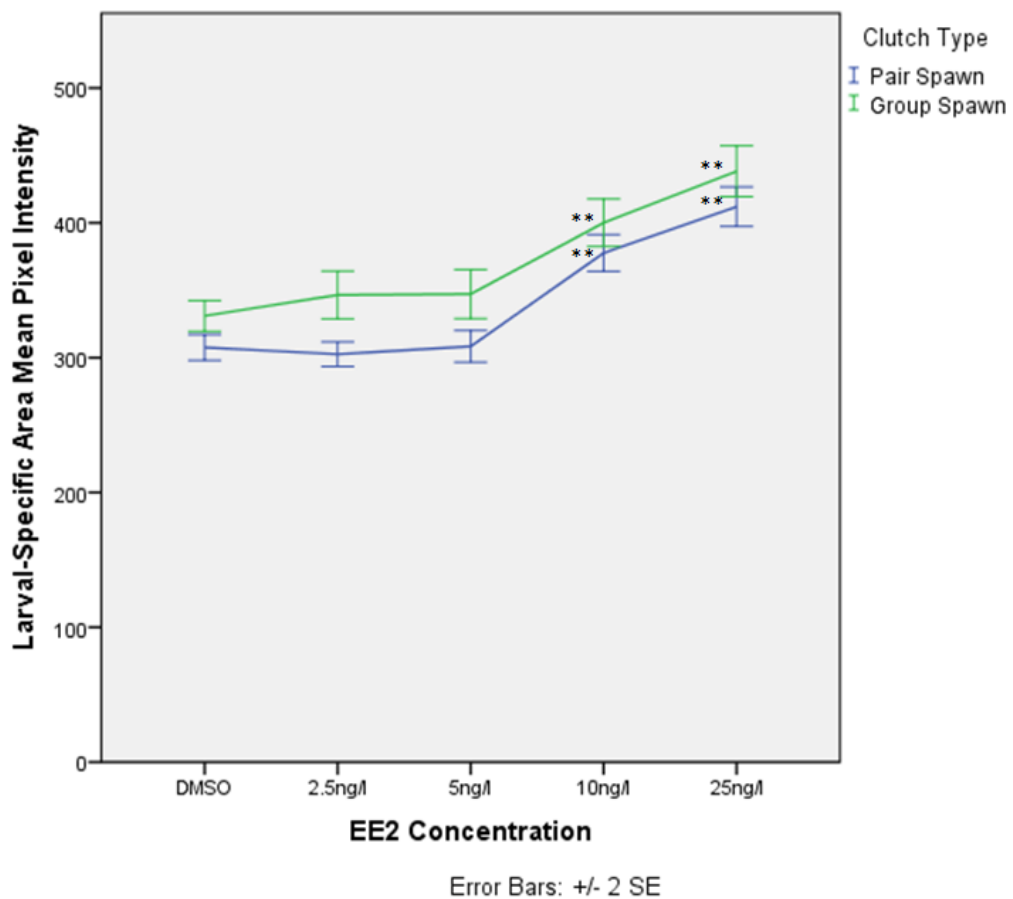


Figure 3.19. Larval-mask mean fluorescence intensity responses to EE2-exposed pair- ($n=438$) and group-spawned ($n=369$) larvae reported as mean \pm 2SEM (asterisks indicate significant difference compared with DMSO control, $p < 0.01$).

Pair- and group-spawned larvae were also compared at the Top-300 pixel thresholding level. An LSR at the 5ng/L EE2 dosing condition was observed for larvae of both spawning types (Figure 3.20.), with a %RSD around the mean fluorescent inflection point of 725.81 ±51.3% and 1034.47 ±80.78% for pair- and group-spawned larvae, respectively.

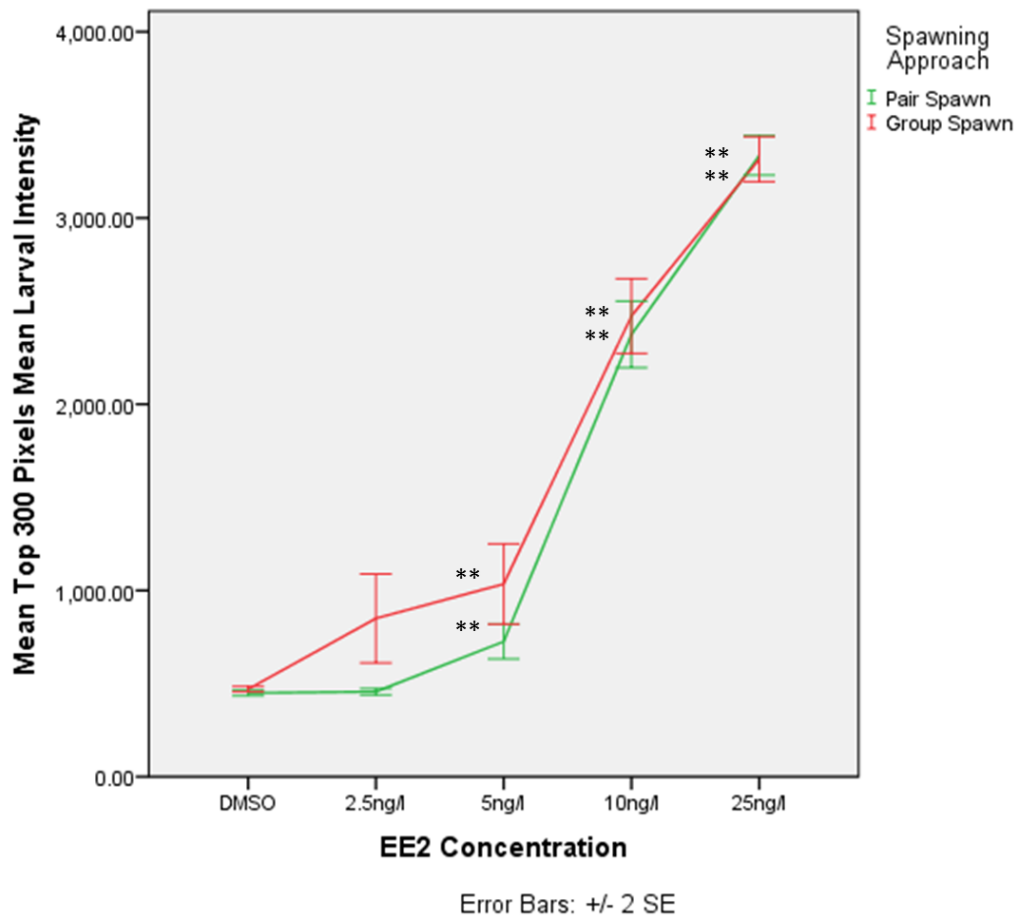


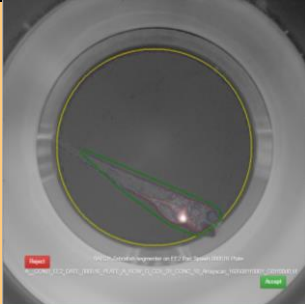
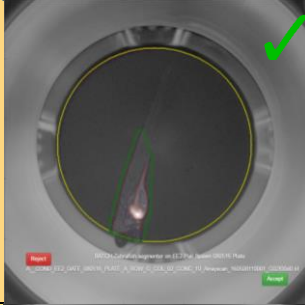
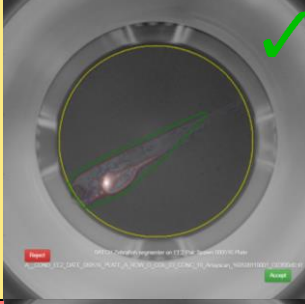
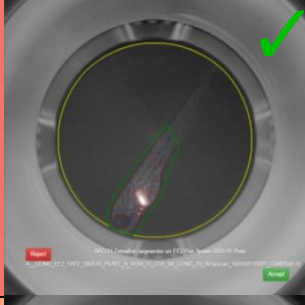
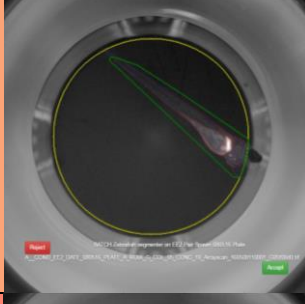

Figure 3.20. Top-300 pixel intensity threshold fluorescence responses to EE2 in pair- and group-spawned larvae reported as mean ± 2SEM (asterisks indicate significant difference compared with DMSO control, ** $p < 0.01$).

Post hoc sample size analyses were also conducted using GPower software (Erdfelder et al., 1996) to ascertain sample sizes required to observe statistically significant difference compared with DMSO controls for 5ng/L EE2 exposed group- and pair-spawned larvae at the .01 level, with power set at 0.80. The analyses indicated that total sample sizes of 44 and 28 larvae for group- and pair-spawned larvae, respectively, were required to achieve significantly different

responses at the 5ng/L exposure level compared to their respective DMSO controls.

3.3.3 Comparison of laterally- vs variably-orientated EE2-exposed larval fluorescence responses

The larval masking algorithm outlines and extracts fluorescence intensity data from larvae of varying orientations across a singular run, incorporating a wide range of fluorescence variation between individual larvae, even within a single dose condition (Figure 3.21., green ticks indicate images where larvae are 'ideally' laterally orientated, left side facing the objective lens, capturing the most unobstructed view of the liver).

Column #	10ng/L EE2	
1	3604.57	
2	3570.60	
3	3464.77	
4	3836.10	
5	3703.04	
6	3786.21	

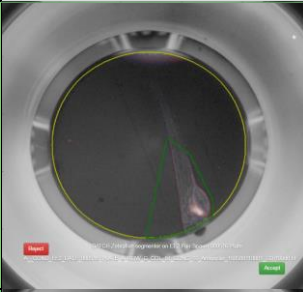

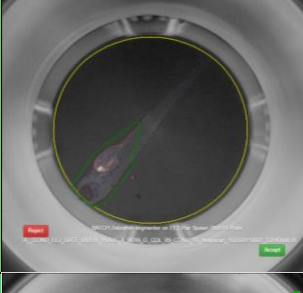
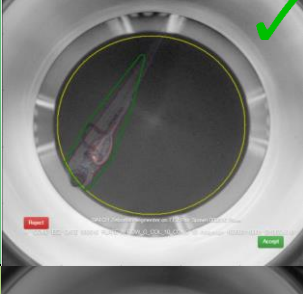
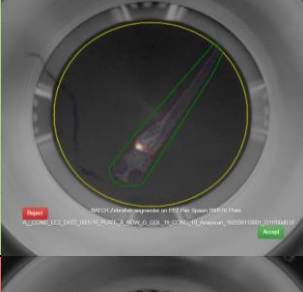
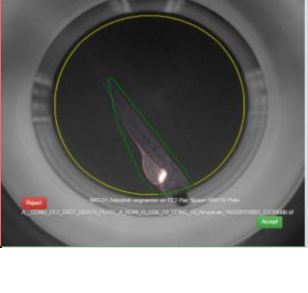
7	1219.65	
8	750.66	
9	995.74	
10	505.95	
11	2001.79	
12	3853.20	

Figure 3.21. Top 100 pixel intensity values for all larvae exposed to 10ng/L: green ticks indicate 'ideally' orientated larvae (08.05.16, Pair Plate A).

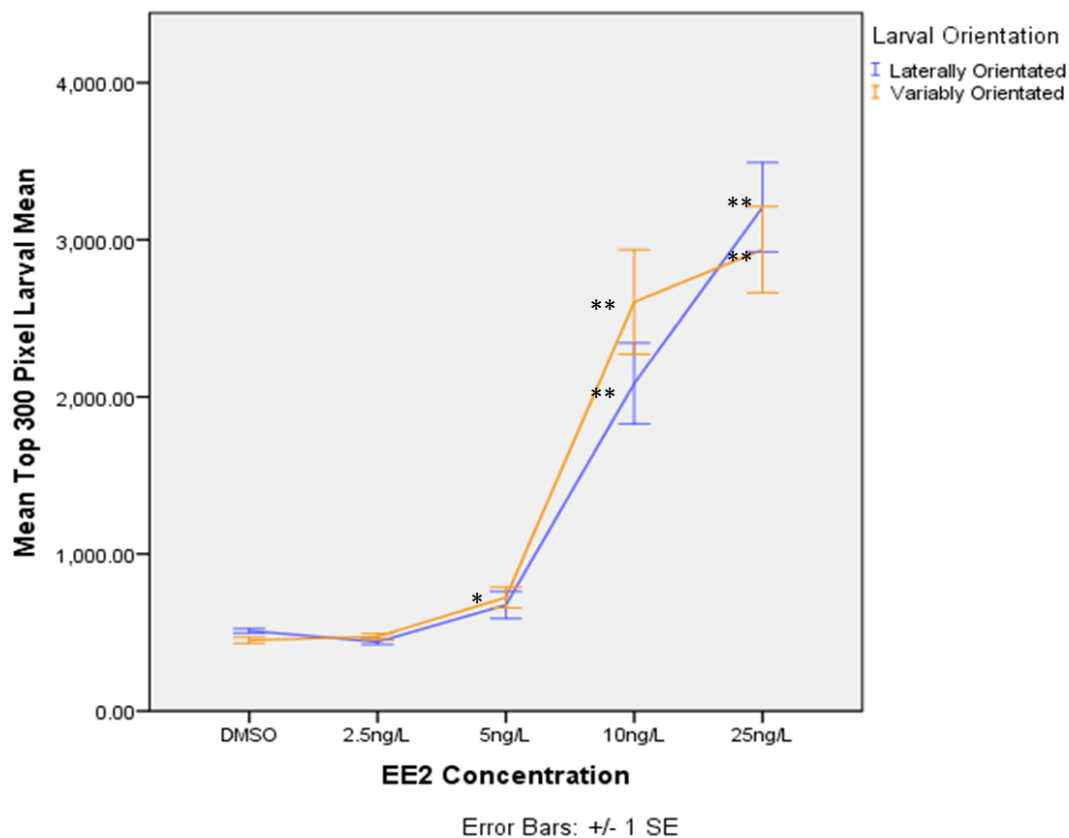


Figure 3.22. Mean Top-300 pixel fluorescence intensities for laterally- and variably-orientated EE2-exposed ERE:GFP:Casper larvae reported as mean ± 1 SEM (asterisks indicate significant difference compared with DMSO control, * $p < 0.05$ and ** $p < 0.01$).

ArrayScan images of laterally-orientated, left side-down, pair-spawned EE2-exposed larvae from 4 datasets (~55 larvae/orientation) were hand-selected from the online interface and compared with randomly-selected, variably-orientated larvae from the same exposure plates in order to compare sensitivity and variability (Figure 3.22.). The mean Top-300 mean pixel threshold was used to extract fluorescence data from ‘ideally’ orientated larvae for comparison against variably orientated animals.

An LSR was observed at 5ng/L EE2 for the variably-orientated larvae ($p < 0.05$) and at 10ng/L EE2 for the ‘ideally’ laterally uniformly-orientated larvae ($p < 0.01$). At the 10ng/L EE2 dosing condition (Figure 3.22.), where both larval orientations exhibited highly significant elevated fluorescence responses in comparison to the control fish ($p < 0.01$), %RSD around the mean was calculated as being $2085.75 \pm 34.84\%$ and $2603.9 \pm 36.12\%$ for laterally-orientated and variably orientated

larvae, respectively, demonstrating a slight improvement in terms of robustness using the 'ideally' orientated animals.

3.3.4 Comparison of EE2-exposed larval fluorescence responses quantified using the semi-automated ArrayScan system and manual Zeiss system

Larvae were taken directly from the 96-well optiplate after ArrayScanning and embedded for manual image acquisition using the Zeiss inverted microscope. Background fluorescence was much lower for the Zeiss-acquired images, resulting in an LSR at 5ng/L EE2 compared to 10ng/L EE2 for the ArrayScan-acquired images (at the Top-100 mean pixel thresholding level), demonstrating the superior sensitivity of the Zeiss when using small sample sizes ($n=52$, Figure 3.22.).

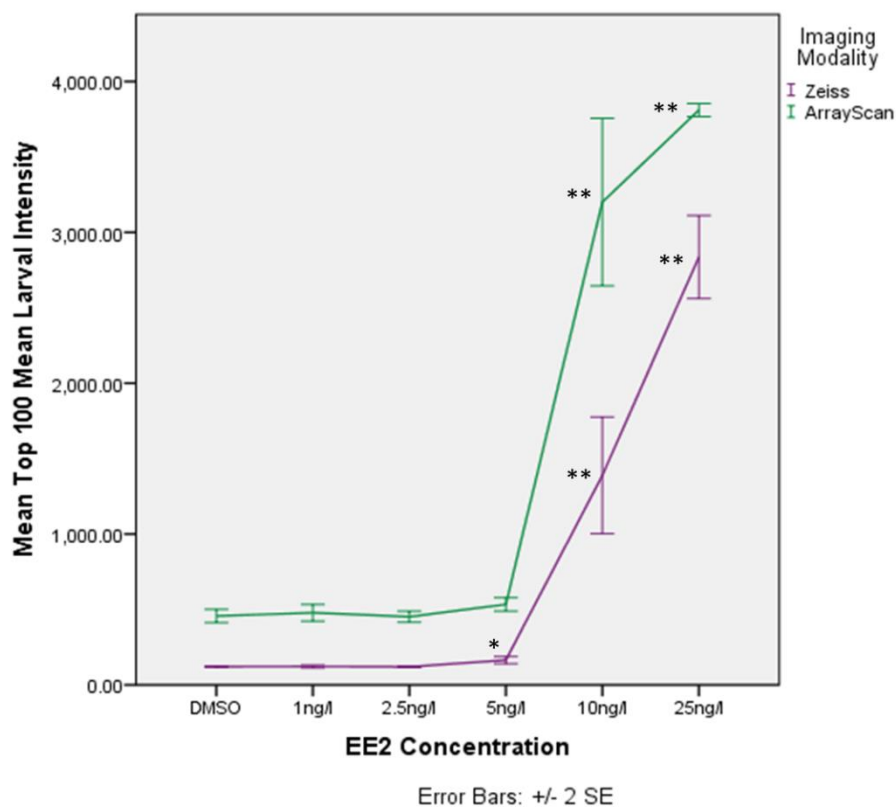


Figure 3.23. Comparison of EE2-exposed larval fluorescence responses quantified using the semi-automated ArrayScan system (larvae variably orientated within a 96-well plate ($n=56$)) and manual Zeiss system (larvae embedded and laterally orientated in agarose ($n=52$)) reported as mean values ± 2 SEM (asterisks indicate significant difference compared with DMSO control, * $p < 0.05$ and ** $p < 0.01$).

The Zeiss manual approach demonstrated more sensitive fluorescence-detection capabilities, with an LSR at 5ng/L EE2, compared to 10ng/L EE2 for the ArrayScan system. Fluorescence responses were significantly elevated compared to control ($p < 0.01$) for both imaging modalities at the 10ng/L dosing condition using the Top-100 mean pixel thresholding approach (Figure 3.23.), with %RSD around the mean calculated as being $1388.72 \pm 39.44\%$ and $3200.89 \pm 26.02\%$ for the Zeiss and ArrayScan systems, respectively. Thus, the ArrayScan acquired fluorescence data with less between-larval response variation.

3.4 Discussion

The ERE:GFP:Casper estrogen-responsive larval zebrafish was used as a model for assessing the sensitivity, signal-to-noise capacity, and robustness of the semi-automated ArrayScan system for detecting EE2-induced increased GFP expression *in vivo*. A number of different assay parameters and fluorescence response extraction approaches were implemented and compared in order to ascertain the variables that would output the most consistent data with the most effective signal to noise (SNR) achievable using the ArrayScan system. Lowest significant response (LSR) analysis was used to indicate a statistically significant difference in fluorescence response compared to control animals (0.5% DMSO). Robustness was quantified and defined by fluorescence response relative standard deviation (%RSD), which described the variability of the data in relation to the mean, and thus an indication of the ability of the assay to extract consistent dose-response data from the EE2-exposed model.

In terms of the quantified fluorescence response, whole-image and whole-well approaches provide no meaningful data due to excessive background (autofluorescence) generated by the plates themselves and artefacts within the well. This effect could potentially be overcome by using different plates for imaging – for example, plates with black well walls and an optically clear bottom could be trialled for improved fluorescence data robustness. The first level of larval masking – whole-larvae – showed a marked improvement on the whole-image and well-masking approaches, with significant ERE-GFP responses

recorded at 10 and 25 ng/L. The whole-larval masking approach may have some limited application where relatively high exposure concentrations are being screened, but is not suited to general screening work as it is too insensitive.

The image data extraction approach at the larval-specific top pixel thresholding levels generated data with the best SNR. In this case, the lowest significant dose in comparison to control detected was at 5ng/L EE2. The Top-100, -300 and -600 pixel thresholding approaches all indicated an LSR at 5ng/L EE2, but the robustness varied, with the Top-100 and -300 pixel approaches having large ($\pm 76.32\%$ and $\pm 80.78\%$, respectively) relative standard deviation at the 5ng/L (response threshold) EE2 exposure (Table 3.1.). The values generated by the Top-100 mean pixel value threshold approach also meant that larval responses began to saturate slightly (for some of the assay repeats) at the 10ng/L to 25ng/L EE2 dosing conditions, causing pixel information to be lost at the higher exposure concentrations. The Top-100 pixel thresholding approach was therefore slightly more sensitive than the other approaches, but the responses were still variable. Data loss due to saturation at the higher EE2 concentrations meant that the Top-100 approach was most suited for low-level/less potent EEDC exposures. The Top-600 mean pixel value strategy resulted in a further reduction in the %RSD of $\pm 64.68\%$ but sensitivity began to be compromised - a concern if less potent estrogenic compounds were to be screened using this assay.

Table 3.1. Mean and %RSD fluorescence response values at different larval-specific pixel thresholding approaches for group-spawned larvae exposed to 5ng/L EE2.

Pixel thresholding level	Mean fluorescence	%RSD
Mean Top-100	1438.6	$\pm 76.32\%$
Mean Top-300	1034.47	$\pm 80.78\%$
Mean Top-600	768.53	$\pm 64.68\%$

As described above, the teleost fish liver has been shown to consist of two lobes, the left of which is bigger and spreads through most of the corporeal cavity, rendering the left side of the larvae the most unobstructed from the perspective for imaging responses in the liver (Vicentini et al., 2005). The variable orientation of the anaesthetised live larvae during ArrayScan imaging was postulated as having an influence on recorded intra-individual fluorescence variability. It was assumed that by taking fluorescence intensity readings from uniformly laterally-orientated, left side-down (liver nearest to objective) larvae exclusively, variation in fluorescence readings across the range of dosing conditions might be reduced and SNR increased.

Although orientation of the larvae did not appear to significantly influence %RSD, variability between larval responses was slightly reduced for uniformly-orientated larvae at the 10ng/L EE2 dosing condition, at which both orientation approaches elicited highly significant ($p < 0.01$) fluorescence responses ($\pm 34.84\%$ and $\pm 36.12\%$ for uniform laterally- and variably-orientated larvae, respectively). As the liver has been found previously to be the most responsive tissue to EE2 (Green et al., 2016), it was not surprising that taking fluorescence intensity readings from larvae uniformly orientated in a way that gave the most unobstructed view of the liver might elicit less between-larval GFP response variation. However, as SNR was not significantly improved, it could be assumed that natural variation between individual larval responses might be having a stronger impact on recorded intensity than any effect of animal orientation. Again, a comparison of uniformly- versus variably-orientated larval responses acquired using a more sensitive, designed-for-purpose system, together with a larger sample size (n was just ~ 55 for each orientation type in this study), might elucidate whether inherent variation or larval orientation is having more of a profound effect on observed GFP responses.

Lack of any significant difference in responses between the two spawning conditions could be due to the 'noisiness' of the images acquired by the ArrayScan system used. This could be subject to further investigation with an imaging modality designed for the specific role of screening fluorescent transgenic larvae. We employed a manual system to assess whether sensitivity and robustness could be improved within a single assay run (one 96-well plate of

exposed larvae). The ArrayScan was capable of acquiring one GFP-channel image per well of a 96-well optiplate automatically at a rate of approximately 1.5 hours per full plate. Using the Zeiss system, it took a team of two approximately 2 hours to embed, image, and then manually save image files (in both GFP and bright field channels) for the full complement of EE2-exposed anaesthetised larvae extracted directly from the 96-well optiplate after ArrayScan imaging. Thus, using the Zeiss manual-screening approach would take approximately twice as long to generate the same set of images as using the ArrayScan.

The smaller dataset collated from the Zeiss imaging ($n=52$) was due to mechanical damage caused to the larvae during manual embedding – an occasional unfortunate by-product of larval manual handling, that is largely circumvented by the ArrayScan system ($n=56$ 'accepted' images). As larvae were also manually laterally uniformly-orientated before being imaged using the Zeiss system with no improvement in robustness (fluorescence %RSD was $\pm 39.44\%$ and $\pm 26.02\%$ for the Zeiss and ArrayScan systems at 10ng/L EE2, respectively), it seems likely that natural variation between individual larvae was strongly affecting the variation seen in fluorescence responses. However, a single run of each system using the same larvae resulted in a lower LSR from the Zeiss-imaged dataset, detected at 5ng/L EE2 ($p < 0.05$) compared to 10ng/L for the ArrayScanned images ($p < 0.01$) – this represented good sensitivity considering the small sample sizes used in this comparison.

Variability in drug responses is well-recognised in humans (Xie et al., 2001), and has been shown to be influenced by drug pharmacodynamics and pharmacokinetics (Derendorf et al., 2000; Reigner et al., 1997; Sheiner & Steimer, 2000). However, little is known about pharmacodynamics and pharmacokinetics in fish despite similarly large variation between individuals being observed in their responses to other chemicals, such as the anti-inflammatory ibuprofen (Patel et al., 2016). Pharmacogenetics describes a genome-wide approach to identifying the genetic determinants of drug responses which can affect individual responses to drugs due to heredity. It would thus be expected that pair-spawned animals would exhibit reduced variation in their ERE-driven responses to EE2 compared to group-spawned larvae, which was

observed at the 5ng/L LSR ($725.81 \pm 51.3\%$ and $1034.47 \pm 80.78\%$ for pair- and group-spawned larvae, respectively).

There was still a high degree of variation observed for the pair-spawned larvae, and this could, in part, be due to the fluorescence results of 7 different pair-spawning events being pooled. Average variation within each pair-spawned larval group was 26.01% RSD around the 5ng/L fluorescence average, almost half the variation of the 7 pooled pair-spawned larval responses. This potential limitation could be usefully explored by using the same adult pair to produce all eggs across several exposure days, minimising genetic variation, while ensuring that group-spawned batches are generated by different animals at every spawning event by selecting eggs from multiple pairs and pooling these to ensure a randomised contribution of parent fish. It should be acknowledged that any minimisation of genetic diversity in groups of the exposed model might skew fluorescence results and lead to false interpretation of data. Loss of individual genetic variability in animals depresses their ability to cope with environmental challenges (Lacy, 1997). This could manifest as exaggerated or attenuated overall responses in study groups and would limit the capacity to extrapolate findings to natural populations.

It should also be considered that the levels of EE2 used in this study were very low. EE2 has a Log P of ~ 3.9 (Han et al., 2012) and therefore a tendency to be hydrophobic, adhering to well surfaces in an inconsistent manner. Larvae could be exposed at different EE2 concentrations *en masse* in a Petri dish (prior to image acquisition) and compared to larvae exposed in well plates to assess whether minimising the potential variation of differential adsorption between dosing-plate wells has any effect on individual-level variation within EE2 exposure groups. Tissue concentrations of EE2 could also be analysed in order to assess whether larvae are experiencing different rates of uptake due to the variable adherence tendencies of EE2. However, it is very difficult to measure for internal concentrations of EE2 in individual larvae as existing methods need to combine several larvae to get the sensitivity for measurement, and combining animals would average out the variation.

Using the ArrayScan system, the most sensitive assay for detecting the ERE:TG:Casper larval-specific fluorescent signal in response to EE2 could be achieved by exposing pair-spawned larvae for 4 days before using the Top-100 larval-specific pixel thresholding approach to extract fluorescence intensity response values from variably-orientated larvae. The most robust data could be acquired using uniformly-orientated pair-spawned larvae and extracting fluorescence data using either the Top-100 or Top-600 mean pixel thresholding approaches (depending on test compound potency).

The optimum LSR that could be identified using this semi-automated assay was 5ng/L EE2 in 4dpf larval fish. This represents an important improvement in terms of experimental timescale on previous work using the ERE:GFP:Casper (Green et al., 2016), where 5dpf larvae were used to obtain an LSR at the same EE2 dose concentration. This assay therefore represents an improvement in screening throughput using the transgenic model without compromising sensitivity. An additional benefit of using larvae at 4dpf is that they feed endogenously on their yolk sac (Wilson, 2012), so do not require the provision of exogenous food which could potentially alter uptake of test chemicals. Our assay also compares favourably to ArrayScan work by Green et al. (2016) in terms of between-larval fluorescence specificity, with an SEM across all EE2 exposure concentrations of $\leq \pm 10\%$ mean intensity at the Top-600 mean pixel value level of thresholding compared to an SEM of $\leq \pm 14\%$ reported in their work.

Screening using the ERE:GFP:Casper line represents a marked improvement in sensitivity in comparison to one of the first estrogen-responsive transgenic medaka models which employed a vitellogenin promoter-driven GFP reporter (Zeng et al., 2005). This model required 50ng/L EE2 exposures to induce detectable levels of fluorescence using whole-fish RNA extraction and 1000ng/L EE2 exposures to elicit detectable GFP expression in live animals. A further estrogen-sensitive transgenic medaka model was developed using gene regulatory elements of *choriogenin H* line capable of eliciting a more sensitive *in vivo* GFP response at 50ng/L EE2 after a 24 hour exposure (Kurauchi et al., 2005). However, the model was not sufficiently sensitive enough to generate a fluorescence response significantly brighter than baseline for environmentally-relevant exposures.

The 5ng/L EE2 optimum level of detection achieved using this assay falls within the range reported in effluents and surface waters throughout Europe, from below the detection limit of 0.5ng/L up to 15ng/L (Belfroid et al., 1999; Desbrow et al., 1998; Johnson et al., 2000; Svenson et al., 2002; Ternes et al., 1999). In other parts of the world, much higher concentrations of EE2 have been recorded, for example 42ng/L in a Canadian sewage affluent (Ternes et al., 1999) and 831ng/L in an investigation of US streams (Kolpin et al., 2002). In a study of Brazilian surface waters EE2 concentrations were found to reach 25ng/L (Sodré et al., 2010).

The 5ng/L EE2 exposure level has also been suggested to be a concentration at which fish anxiety and shoaling behaviour could be adversely effected. A dose concentration of 5ng/L EE2 for 14 days caused adult male zebrafish to have an increased latency period compared to control fish, while a 25ng/L EE2 exposure resulted in reduced latency (Reyhanian et al., 2011). Exposure to a dose of 25ng/L also caused a significant reduction in swimming activity, with fish tending to spend more time at the surface compared to controls, while those exposed to 5ng/L spent significantly less time away from the shoal than control fish.

3.5 Conclusions

An interesting extension of this project could be to delineate and quantify the ERE:GFP:Casper heart valve fluorescence response in the same semi-automated manner that the larval body can currently be delimited. This could be achieved by uniformly orientating the larvae and acquiring a brightfield image in addition to GFP, so that the heart valves could be automatically outlined and fluorescence values acquired from this region alone. Integrating this image data with observations of cardiac contractile strength could generate some compelling evidence regarding the influence of EE2 on cardiac muscle. There are a range of novel automated screening systems available that would allow for the generation of tissue-specific fluorescence response quantification in live zebrafish.

Based on technology generated by the Yanick lab (Chang, 2012; Pardo-Martin, 2010), the VAST (Vertebrate Automated Screening Technology) Bioimager

system is an automated larval handling, positioning and orientation toolset that can be mounted on an upright fluorescence or confocal microscope, allowing for optimised imaging of specific tissues and organ systems in an automated and high-throughput manner. Designed specifically for the imaging of 2-7 day old anaesthetised larvae, the system negates the rejection of images due to poor orientation affecting shape recognition and could reduce the loss of larvae caused by mechanical damage sustained during manual pipetting. The VAST bioimager would also allow for multi-channel, high-content images to be taken of the same specific region in multiple animals. One of the major drawbacks of the ArrayScan system is its inability to create composite brightfield and GFP images without the addition of an extra transmitted light module. These overlay images would allow for automated recognition of non-fluorescent organ outlines that could be used to delineate them and record organ-specific fluorescence responses across a concentration range in uniformly-orientated animals. The VAST system is capable of overcoming both these drawbacks, generating more useful, higher-content images. It takes the VAST system around 80 minutes to generate images of 96 larvae collected from a 96-well plate with a failure rate of approximately 14%, representing an improvement on the efficiency of the ArrayScan system (Pulak, 2016). The VAST platform can be mounted on many types of upright microscope such as the Leica DM5000B - as demonstrated using an mCherry expressing transgenic zebrafish strain (Jarque et al., 2015) making it simpler to generate many high-resolution fluorescent images *in vivo*.

Although the concentrations of EE2 we used to generate a statistically elevated, reliable and robust fluorescence response in the ERE:GFP:Casper model were higher than those observed in some higher-content analyses (i.e. 1ng/L EE2 in 5dpf larvae using confocal microscopy, Green et al., 2016), it should be acknowledged that this bioimaging assay permits the detection of an increased ER response after only 96 hours of exposure in a semi-automated manner, and has the potential to elucidate the effects of a range of EEDCs on ER-signalling pathways at critical early-life developmental stages. Furthermore, the fact that larvae are kept alive under anaesthetic during imaging, and can be revived, makes repeat-screening of the same larvae a possibility.

Continuation of work using the ArrayScan with high environmental relevance could be carried out using the newly developed ERE:Kaede:Casper zebrafish strain (developed by Green et al., 2016). Upon exposure to estrogenic compounds, the model expresses a fluorescent Kaede protein which can be quantified before being UV-photoconverted from green to red, thereby allowing any sensitizing effects of the initial exposure on subsequent exposures to EEDCs to be investigated. As environmental organisms are likely to be exposed to a variety of stressors as well as complex combinations of hormonally-active chemicals exerting both agonistic and antagonistic effects, further work using either the ERE:GFP:Casper or ERE:Kaede:Casper lines could centre on fish being exposed to a range of abiotic conditions in conjunction – or prior to – EEDC exposure. Subsequent fluorescence data quantification could then be analysed for evidence of resultant modulations or sensitisations in estrogenically-induced responses exacerbated by the abiotic stressor.

Chapter 4

Effects of Water Temperature on Responses to 17 α -Ethinylestradiol Assessed in a Larval Estrogen-Responsive Transgenic Zebrafish Model.



Chapter 4.

The interactive effects of water temperature and 17 α -ethynylestradiol exposure assessed in a larval estrogen-responsive transgenic zebrafish model

4.1 Introduction

4.1.1 Effects of EDC exposure on teleost fish during critical life stages

Many species of teleost fish have been shown to exhibit a high degree of developmental plasticity in response to EDC exposure, with several studies demonstrating the potential for estrogenically-active compounds to disrupt sexual development and reproductive capabilities (Gimeno et al., 1998; Lange et al., 2001; Segner et al., 2003; Tyler et al., 1998). Estrogenic EDC (EEDC) exposure during periods of larval development and following sexual maturity have been found to result in particularly adverse effects at the molecular, behavioural and physiological levels (McGee et al., 2009; Panter et al., 2002; Van Aerle et al., 2002).

EEDCs can cause effects on fish populations at both juvenile and adult life-stages. For example, fathead minnow (*Pimephales promelas*) populations continuously exposed to environmentally relevant concentrations of EE2 (3.2ng/L) demonstrated reduced male survival rates (17%) and diminished juvenile recruitment (40% compared to controls; Schwindt et al., 2014). The exposed F1 generation completely failed to reproduce and, even after being transferred to clean water, while previously exposed fish demonstrated a reduction in reproduction of 70–99% when compared with controls.

Studies at the individual-morphological level have evidenced EEDCs as being key factors affecting teleost development: Fathead minnow exposed to EE2 (<1-32ng/L) during early life stages have been found to exhibit decreased growth (length/weight) and alterations in gonadal development (male feminisation and fewer spermatozoa), which are likely to impart population-level effects (Van Aerle et al., 2002; Länge et al., 2001). Zebrafish (*Danio rerio*) exposed to 25ng/L EE2 immediately post-fertilisation until the age of three months also showed a

significant reduction in body length and weight in comparison to unexposed control fish (Van den Belt et al., 2003).

Studies addressing the effects of exposure to EEDCs in early life-stage fish have not received the same degree of attention as those concerning their impacts in adult fish. Those which have addressed EEDC-induced activity in larval fish, have largely been concerned with alterations in morphological sexual characteristics (i.e. ovipositor index, gonad morphology) as these tended to be more readily observable than molecular biomarkers (i.e. vitellogenin).

Considering that molecular responses are often signals for subsequent phenotypic effects, morphological endpoints are arguably more important quantitative traits in the assessment of chemical toxicity. However, being able to quantify hormonally-induced responses at the molecular level can provide useful insight into chemical modes of action (MOA). Furthermore, the ability to measure low-level endocrine disruption events is crucial for the sensitive assessment of a chemical's endocrine-disrupting potential, being that such disruption may not actually induce measurable phenotypic abnormalities.

4.1.2 Effects of temperature variation on ectothermic fish

Fish, along with amphibians and reptiles, belong to a group of organisms known as ectotherms. These animals do not produce their own heat, and instead rely on the surrounding environment and their own behaviour to regulate their temperature. The body temperatures of most fish therefore equilibrate with ambient water temperatures (Donaldson et al., 2008). Many species of fish, including zebrafish, are also poikilothermic, meaning that their body temperature is variable and fluctuates over time depending on external temperature conditions. Close contact between the surrounding water and blood at the fish gill results in an efficient heat exchange system, ensuring that internal temperature varies directly and rapidly with the ambient water temperature (Crawshaw, 1979).

Considered the 'abiotic master factor' in aquatic ectotherms, temperature is a fundamental physical regulatory factor for fish, with its influence being seen most strongly in the control of reproductive processes (Pankhurst & Munday, 2011). Temperature is pivotal in the regulation of reproductive mechanisms such as

ovulation, and gamete development and maturation, as well as influencing behaviour, metabolism, distribution and other physiological responses (Brett, 1971; Pankhurst & Munday, 2011). Temperature also influences growth, body size, meristic characters, and muscle differentiation (Blaxter, 1991). All aquatic organisms have a thermal tolerance zone, e.g. a range of temperatures that can be tolerated for the duration of their lifespans. These tolerance zones are dictated by a number of factors, including developmental and genetic influences, as well as the organism's life stage, physiological condition, and the point that it is at in its life history (Fry, 1971).

A three-year study of Atlantic halibut (*Hippoglossus hippoglossus*) exemplified the pivotal role that water temperature plays in the reproductive physiology and development of the species (Brown et al., 2006). Eggs spawned under a warmer ambient temperature regime tended to be of lower viability, and spawning season duration tended to be shorter than those generated under 'chilled' temperature conditions. This reduction in quantity and quality of eggs would likely have a projected negative impact at the population-level if elevated temperatures were maintained.

The embryonic and larval stages of life represent two of the most thermally vulnerable time windows for poikilothermic fish (Rombough, 1997). Elevated temperatures during embryogenesis have been shown to increase mortality (Janhunen et al., 2010; Pankhurst & Thomas 1998), with many species of fish having thermal tolerance limits within $\pm 6^{\circ}\text{C}$ or less of their spawning temperatures (Rombough; 1997).

Temperature has also been shown to strongly influence growth, metabolism and developmental stage duration in larval fishes (Benoît et al., 2000; Blaxter, 1991; Houde, 1989). The higher metabolic rate of larvae maintained under elevated temperature conditions results in them having higher basal energy demands in warmer environments. Larval growth rates have thus been shown to increase with water temperature in temperate and tropical species of fish (Benoît et al., 2000; Blaxter, 1991; Green & Fisher, 2004; McCormick & Molony, 1995; Meekan et al., 2003).

Despite larval growth rate increasing with temperature in many fish species, growth efficiency (the efficiency with which ingested food is converted into a unit of body substance, Aryal et al., 2008) does not seem to follow the same trend (Houde, 1989; Rombough, 1997). Hence, the number of larval fish surviving to sexual maturity has been shown to increase with rising temperature, but also becomes more variable (i.e. in bluehead wrasse, *Thalassoma bifasciatum*; Sponaugle & Cowen, 1996). This could be caused partly by increased food requirements at increased metabolic rates making larvae more susceptible to starvation at elevated temperatures. Temperatures beyond the thermal tolerance limits of some species may also negatively impact fish health by increasing oxygen consumption, as well as the occurrence and virulence of pathogens, which can lead ultimately to fish death (Dalvi et al., 2009; Gordon, 2005).

Zebrafish, like many teleost species, are vulnerable to the modulating effects of temperature across all levels of organisation, from molecular (i.e. levels of vtg expression and multiple key genes; Brian et al., 2008; Körner et al., 2008, Long et al., 2012) to physiological (i.e. standard length and eye diameter; Long et al., 2012) and life history activities (i.e. the timing and duration of reproductive processes; Donaldson, 2008; Gillet & Quetin, 2006). The most commonly used laboratory temperature for breeding and raising zebrafish is 28.5°C, which is generally considered to be the optimal temperature for zebrafish development (Westerfield, 2000).

Many studies have found zebrafish larval developmental rates to increase with rising temperatures, highlighting the vulnerability of early life-stages to temperature variation (Barrionuevo & Burggren, 1999; Dekens et al., 2003; Hallare et al., 2005; Schröter et al., 2008; Schmidt & Starck, 2010). Zebrafish embryos kept at three different temperatures (25, 28 and 30°C) were found to hatch on days 4, 2.5 and 1.5 post-fertilization, respectively (Dekens et al., 2003). This variation in developmental speed could be due to the influence of temperature on the duration of somitogenesis, which has been reported to decrease in zebrafish with increasing temperatures (Schröter et al., 2008). This difference in somitogenesis rate could be explained by the effect of temperature on the biochemical reactions involved in the process. Dechoriation procedures therefore need to be employed if larval growth rates need to be monitored from ≤ 2 days post-fertilisation (dpf) under modified temperature conditions.

Although larval development has been shown to increase with elevated temperatures, this does not seem to be reflected by overall body size. Evaluation of morphological parameters for embryos maintained at three different temperatures (24, 27 and 30°C) showed that the greatest embryo lengths were seen in zebrafish embryos kept at the lowest temperature, 24°C (Schmidt & Starck, 2010). Zebrafish were developing more slowly but were larger at lower temperatures, an effect that has also been observed in other ectothermic organisms which, despite growing more rapidly in elevated temperatures, appear to develop into smaller adults (Atkinson, 1994). It is suggested that this phenomenon occurred adaptively in response to the increased risk of predation by ectothermic predators, which tend to be more prevalent in warmer environments (Atkinson, 1994; Sibly & Atkinson, 1994).

Reproduction and sex determination represent further windows of vulnerability to temperature modulation in many species of fish. Two main types of sex-determination processes have been reported in gonochoristic vertebrates: environmental sex determination (ESD), where there are no genetic differences between the sexes, and sex is determined by environmental factors after fertilization; and genotypic sex determination (GSD), where sex is determined at the point of conception (Ospina-Álvarez & Piferrer, 2008; Penman & Piferrer, 2008). In ESD vertebrates, the most influential environmental factor affecting sex determination is temperature, hence the term 'temperature sex determination' (TSD), the most studied type of ESD in fish (Ospina-Álvarez & Piferrer, 2008).

Juvenile zebrafish first develop as females, with ovary-like undifferentiated gonads disappearing in males 20-30 days after hatching, along with the occurrence of testicular differentiation (Takahashi, 1977). This process is known as juvenile hermaphroditism, and the reversal of the ovary-like gonads into male-gonads occurs via the apoptosis of oocytes prior to the development of male testes and spermatogonia (Uchida et al., 2002). In zebrafish, this female-to-male transition has been shown to be heavily regulated by water temperature, with biased sex ratios occurring at temperatures close to species maximum thermal tolerance (Cortemeglia & Beitinger, 2005).

For example, elevated water temperature conditions were applied to an all-female population of zebrafish (raised initially at a control temperature of 28.5°C) from days 15-25 post-hatch in order to investigate temperature-induced sex reversal (Uchida et al., 2004). The 35°C and 37°C temperature conditions investigated induced sex reversal in the fish at a proportion of 68.8% and 100% males, respectively, demonstrating the powerful influence of temperature on sex determination.

Despite little being known about the physiological mediators of temperature-induced sex determination in fish, the enzyme aromatase appears to play a pivotal role in the process of female differentiation (Godwin et al., 2003). Aromatase is responsible for catalysing a key step in the biosynthesis of estrogens from androgens, including those estrogens essential for female differentiation. In the Japanese flounder (*Paralichthys olivaceus*), levels of these estrogens have been shown to be reduced at high temperatures (27°C) known to induce male-biased sex ratios in this species, and elevated at low temperatures (18°C) at which female-biased sex ratios are seen (Kitano et al., 1999).

It is evident that temperature variation has a marked influence on teleost embryo survival, larval development and sexual determination. It therefore seems pertinent that, when interpreting results of studies considering larval development or response to endogenous estrogens, incubation temperature is controlled for and taken into consideration as a potential extraneous variable.

4.1.3 Effects of EDCs and temperature interactions in teleost fish

The ever-changing environmental pressures to which many organisms are subjected can often interact with chemical stressors to generate unpredictable responses (Brian et al., 2008). Despite this widely-accepted conjecture, there are very few studies that have examined the interaction between the two factors. However, the effects of temperature stress (measured as cortisol response) and EE2 exposure have been analysed for their combined impact on vitellogenin (vtg, a biomarker of estrogen exposure) expression levels in juvenile brown trout (*Salmo trutta*) (Körner et al., 2008). At elevated temperatures, estrogen-induced expression of vtg was found to be significantly elevated, highlighting the

importance of considering the integrated effects of EDCs and temperature when interpreting environmental monitoring studies.

Increases in temperature have also been shown to amplify skewed sex ratios induced by EDCs in zebrafish. For example, 33°C temperature conditions in conjunction with exposure to the EDC clotrimazole (at 8µg/L) was shown to induce male skews of ~97% and ~82% in inbred and outbred zebrafish populations, respectively (Brown et al., 2015). In comparison, the 33°C temperature treatment alone (without chemical exposure) induced a lower male skew of ~72% under inbred conditions, and resulted in a ~48% male population in the outbred group.

Similarly, the effects of 17β-estradiol (E2; 50ng/L) and nonylphenol (NP; 50ng/L) on juvenile Japanese medaka (*Oryzias latipes*) were shown to intensify at higher water temperatures (Jin et al., 2011). For example, estrogen-responsive gene transcription levels in medaka exposed to E2 and NP for seven days were shown to increase by 605- and 5-fold under 10°C temperature conditions, while they increased more than 5000-fold (E2 treatment) and 8 - 21-fold (NP treatment) in the 20°C and 30°C temperature groups, respectively, compared to their respective controls.

At elevated temperatures, exposure to endocrine disrupting pesticides has also been shown to increase mortality and perturb embryogenesis in fish (Osterauer & Kohler, 2008). Zebrafish embryos were exposed to five different concentrations of thiacloprid (1, 5, 10, 15 and 20mg/L) and diazinon (100, 500, 1000, 2000 and 3000 mg/L) under four different temperature regimes (26, 28, 30 and 33.5°C). For diazinon, mortality was shown to increase strongly with higher temperatures (97.5% mortality at 33.5°C) and hatching of the surviving embryos was found to be delayed. For both thiacloprid and diazinon, effects on heart rate were observed to increase in severity under the influence of increasing temperature.

It is widely acknowledged that temperatures which exceed the optimum temperature range for a respective species may also increase the toxicity of potentially harmful chemicals (Fisher & Wadleigh, 1985; Heugens et al., 2001; Persoone et al., 1989; Van Wezel & Jonker, 1998). Due to increased metabolic rates in ectothermic organisms, oxygen demands and heart rate are also elevated under higher temperature conditions, further potentiating the deleterious effects

of toxic substances as the organism is already subject to stress. This may be further exacerbated by the decreased oxygen solubility of warmer water (Mortimer, 2003).

Additionally, the better solubility of chemicals at higher temperatures results in elevated uptake by aquatic organisms, aided by increased diffusion and active uptake rates of water-borne substances across gills and body surfaces (Heugens et al., 2001). Toxic effects on ectothermic organisms may therefore be seen to be strongly potentiated by elevated temperature conditions. Despite this well-supported conjecture, established protocols for studies of ecotoxicology often fail to take variable abiotic environmental factors in conjunction with chemical exposure and more highly vulnerable life-stages into account (Jin et al., 2009).

There is an urgent need for the interactions between temperature and chemical exposures in aquatic organisms to be considered within studies of ecotoxicology, particularly where vulnerable life stages and endocrinological responses are being considered. Both temperature stress and EDCs have been shown to dramatically influence growth, survival and reproductive success.

4.1.4 Selection of experimental temperatures

Lab studies have shown zebrafish embryonic development to be most successful at temperatures between 22-32°C, as reflected by high proportional survival to hatching ($\geq 88\%$) within this temperature range. At 34°C, survival was observed to decline to $\sim 43\%$ and was negligible both above 34°C and below 22°C (Schnurr et al., 2014). $28 \pm 1^\circ\text{C}$ is widely regarded as the recommended maintenance temperature for zebrafish in culture (Westerfield, 1995). This assertion has been supported by work showing that zebrafish exhibit a marked increase in growth when maintained at 28°C, as opposed to lower or fluctuating temperatures (Schaefer & Ryan, 2006).

It is probable that the zebrafish thermal preference range extends considerably above and below the 28°C recommended temperature, and a wider holding temperature range of 24–30°C has been suggested as being appropriate (Matthews et al., 2002). Natural populations of zebrafish have been found to inhabit temperatures ranging from 16.5 to 33 °C (Spence et al., 2006), thus, the

test temperature conditions of 24°C and 32°C were chosen for their environmental relevance, in addition to the high rates of embryonic survival reported within this range (Schnurr et al., 2014).

The aim of the current study was to assess the effects of temperature on responses to the estrogen EE2 and their combined influence on growth in zebrafish, using the ERE-Casper transgenic model. Specifically, we tested the hypothesis that elevated water temperatures would amplify physiological and molecular responses for a given level of EE2 exposure (i.e. Green et al., 2016; Van den Belt et al., 2003). The test temperature conditions chosen for the present study were environmentally relevant low and high thermal regimes (24°C and 32°C, respectively), and the widely-accepted 'optimal' zebrafish rearing temperature of 28°C was chosen as the thermal control. These temperatures were within the range of thermal tolerance for zebrafish embryos, ensuring that temperature would not induce any mortality but would present an abiotic stress.

4.2 Materials and Methods

4.2.1 Egg collection and sorting

A pair-spawned batch of ≥ 108 healthy fertilised embryos were required to carry out one full run of the assay (12 embryos per dose condition, per temperature regime), thus, only pair-spawned batches of > 150 viable embryos were kept for dosing. This allowed some scope for embryo losses (e.g. due to fungal infection) during the first few hours post-fertilisation.

4.2.2 Staging of embryos

As in the previous study (Chapter 3.), following collection and sorting, embryos were stored in rig water at $28 \pm 1^\circ\text{C}$ and checked regularly using a dissection microscope until the majority of embryos ($> 80\%$) had reached the readily-definable $5\frac{2}{3}$ hour germ-ring stage (Kimmel et al., 1995). This ensured that all embryos were at an equivalent stage of development before being exposed to the treatment conditions.

4.2.3 Test chemicals

EE2 (Chemical Abstracts Service CAS no. 57-63-6) was chosen as the estrogenic chemical for this assay due to its environmental relevance, its high binding affinity for all piscine ER subtypes (Shyu et al., 2011), and the low (ng/L) levels at which it has been shown to elicit deleterious effects in fish. EE2 was purchased from Sigma-Aldrich Chemical Co. ($\geq 98\%$) and the stock chemical was dissolved in analytical grade dimethyl sulfoxide (DMSO) to give final nominal dosing concentrations.

4.2.4 Experimental design

5ng/L EE2 was chosen as the low exposure concentration, as equivalent to, or greater than, this level of EE2 has been measured in the aquatic environment (i.e. Al-Ansari et al., 2010; Chen et al., 2007; Johnson et al., 2000; Pojana et al., 2007; Ternes et al., 1999a; Zhou et al., 2012), it is also the lowest concentration previously found to generate detectable significant fluorescence responses in the ERE:GFP:Casper zebrafish model (using the Thermo-Fisher Cellomics ArrayScan II HCS Integrated High Content Screening System) compared to control animals under optimum 28°C temperature raising conditions at 96 hours post-fertilisation (hpf) (Chapter 3.).

25ng/L EE2 was chosen as the high dosing concentration as this exposure generates a strong fluorescence response in the ERE:GFP:Casper model across a wide selection of different larval body tissues (as imaged using a confocal microscope) at 4dpf (Green et al., 2016). 25ng/L EE2 was consistently shown to generate very highly significant GFP-response in 4dpf zebrafish maintained at $28\pm 1^\circ\text{C}$ (Chapter 3.) at all larval orientations using the semi-automated ArrayScan imaging approach. Unexposed larvae were raised in 0.5% DMSO vehicle control solution.

Working EE2 solutions were serially diluted in DMSO from a concentrated stock of 1.25g/L EE2/DMSO in order to give dilute solutions of 6.25 and 1.25 EE2/DMSO with $\sim 5\text{s}$ vortexing at each dilution step to ensure thorough mixing. 60 μL of each working solution was further diluted in fresh rig water in glass vials

on the day of exposure to give 1.25 x working solutions of 6.25 and 31.25ng/L, which were mixed thoroughly on a magnetic stirrer for ≥ 10 minutes.

800 μ L dosing and vehicle control solutions were pipetted into the wells of 6 x 24-well plates to give 12 well columns of 0.5% DMSO, 5ng/L and 25ng/L EE2 in triplicate (for maintaining at 3 different temperature regimes). Embryos were pre-arrayed in 200 μ L media/well, to give 1ml of the final nominal desired control and EE2 concentrations.

Stock control and EE2 solutions were kept refrigerated at 2-8 °C overnight after the initial dosing to minimise degradation. On the mornings of media changes, the solutions were placed on magnetic stirrers for ≥ 1 h and allowed to warm to laboratory temperature ($28\pm 1^\circ\text{C}$) before being used.

A multi-draw incubator (INFORS-HT Multitron Pro) was used to maintain the larvae at the chosen temperature regimes for the duration of the experiment (~6 – 96 hpf). Larvae were kept at either control temperature $28\pm 1^\circ\text{C}$, $24\pm 1^\circ\text{C}$, or $32\pm 1^\circ\text{C}$. The glass windows of the incubator doors were covered and the photoperiodic conditions set to a 12:12 light:dark cycle. A lux meter was used to ensure that during the 'light' period, conditions were kept as constant as possible at ~340 LUX (recalibrated at the beginning of each assay run).

Temperature was monitored using mercury thermometers placed in 500ml glass beakers of water in each drawer of the incubator. These were regularly checked to ensure that ambient temperature did not deviate more than $\pm 1^\circ\text{C}$. Embryos were incubated shortly after initial chemical exposure (~6 hpf) until termination of the assay (96 hpf) in 24-well plates covered in PVC-free Clingfilm to minimise media evaporation during exposure.

4.2.5 Dechoriation

Manual dechoriation was performed on all embryos at 24 hpf using Dumont™ no. 5 forceps (as per protocol outlined in Henn & Braunbeck, 2010). This was done partly to expose them to EE2, but also to allow the body axis to straighten before animals were imaged at 48 hpf. Discrepancies have been reported in zebrafish embryo toxicity screening systems due to varying uptake and

metabolism of chemicals between embryo and adult fish. These have been shown to be resolved when embryos are dechorionated prior to chemical exposure (reviewed in Lammer et al., 2009). Dechorionating all embryos at the same 24 hpf timepoint also helped to improve developmental synchronicity. Dechorionated embryos showed ~15% mortality, as a consequence of mechanical trauma, as opposed to chemical toxicity.

4.2.6 ArrayScan live imaging

At 48 hpf, following initial chemical exposure, dechorionation, and incubation, all larvae were temporarily anaesthetised in 0.4% tricaine methanesulphonate (MS222) solution and transferred to 3 x half-area 96-well Optiplates (Corning®) in 50µl 0.4% MS222 solution (1 plate per temperature regime, Figure 4.1.). 96-well plates were always loaded on to the automated ArrayScan system in the following order, according to temperature regime: 32°C, 28°C, 24°C.

Imaging of each plate was carried out automatically at a rate of ~45 mins/plate, after which larvae were quickly washed to remove as much MS222 as possible, before being re-exposed to test solutions and returned to their respective temperature conditions to revive (whole process ~90 mins). Imaging under anaesthesia was carried out again at 72 hpf, with subsequent washing, revival, and re-exposure, and again at 96 hpf, after which larvae were humanely terminated according to protocol.

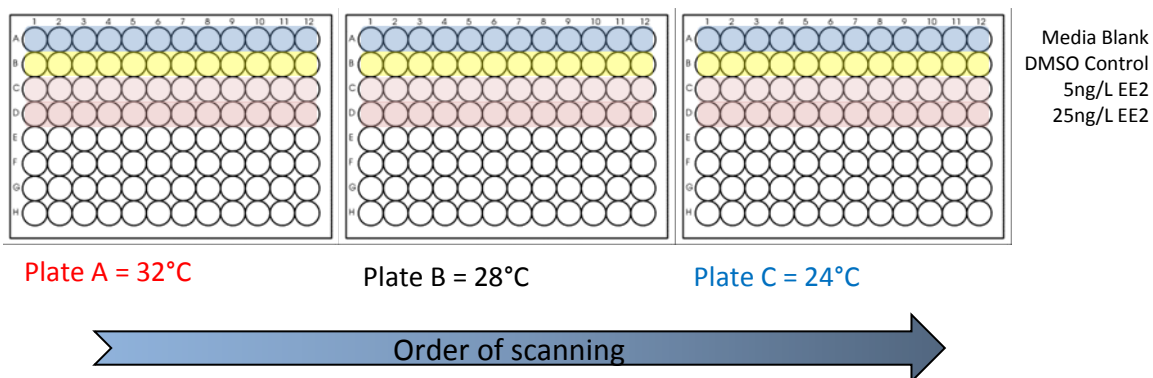


Figure 4.1. 96-well plate layout and order of screening for semi-automated ArrayScan imaging.

4.2.7 Larval fluorescence response analysis

After uploading the ArrayScan images to the online interface, a Python masking algorithm was applied to each GFP-channel ArrayScan image, which automatically outlined the larval body, before selecting the brightest 100 pixels within the larval-specific area (Figure 4.2.). The 100 top pixel intensities were then averaged to give the Mean Top 100 Pixel Intensity value for each larva. The images were then subject to a manual verification process, where correctly identified larvae were 'accepted' for data collation or 'rejected' and excluded from analyses.

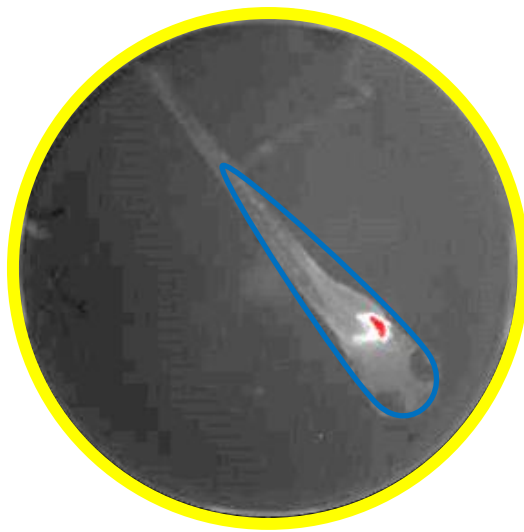


Figure 4.2. Algorithm initially identifies i) the well outline (yellow circle); ii) the larval outline (blue); iii) 100 brightest pixels within larval outline (red area).

4.2.8 Larval growth

Larvae were measured at each sampling timepoint (48, 72, 96 hpf) using the ImageJ open source image processing program to calculate total length (TL, from the tip of the snout to the tip of the caudal fin). The TL was then converted into microns (μ) using a simple calculation (Figure 4.3.). Larval lengths were averaged for each timepoint to assess growth over time. Larval TLs at 48 and 96 hpf timepoints were then input into an Excel spreadsheet and specific growth calculated for each larva using the following formula: $= ((\text{length at 48hpf} - \text{length at 96 hpf}) * 100) / 2$.

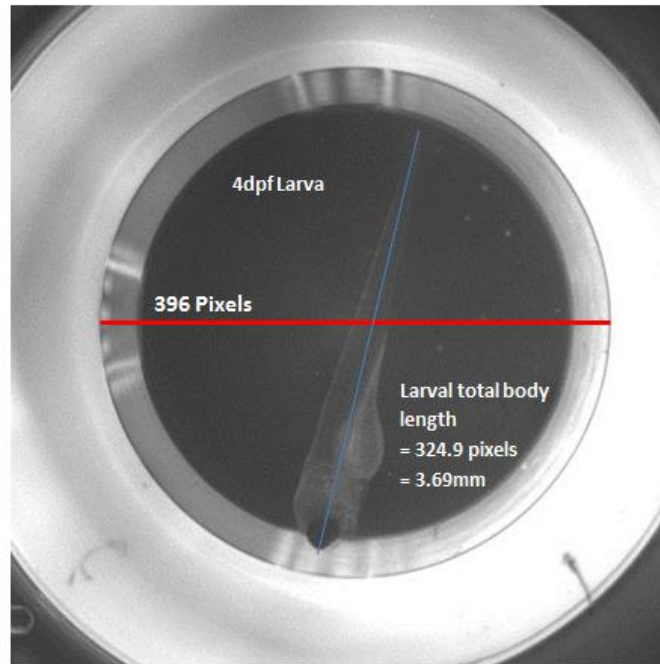


Figure 4.3. Calculating larval total length from ArrayScan image.

4.2.9 Statistical analysis

All values were presented as mean \pm SEM with statistical significance indicated at the $p < 0.05$ (*), < 0.01 (**) or < 0.001 (***) level using ANOVA and the Mann-Whitney U test to compare differences between groups. Fluorescence response robustness at a given dose concentration was calculated using relative standard deviation (%RSD) and stated as \pm 'x' % about the mean.

4.3 Results

4.3.1 ArrayScan runs

Three runs of the assay were included in the results, with an average of ~76 animals for each complete experiment. Excluded data comprised of larvae that had not been correctly identified by the algorithm ($< 90\%$), non-viable larvae, and those that had been damaged by mechanical dechoriation. No increases in mortality were observed as a result of chemical exposure or stressful temperature conditions.

4.3.2 Larval length over time

Mean larval lengths for chemically-unexposed animals reared under temperature stress conditions ($24\pm 1^\circ\text{C}$ and $32\pm 1^\circ\text{C}$) were compared against chemically-unexposed larvae maintained at control temperature ($28\pm 1^\circ\text{C}$, hereafter referred to as 'control-control') over three sampling time-points (48, 72, and 96hpf).

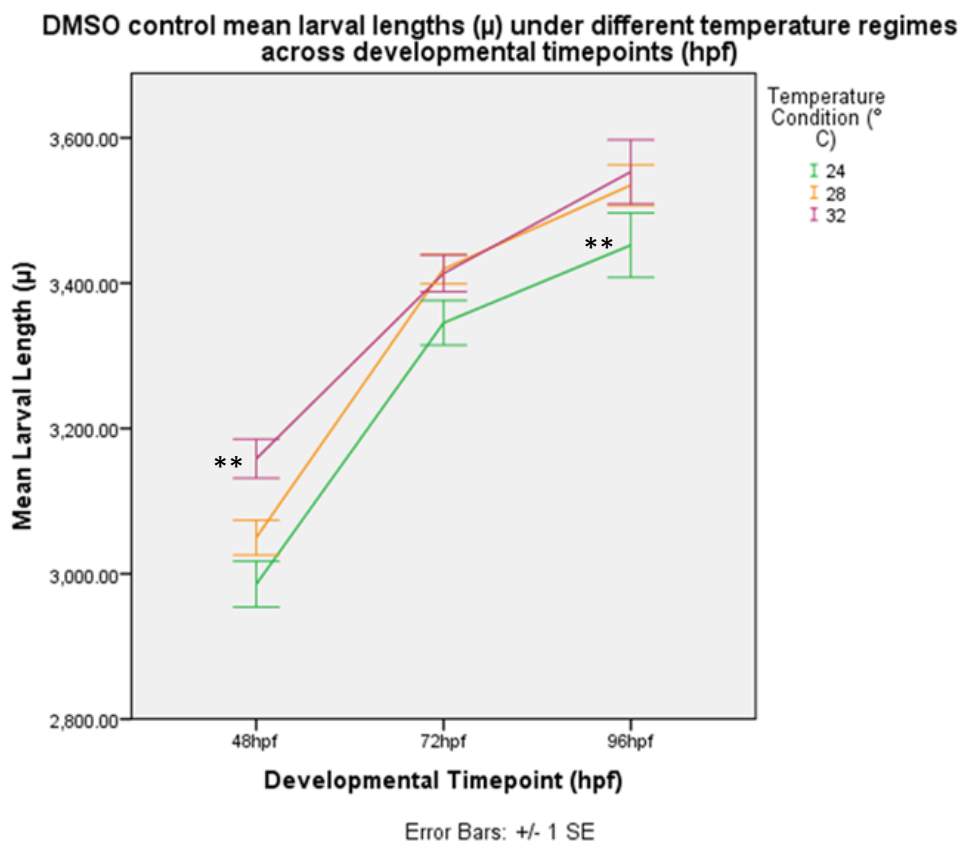


Figure 4.4. Mean larval length at each sampling time-point under different temperature regimes for chemically-unexposed larvae, reported as mean \pm 1SEM (asterisks indicate significant difference compared with chemically-unexposed larvae raised at control $28\pm 1^\circ\text{C}$, ** $p < 0.01$).

Temperature alone appeared to have a significant influence on larval length in chemically-unexposed larvae, with the higher temperature condition animals measuring larger than the larvae incubated at the other two temperatures at the first time-point. However, this size advantage was not sustained and growth-rate slowed, producing larvae of similar size to 28°C larvae by 96hpf. Chemically-unexposed larvae raised at $32\pm 1^\circ\text{C}$ were found to be significantly larger (larval length = $3158.5 \pm 146.7\mu$) compared to control-control larvae (larval length =

3049.8 ± 117.5 μ) at the 48hpf time-point (Figure 4.4.), $t(52) = 2.952$, $p = 0.005$. At 24°C, the lower test temperature, larvae showed a consistent reduced size throughout compared to the other two temperatures. Chemically-unexposed larvae raised at 24±1°C were found to be significantly smaller (larval length = 3448 ± 156.1μ) compared to control-controls at the 96hpf time-point (larval length = 3570.5 ± 126.4μ), $t(44) = 2.857$, $p = 0.007$.

4.3.3 Mean specific growth rate

Specific growth rate was calculated for all larvae from 48–96 hpf and averaged for each temperature regime. Mean specific growth rates for chemically-unexposed larvae maintained at the three temperature conditions were initially compared in order to investigate the influence of temperature alone on growth (Figure 4.5.).

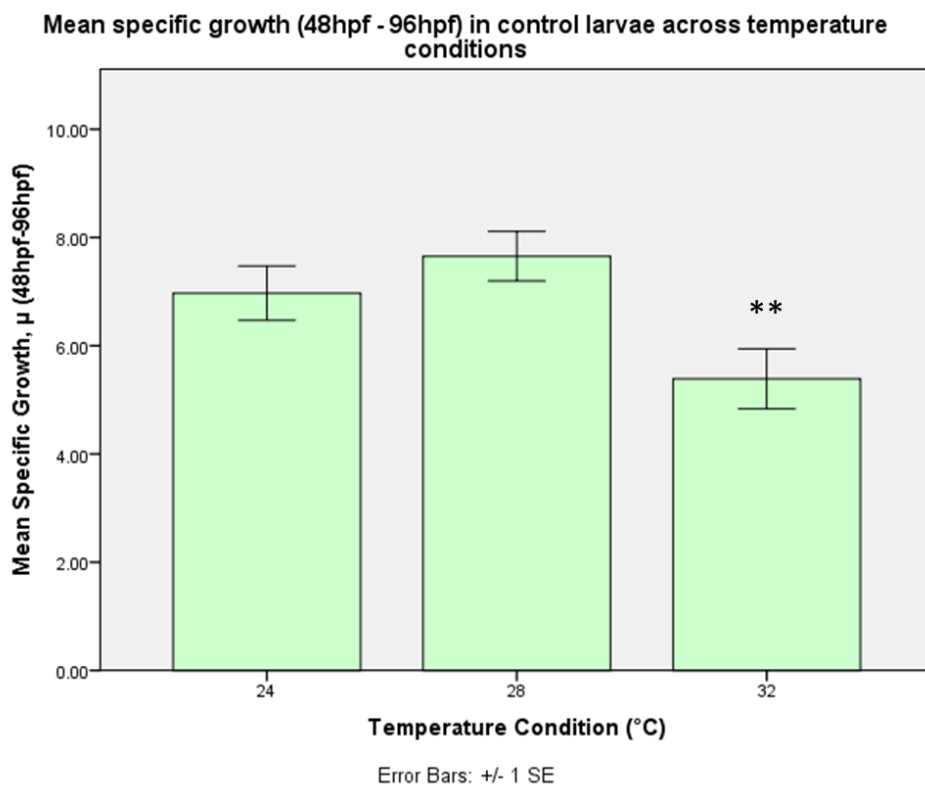


Figure 4.5. Mean specific growth rates (48 – 96 hpf) for all chemically-unexposed larvae raised under three different temperature regimes, reported as mean ± 1SEM (asterisks indicate significant difference compared with chemically-unexposed larvae raised at control 28±1°C, ** $p < 0.01$).

Specific growth rate was found to be significantly reduced in the chemically-unexposed larvae raised at $32\pm 1^\circ\text{C}$ (mean specific growth = $5.4 \pm 2.2\mu$) compared with control-control larvae (mean specific growth = $7.7 \pm 1.9\mu$), $t(32) = 3.173$, $p = 0.003$. The effect size for the analysis of chemically-unexposed larvae at $28\pm 1^\circ\text{C}$ versus chemically-unexposed larvae at $32\pm 1^\circ\text{C}$ ($d = 1.09$) was found to exceed Cohen's (1988) convention for a large effect ($d = 0.8$), meaning that temperature was having a strong influence on reducing larval growth at $32\pm 1^\circ\text{C}$ compared to the control temperature condition. No significant difference was seen in specific growth between chemically-unexposed larvae raised at $24\pm 1^\circ\text{C}$ compared to larvae raised at $28\pm 1^\circ\text{C}$, at the $p < 0.05$ level.

Mean specific growth rate for EE2-exposed larvae was not found to significantly differ compared with chemically-unexposed larvae when all fish were reared at $28\pm 1^\circ\text{C}$ optimal temperature conditions (Figure 4.6). This result suggested that, in the absence of a thermal stressor, zebrafish larvae grew at similar rates despite being exposed to an estrogenic chemical.

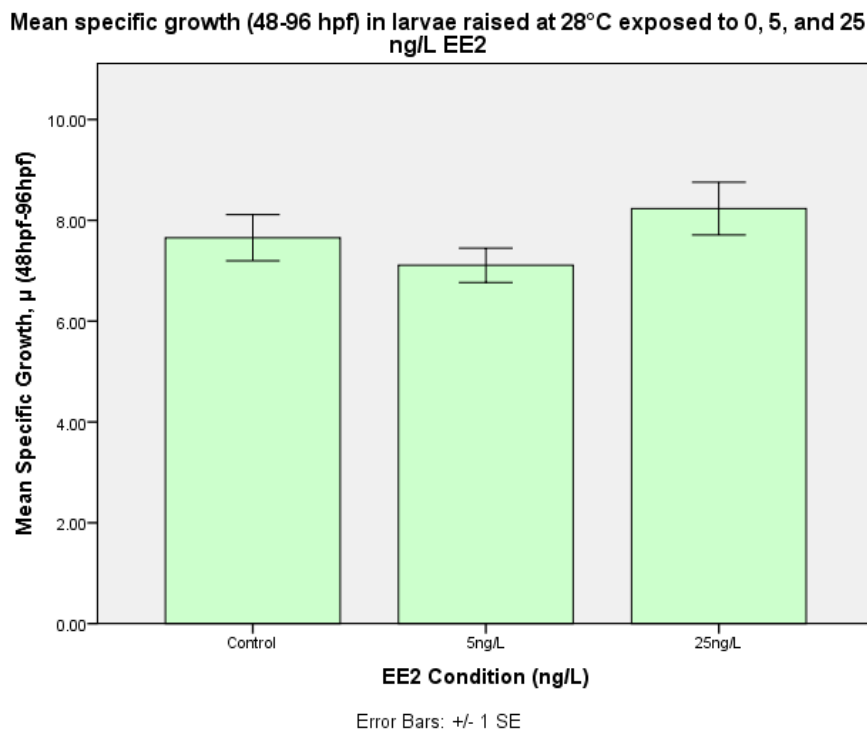


Figure 4.6. Mean specific growth (48–96 hpf) for chemically-unexposed and EE2-treated larvae reared at $28\pm 1^\circ\text{C}$, reported as mean ± 1 SEM.

Mean specific growth rate was found to occur more slowly in 5ng/L EE2-exposed larvae raised at 32±1°C (mean specific growth = 4.6 ± 2.0 μ) compared to chemically-unexposed larvae raised at 28±1°C (mean specific growth = 7.7 ± 1.9 μ), $t(34) = 4.605$, $p = 0.000$ (Figure 4.7). The 28±1°C chemically-unexposed larval growth data was used here as the optimal raising condition ‘control-control’ baseline from which to compare the interactive influence of chemical exposure plus temperature stress. The effect size for this analysis ($d = 1.54$) was found to exceed Cohen’s (1988) convention for a large effect ($d = 0.8$). The difference observed between 5ng/L EE2 + 32±1°C larval growth compared with chemically-unexposed + 28±1°C larvae was more highly significant than that observed between larval growth in the 28±1°C and 32±1°C chemically-unexposed larvae. This result suggested that the independent variables of temperature and chemical treatment may have been acting additively at these levels (5ng/L EE2 + 32±1°C) to impact specific larval growth.

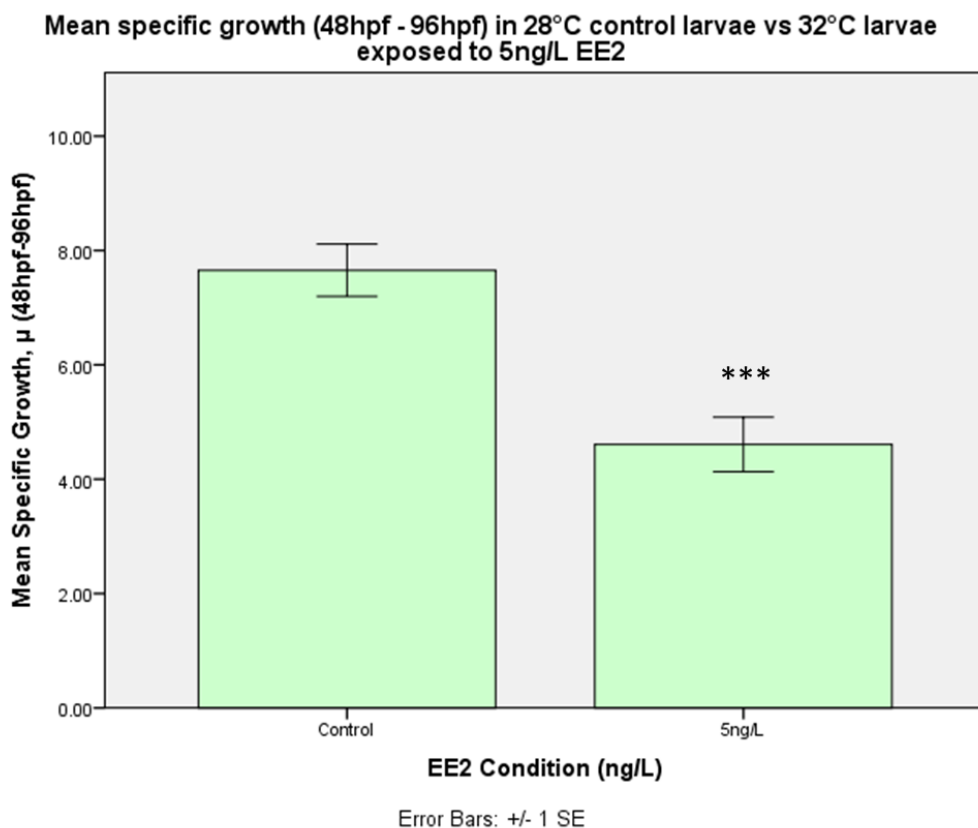


Figure 4.7. Mean specific growth (48–96 hpf) for chemically-unexposed larvae raised at 28±1°C compared to 5ng/L EE2-exposed larvae raised at 32±1°C, reported as mean ± 1SEM (asterisks indicate significant difference compared with ‘control-control’ chemically-unexposed + 28±1°C larvae, *** $p < 0.001$).

Mean specific growth was significantly reduced for larvae exposed to 25ng/L EE2 and maintained at 32±1°C (mean specific growth = 5.62 ± 2.4 μ) compared to chemically-unexposed larvae raised at 28±1°C (mean specific growth = 7.7 ± 1.9 μ), $t(40) = 2.919$, $p = 0.006$ (Figure 4.8.). The 28±1°C unexposed larvae were used here as control-control baseline from which to compare the interactive influence of chemical exposure plus temperature stress. The effect size for this analysis ($d = 0.92$) was found to exceed Cohen's (1988) convention for a large effect ($d = 0.8$). Larval specific growth was no more significantly higher for 32±1°C + 25ng/L EE2-larvae compared to chemically-unexposed larvae, suggesting that EE2 exposure was not influencing growth in addition to temperature conditions

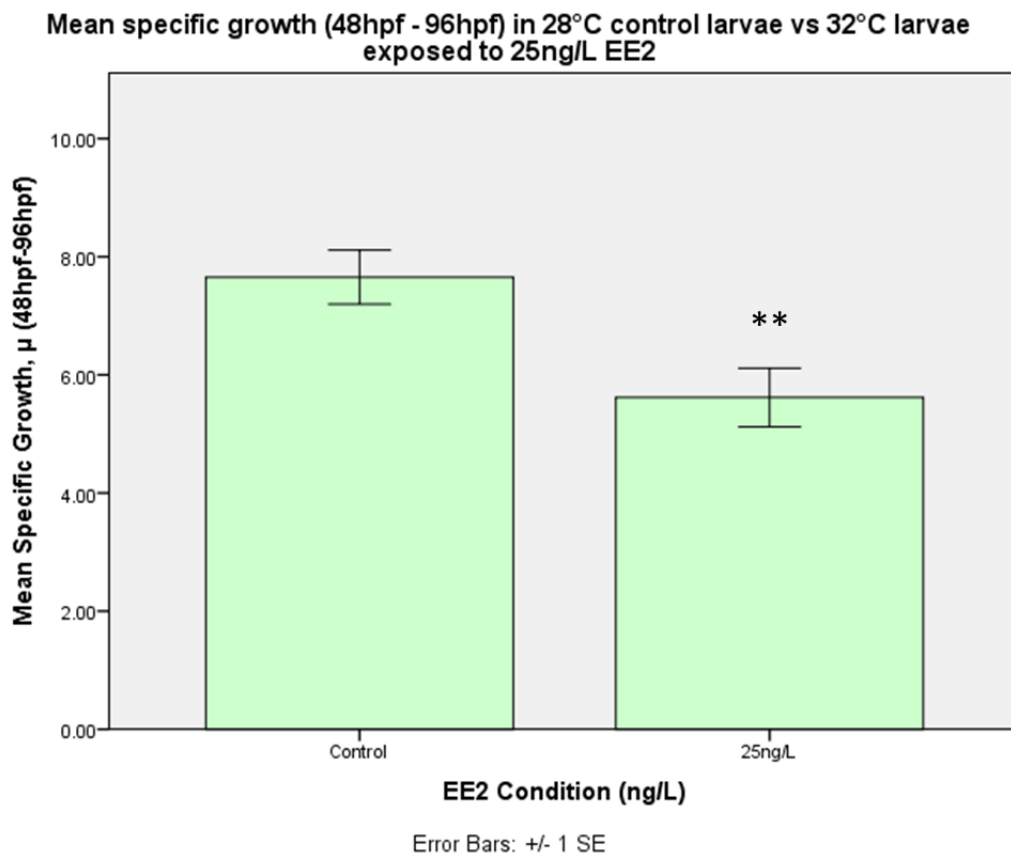


Figure 4.8. Mean specific growth (48 – 96 hpf) for chemically-unexposed larvae raised at 28±1°C compared to 25ng/L EE2-exposed larvae raised at 32±1°C, reported as mean ± 1SEM (asterisks indicate significant difference compared with chemically-unexposed + 28±1°C larvae, ** $p < 0.01$).

4.3.4 Mean larval fluorescence

Mean larval fluorescence was calculated using the Mean Top 100-pixel intensity masking strategy value for all larvae before averaging across the three datasets, giving mean larval intensity readings for each chemical treatment + temperature condition at each of the 3 sampling timepoints.

Mean larval fluorescence responses for all chemically-unexposed larvae raised under the high and low temperature conditions ($24\pm 1^\circ\text{C}$ and $32\pm 1^\circ\text{C}$) across time (48hpf – 96hpf) were compared with chemically-unexposed larval responses at control temperature $28\pm 1^\circ\text{C}$ (Figure 4.9.). No significant differences in larval GFP were seen at any of the timepoints at the $p < 0.05$ level. These results indicated that there was no effect of temperature alone on GFP induction levels.

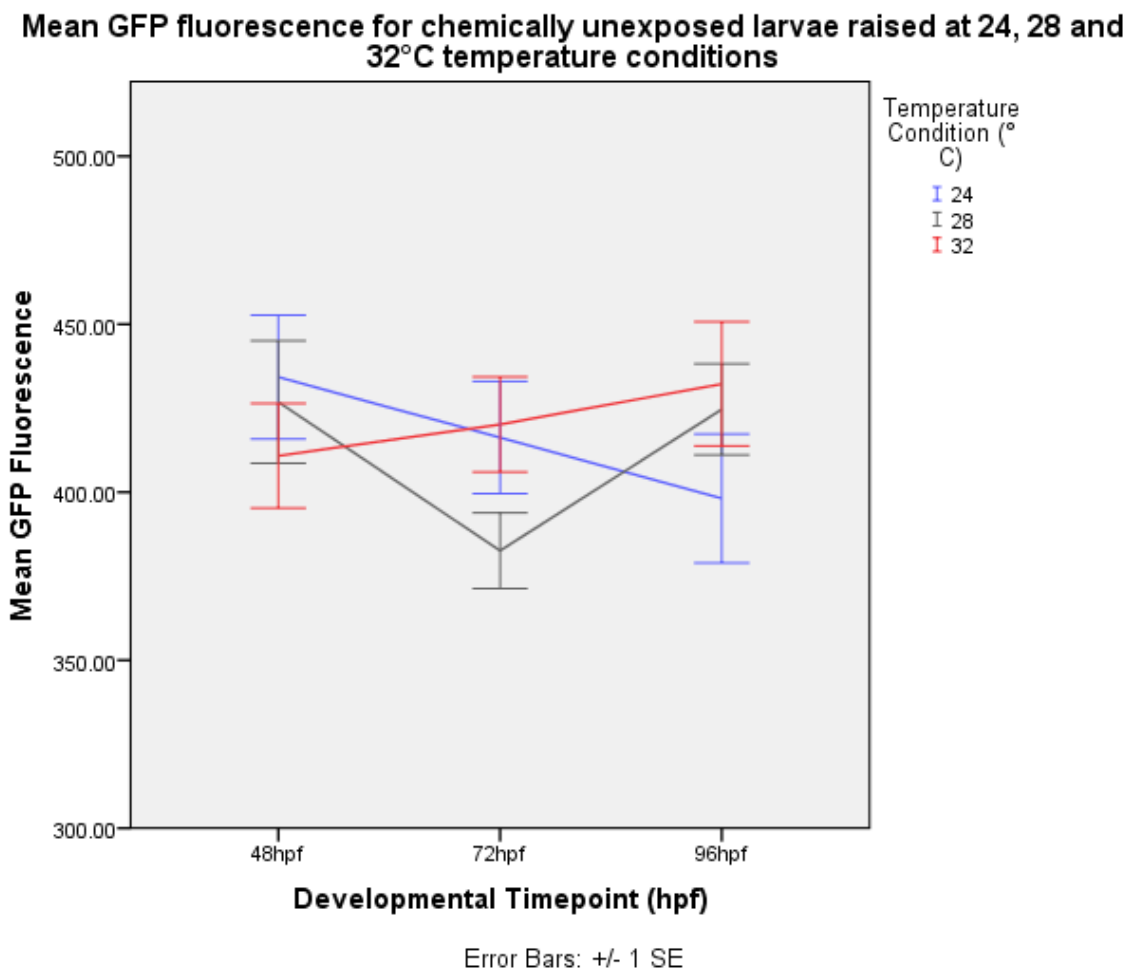


Figure 4.9. Larval fluorescence responses for all chemically-unexposed larvae raised under three different temperature conditions, reported as mean \pm 1SEM.

Mean larval fluorescence responses for all 5ng/L EE2-exposed larvae raised under experimental temperature conditions ($24\pm 1^\circ\text{C}$ and $32\pm 1^\circ\text{C}$) across time (48hpf – 96hpf) were compared with 5ng/L EE2-exposed larval responses at $28\pm 1^\circ\text{C}$ (Figure 4.10.). We found no significant differences between the different incubation temperatures at any of the timepoints at the $p < 0.05$ level. A two-way independent ANOVA demonstrated that there was, however, an overall significant main effect of the incubation temperature on GFP expression at each timepoint: 48 hpf: $F(2,236) = 13.33$, $p < 0.001$; 72 hpf: $F(2,228) = 5.74$, $p < 0.01$; 96 hpf: $F(2,195) = 3.04$, $p < 0.05$.

Mean GFP fluorescence for 5ng/L EE2-exposed larvae raised at 24, 28 and 32°C temperature conditions

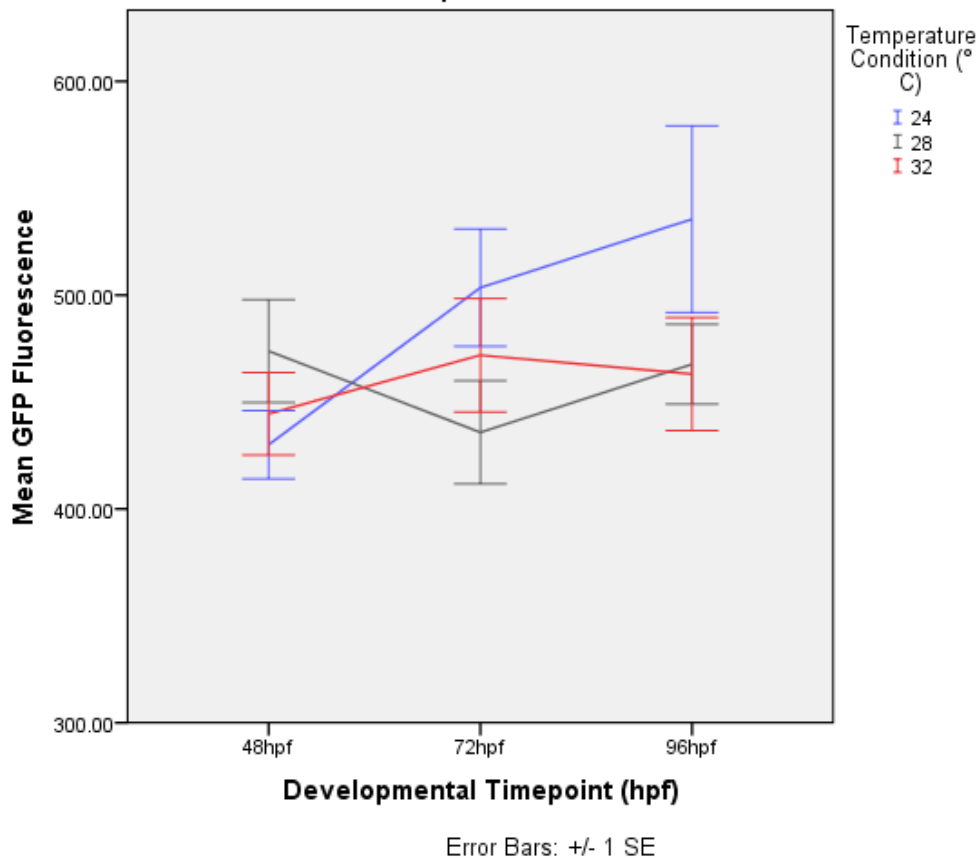


Figure 4.10. Larval fluorescence responses for all 5ng/L EE2-exposed larvae raised under the three different temperature conditions, reported as mean \pm 1SEM.

Mean larval fluorescence responses for all 25ng/L EE2-exposed larvae raised under experimental temperature conditions ($24\pm 1^\circ\text{C}$ and $32\pm 1^\circ\text{C}$) across time (48hpf – 96hpf) were compared with 25ng/L EE2-exposed larval responses at control temperature $28\pm 1^\circ\text{C}$ (Figure 4.11.). Fluorescence response was significantly lower in the EE2-treated $24\pm 1^\circ\text{C}$ larvae compared to EE2-treated $28\pm 1^\circ\text{C}$ larvae at 72 hpf (** $p < 0.01$) and significantly lower in the EE2-treated $32\pm 1^\circ\text{C}$ larvae compared to $28\pm 1^\circ\text{C}$ larvae at 96 hpf (* $p < 0.05$).

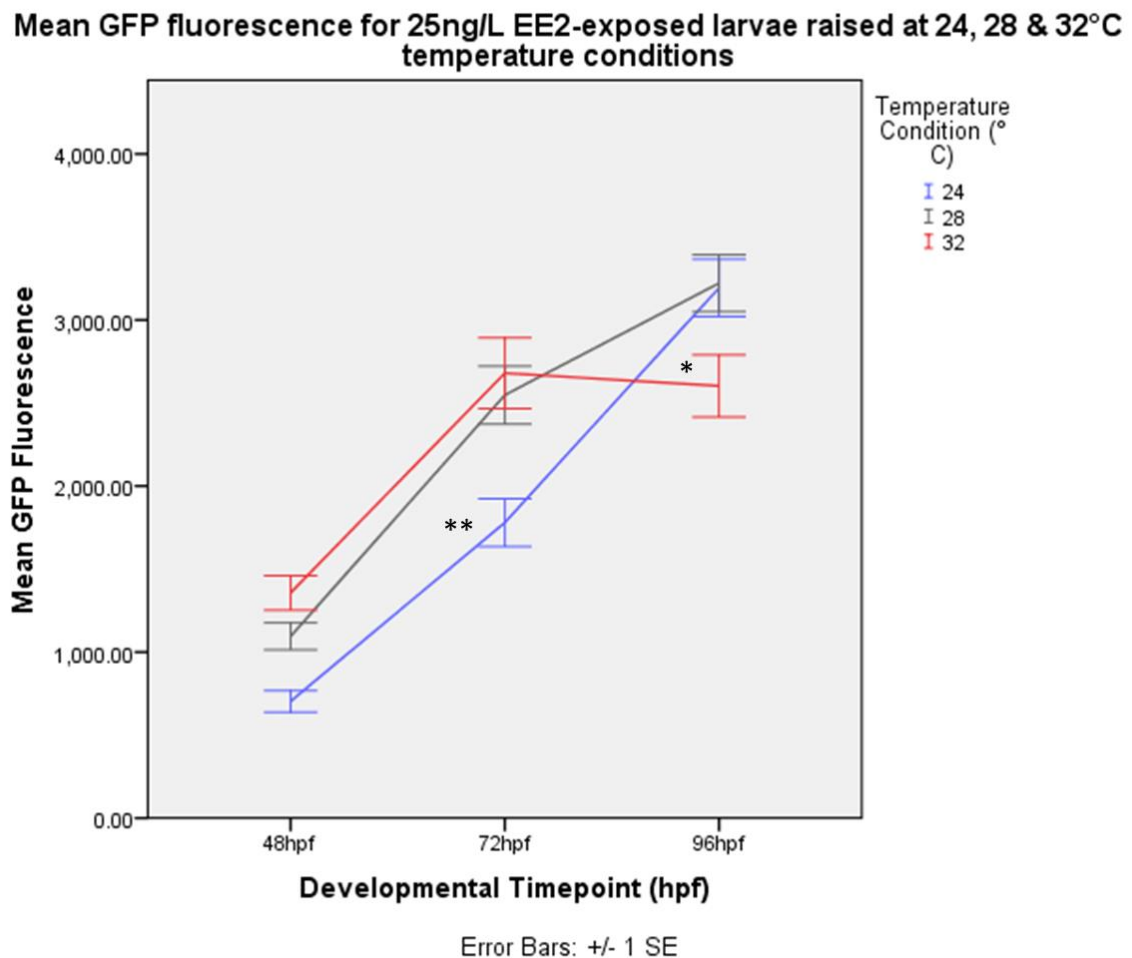


Figure 4.11. Larval fluorescence responses for all 25ng/L EE2-exposed larvae raised under the three different temperature conditions, reported as mean \pm 1SEM (asterisks indicate significant difference compared with 25ng/L EE2-exposed + $28\pm 1^\circ\text{C}$ larvae, * $p < 0.05$, ** $p < 0.01$).

4.3.5 Comparison of control temperature, chemically-unexposed larvae with test temperature, EE2-exposed larval fluorescence responses

Mean larval fluorescence responses in chemically-unexposed larvae raised at control temperature $28\pm 1^\circ\text{C}$ (hereafter 'control-control') were used as a baseline for comparison with EE2 treatment + experimental temperature larvae to investigate the potential interactive effects of chemical stressor (EE2) + temperature stressor on larval estrogen responses. Fluorescence responses in 25ng/L EE2-exposed treatment groups were found to be significantly higher than in control-control larvae regardless of temperature conditions and life stage (timepoints) hence, we did not run any comparisons on these data for the purposes of comparing fluorescence responses in conjunction with test temperatures.

No significant differences were found between 5ng/L EE2-exposed + $28\pm 1^\circ\text{C}$ larval responses compared with control-control larval responses over time (Figure 4.12.). Although EE2-induced larval fluorescence responses in the 5ng/L EE2-exposed + $28\pm 1^\circ\text{C}$ treatment group were consistently higher than control-control larval fluorescence responses for all timepoints, these differences were not found to be significant at the $p < 0.05$ level.

Mean GFP fluorescence responses in control vs larvae exposed to 5ng/L EE2 maintained at 28°C

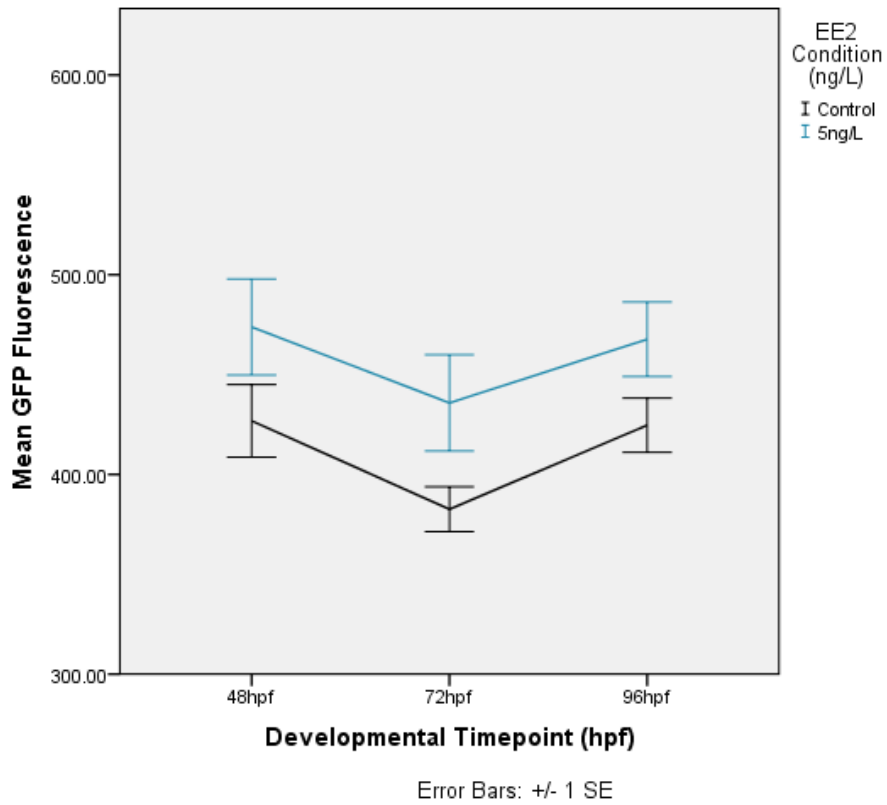


Figure 4.12. Mean control-control larval fluorescence responses compared with 5ng/L EE2-exposed + $28\pm 1^\circ\text{C}$ larval responses, reported as mean ± 1 SEM.

The interaction between the $24\pm 1^\circ\text{C}$ temperature + EE2 (5ng/L) exposure shows a steady increase in fluorescence with increasing time compared to 28°C control-control. The combined influence of 5ng/L EE2 and low temperature appeared to be having a strong influence on larval fluorescence induction at the 72 hpf timepoint, with a significantly enhanced estrogen-induced GFP response above the control-control baseline response. A Mann-Whitney U test indicated that the mean 5ng/L EE2-induced larval fluorescence response was significantly elevated in larvae raised at $24\pm 1^\circ\text{C}$ at the 72 hpf screening timepoint (Figure 4.13.) compared to control-control larvae ($U = 147, p = 0.001$).

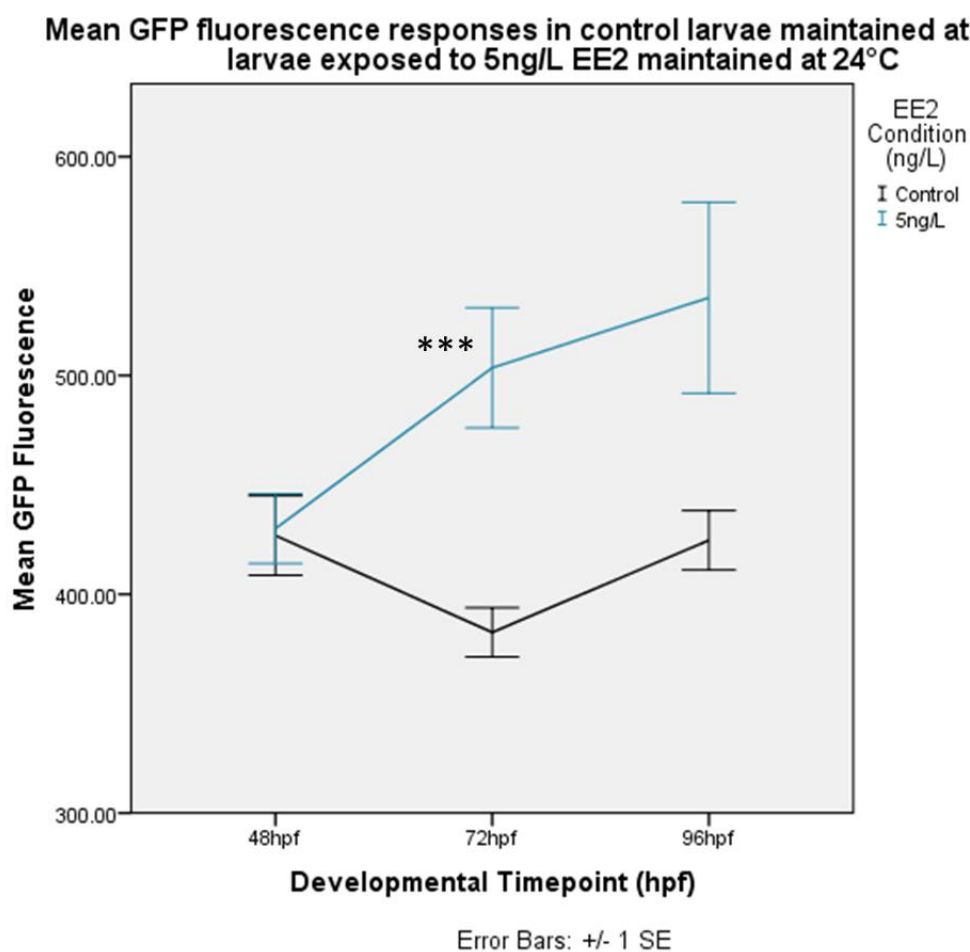


Figure 4.13. Mean control-control larval fluorescence responses compared with 5ng/L EE2-exposed + $24\pm 1^\circ\text{C}$ larval responses, reported as mean ± 1 SEM (asterisks indicate significant difference compared with control-control larval response, *** $p < 0.001$).

A Mann-Whitney U test indicated that the mean fluorescence response under the combined influence of $32\pm 1^\circ\text{C}$ + 5ng/L EE2 was significantly elevated at the 72 hpf screening timepoint (Figure 4.14.) compared with the control-control larvae ($U = 128, p = 0.003$). The interaction between the $32\pm 1^\circ\text{C}$ temperature + EE2 exposure appeared to have had a strong influence on larval fluorescence induction at the 72 hpf timepoint, significantly enhancing the estrogen-induced GFP response above the control-control baseline response.

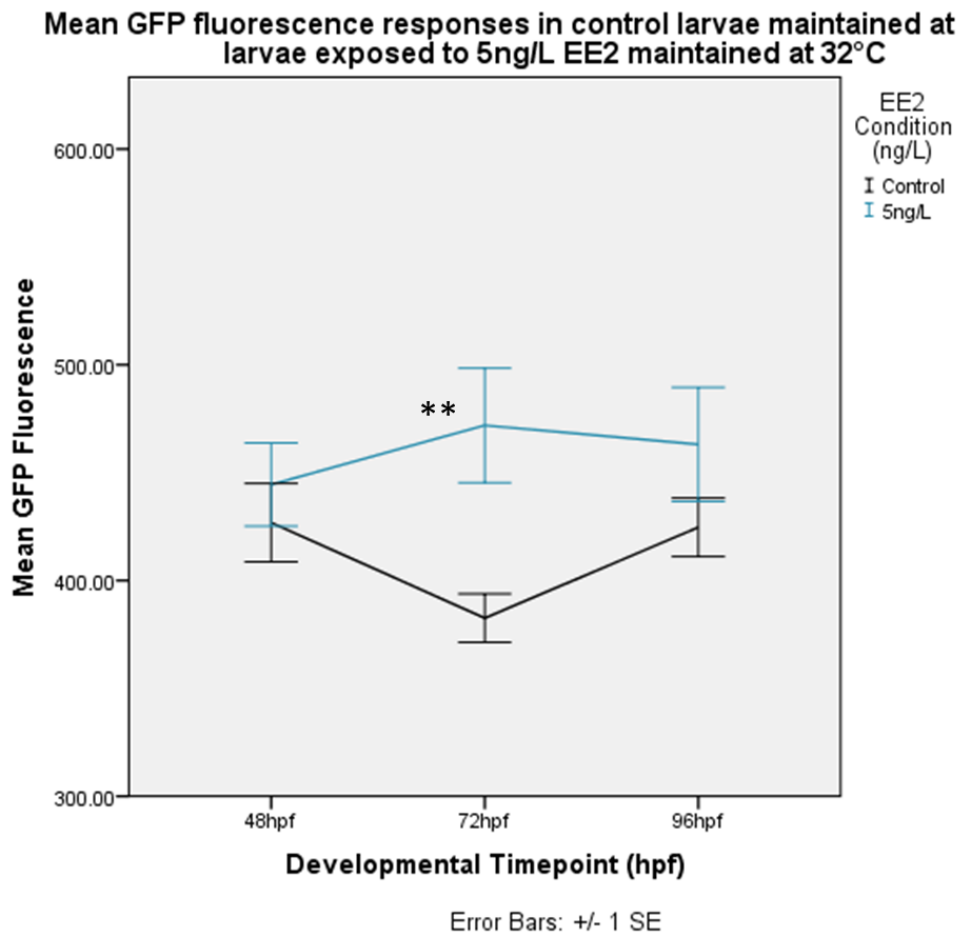


Figure 4.14. Mean larval fluorescence responses for chemically-unexposed control larvae raised under $28\pm 1^\circ\text{C}$ temperature conditions compared to larval fluorescence responses induced in 5ng/L EE2-exposed + $32\pm 1^\circ\text{C}$ larvae, reported as mean ± 1 SEM (asterisks indicate significant difference compared with control-control larval response, ** $p < 0.01$).

4.4 Discussion

4.4.1 Effects of temperature on larval size and specific growth rate

A two-way independent ANOVA showed that there was a significant main effect of the incubation temperature on the overall specific growth rate of the larvae, $F(2,185) = 20.14$, $p < 0.001$.

Looking at the influence of the different incubation temperatures individually, larvae kept at the warmer thermal regime appeared to be initially (< 48 hpf) larger, before their growth rate slowed and their subsequent size (at 72 hrs onwards) matched that of larvae maintained at the optimal temperature ($28\pm 1^\circ\text{C}$). Compared with control-control animals, larvae maintained at $32\pm 1^\circ\text{C}$ were found to be significantly larger at the earliest 48hpf timepoint ($p < 0.01$, Figure 4.4.). Larval size for the $24\pm 1^\circ\text{C}$ condition was consistently smaller than for the other two temperatures, although this was only comparatively significant at 96 hpf ($p < 0.01$, Figure 4.4.).

Looking at chemically-unexposed animals only over time, larvae grew most rapidly within the experimental timeframe (48 hpf – 96 hpf) under optimal ($28\pm 1^\circ\text{C}$) temperature conditions. We found larval growth rate to be slowest at the highest ($32\pm 1^\circ\text{C}$) temperature condition (Figure 4.5.) despite larvae being significantly larger at the initial time-point compared with the control-controls (Figure 4.4.). This finding is not consistent with studies showing higher larval growth rates at increased water temperatures (Benoît et al., 2000; Blaxter, 1991; Green & Fisher, 2004; McCormick & Molony, 1995; Meekan et al., 2003). A possible explanation for this finding is that at 32°C , the larvae were developed to a stage where they could not maintain their initially elevated growth rate (seen at 48 hpf) without feeding (their energy reserves being dictated by the yolk provision).

The zone of thermal tolerance is thought to be significantly narrower in fish embryos and larvae (Blaxter, 1991; Pepin, 1991), and the capacity to tolerate more extreme temperatures increases with the advancement of development, although different species likely acquire these tolerances at varying rates (Rombough, 1997). Larval specific growth rate appeared to be marginally (although non-significantly) slower for larvae reared at the cooler ($24\pm 1^\circ\text{C}$)

temperature regime compared to control-controls. This was reflected in their significantly smaller size at 96hpf, when unexposed larvae were compared against control-controls at each time-point (Figure 4.4.).

Tropical species, like zebrafish, tend to show limited variation in the width of their thermal tolerance zone as development proceeds. For example, embryonic, larval and adult Mozambique tilapia (*Oreochromis mossambica*) all have upper thermal tolerance limits within $\sim 2^{\circ}\text{C}$ of each other (Allanson & Noble, 1964; Subasinghe & Sommerville, 1992). The reductions in larval growth rate (in comparison to fastest growth rates seen at $28\pm 1^{\circ}\text{C}$) which we observed at the lowest ($24\pm 1^{\circ}\text{C}$) and highest ($32\pm 1^{\circ}\text{C}$) temperature conditions, suggested that maximal thermal tolerance limits for normal zebrafish development (at this particular life-stage) may have been reached (Figure 4.5.).

Previous research investigating the effects of temperature on early-life growth rate (standard body length) in zebrafish at 8 and 12 weeks post-hatch, reported a decrease in rate of growth for fish raised at elevated (32°C) temperatures compared with those raised under near-optimal (27°C) thermal conditions (Schnurr et al., 2014). Fish raised at the lowest tested temperature (22°C) were reported to be comparatively larger. However, the rates of growth from post-hatch to point-of-sampling were not interrogated in this study. There is an apparent scarcity of data concerning rates of embryonic and early larval growth in zebrafish raised under temperature conditions close to thermal tolerance thresholds. However, it seems likely that early-life growth rate varies over time, and temperature may have less or more of a prominent influence depending on developmental stage.

Relatively small changes in water temperature can result in a chain of stress events that can disrupt normal growth rate, metabolism, and overall health in fish (Groot, 2010). The stress response is generally assumed to have evolved to help organisms avoid or overcome short-term challenges, but when potentially threatening events cannot be resolved, the hypothalamus-pituitary-interrenal (HPI) axis may be activated for prolonged periods of time, leading to a chronically extended maladaptive stress responses (Barton et al., 2002). Exposure to an unalleviated stressor may result in reproductive disruption, loss of immunocompetence and growth suppression in the affected animal (Bonga,

1997). There is a metabolic cost associated with stress presumed to be brought about by a shift in energy resources away from normal functioning in order for the organism to cope with the stressor (Schreck, 1982). It is feasible that the reduced larval growth rate we observed was brought about by maladaptive stress responses induced by chronic undesirable thermal conditions. Results such as ours, in conjunction with what has been reported in the literature, emphasise the need for a focus on experimental temperature when planning studies using early life-stage fish models and interpreting subsequent data. Variations in growth and metabolism are likely to influence a host of molecular and morphological endpoints.

4.4.2 Combined effects of temperature and EE2 on larval specific growth

A two-way independent ANOVA showed that overall there was a nonsignificant interaction between the incubation temperature and the level of EE2 exposure on larval specific growth, $F(2,185) = 1.6$, $p = 0.176$.

EE2 exposure appeared to have no influence on larval specific growth in larvae raised at $28\pm 1^\circ\text{C}$ compared with chemically-unexposed larvae (Figure 4.6.). Previous research has demonstrated a significant reduction in body weight and length in zebrafish exposed to 25ng/L EE2 for 3 months post-fertilisation compared to unexposed controls (Van den Belt et al., 2003). It is likely that we would have seen the same effects on growth in chemically-exposed fish had we extended this study. The combined stressors of high temperature ($32\pm 1^\circ\text{C}$) and EE2 exposure (low concentration, 5ng/L) did, however, appear to have a significant effect on reducing larval specific growth compared to the control-control larvae ($p < 0.001$, Figure 4.7.). Unexpectedly, this observation was not supported by data for the highest temperature ($32\pm 1^\circ\text{C}$) in combination with the highest EE2 dose (25ng/L); here, larval growth rate was not more reduced than that of the chemically-unexposed larvae at optimal ($28^\circ\text{C}\pm 1$) temperatures compared with larval growth at the elevated ($32^\circ\text{C}\pm 1$) temperature regime (Figure 4.8.). No significant differences in larval specific growth rates were observed for EE2-exposed or chemically-unexposed larvae raised under $24\pm 1^\circ\text{C}$ compared to control-controls.

Previous studies investigating the combined effects of temperature and chemical stressors on developmental parameters in fish have reported temperature-specific perturbations similar to those seen at our low EE2 exposure concentration. For example, cadmium exposure (≤ 27 mg/L) was found not to have any significant effect on the developmental speed of Atlantic salmon (*Salmo salar*) under normal temperature conditions, but at a low temperature (21°C) regime, significantly high mortality was observed (Rombough & Garside, 1982).

An in-depth analysis of zebrafish developmental aberrations in response to cadmium exposure (0, 0.25, 0.5, 2, 5, and 10mg/L) revealed moderate to severe embryological morphological defects only in zebrafish raised at temperatures higher (33°C) and lower (21°C) than control (26°C) thermal conditions (Hallare et al., 2005). Exposure to even the lowest (0.25mg/L) cadmium concentrations caused acute oedema of the heart and head, spirality of the central nervous system, tail degeneration and helical bodies in 8 day post-hatch zebrafish raised at temperatures above and below the control.

It is well-acknowledged that undesirable temperature conditions are capable of provoking stress responses in fish, and these responses can subsequently suppress growth (Bonga, 1997). It is also widely-accepted that environmental pressures (such as temperature stress) can interact with chemical stressors (such as EDCs) to generate unpredictable responses (Brian et al., 2008). Estrogenic pollutants themselves have been shown to cause alterations in growth rate in fish. For example, highly significant retardation of growth has been reported in brown trout (*Salmo trutta*) embryos exposed to a low concentration (3.8ng/L) of the EEDC 17 β -estradiol (E2) at 0 dpf (Schubert et al., 2014). Similar results were observed after exposing 3 hour pre-fertilization rainbow trout (*Oncorhynchus mykiss*) oocytes to the EEDC bisphenol A (BPA), and the effects were found to persist for a year (Aluru et al., 2010). As we found at the low-dose of EE2 (5ng/L), the combination of thermal and chemical stressors appeared to exacerbate larval growth retardation, resulting in a more pronounced reduction in larval growth rate than seen in the chemically-unexposed but thermally-perturbed fish. It should be noted, however, that estrogenic compounds can act as growth promoters in post-embryonic animals: in the U.S., estrogenic implants (often containing E2) and estrogen-enriched feeds are widely used to augment the growth of cattle (reviewed in Kolok & Sellin, 2008).

However, we did not observe the same level of growth retardation in larvae exposed to EE2 at the highest dose (25ng/L) under any of the temperature regimes. A possible explanation for this could be that there is a non-monotonic dose-response, which occurs when toxicant effects are highest at low- to intermediate-exposure levels, and decreased or no effects are observed at high exposures. The endocrine system has evolved to respond to very low doses of hormones during certain life stages (Christiansen et al., 2014) and estrogens have been shown to have potency at low exposure concentrations, despite no effect being evident at high doses (Parrella et al., 2014). This low dose effect may be subsequently exacerbated under additional thermal stress conditions, resulting in the retardation of growth observed in the present study. We have provided here support for the potential existence of non-monotonic dose-responses to EDCs in an early life-stage fish model, while generating discussion for further investigation into how varying experimental temperatures might amplify such effects.

4.4.3 Combined effects of temperature and EE2 on larval estrogenic (GFP induction) responses

A two-way independent ANOVA showed that there was a highly significant interaction between the incubation temperature and concentration of EE2 exposure on larval GFP responses at all timepoints, 48 hpf: $F(4,236) = 13.66$, $p < 0.001$; 72 hpf: $F(4,228) = 7.09$, $p < 0.001$; 92 hpf: $F(4,195) = 3.12$, $p < 0.01$. There was also a significant main effect of the incubation temperature alone on GFP expression, 48 hpf: $F(2,236) = 13.33$, $p < 0.001$; 72 hpf: $F(2,228) = 5.74$, $p < 0.01$; 96 hpf: $F(2,195) = 3.04$, $p < 0.05$. Unsurprisingly, the dose of EE2 also had a significant main effect on the estrogen-induced GFP response, 48hpf: $F(2,236) = 140.57$, $p < 0.001$; 72 hpf: $F(2,228) = 301.48$, $p < 0.001$; 96 hpf: $F(2,195) = 507.17$, $p < 0.001$.

Estrogen-induced larval fluorescence responses to the highest (25ng/L) EE2 exposure were very pronounced and increased substantially over time for fish under all three thermal regimes. The only exception to this was for $32 \pm 1^\circ\text{C}$ + 25ng/L EE2-exposed larvae, where responses between 72-96 hpf appeared to begin to plateau (Figure 4.11.). We observed larval fluorescence responses to be

significantly lower in larvae exposed to 25ng/L at $24\pm 1^{\circ}\text{C}$ and $32\pm 1^{\circ}\text{C}$ ($p < 0.01$, $p < 0.05$ at 72hpf and 96hpf, respectively) compared to larvae raised under control temperature conditions. A possible explanation for these differences could be that the thermal conditions in which the larvae were reared were either accelerating or retarding their responses to the chemical stressor at the high or low temperatures, respectively. For example, at the $32\pm 1^{\circ}\text{C}$ temperature condition, the estrogenically-induced larval fluorescence was the most amplified compared to the other temperature groups, and increased most rapidly between 48-72 hpf, before beginning to plateau and decline between 72-96 hpf. This could be evidence of a modulatory mechanism being activated as a reaction to chronic stress exposure, allowing the larvae to neutralise the stressors and maintain endocrine homeostasis in terms of estrogen receptor signalling. Alternatively, the plateau in fluorescence responses that we observed may have been caused by stress-induced cell apoptosis in the highly EE2-responsive liver. This depletion of liver cells might have resulted in attenuation of liver-specific GFP expression. Further analysis to test this theory could make use of TUNEL staining to visualise and quantify cell apoptosis *in vivo*.

Similar response patterns were observed in juvenile female Atlantic salmon treated with E2 (10mg/kg body weight) implants and maintained at low (14°C) or high (22°C) temperature conditions (Anderson et al., 2012). At 3 days post-treatment, levels of vtg expression were found to be significantly higher in the E2-treated fish reared at the high temperature (22°C) compared with a corresponding group of fish maintained at 14°C , indicating that gene expression had been induced more quickly at the elevated temperature. However, at 7 days post-implant, expression levels of vtg were approximately equal between the two temperature groups, and at 14 days post-implant, vtg expression was lower in the 22°C group than for the 14°C fish.

It has also been suggested that the rate of physiological processing increases in ectotherms in response to increases in temperature (Sokolova & Lannig, 2008). It is therefore possible that the rapid induction and initially increased levels of EE2-induced larval GFP expression at higher temperatures observed during the present study, followed by a later plateau in fluorescence, may be attributed to more rapid utilisation - and subsequent clearance - of EE2. Measuring fish blood

plasma metabolites following exposure to EE2 could be an interesting extension of this work.

Significantly elevated responses to EE2 were observed in larvae exposed to the lowest dose (5ng/L) of EE2 compared with chemically-unexposed $28\pm 1^\circ\text{C}$ (control-control) larvae, but only in the groups reared at the highest ($32\pm 1^\circ\text{C}$) and lowest ($24\pm 1^\circ\text{C}$) temperatures at the 72 hpf timepoint ($p < 0.001$ and $p < 0.01$ respectively, Figures 4.13. and 4.14.). It is interesting that the only significant differences seen in larval fluorescence responses compared to control-control fish at the low-dose EE2 exposure were the elevated levels of GFP expression seen at $24\pm 1^\circ\text{C}$ and $32\pm 1^\circ\text{C}$ at 72 hpf. As with specific larval growth, this transient but highly significant increase in EE2-induced fluorescence could be attributed to the combined effects of thermal and chemical stressors. The 72 hpf timepoint, at which both thermally-stressed groups of 5ng/L EE2-exposed larvae were found to respond most markedly, could be indicative of a window of enhanced vulnerability, where larvae under stressful temperature conditions were most sensitive to estrogenic endocrine disruption. Consideration of such windows may be pertinent when interpreting responses to EDCs in model fish.

The timing of exposure to EDCs is thought to represent a critical factor affecting how an organism responds to the pollutant. This 'critical window' of vulnerability varies depending on the point at which specific organs and tissues develop (Mittendorf, 1995), and it has been suggested that different receptors are likely present in different cell types during advancing stages of development (Watson et al., 2007; Watson et al., 2005). It is therefore probable that EDCs such as EE2 might elicit diverse effects at different developmental stages in an exposed organism, particularly if exposure occurs in conjunction with an additional stressor, such as a temperature regime close to the limits of an organism's thermal tolerance, an important dynamic to consider when conducting studies into teleost EDC exposure responses.

4.5 Conclusions

The results of this investigation indicate that temperature and estrogenic chemicals can interact to alter larval fish responses to an estrogenic chemical at both the molecular and morphological level. However, the subsequent effects were not always predictable and there seem to be both developmental stage and chemical concentration-dependent effects, with apparent windows of sensitivity. It may prove useful for researchers to take these windows of enhanced vulnerability into account when considering the results of early life-stage EDC exposure in model fish. The molecular basis for the enhanced GFP induction observed in larval responses to EE2 under temperature stress at 72hpf is beyond the scope of the present study, but could represent an area of further research in the investigation of periods of vulnerability to endocrine disruption during embryonic development in the presence of additional stressors.

We have shown here that a relatively low concentration of EE2 (5ng/L) can exacerbate the disruption of normal larval growth rate when combined with a thermal stressor. This finding adds emphasis to the need to better understand how ectotherm responses to EEDC exposure will be impacted by the projected climate change scenario and provides greater understanding of how experimental variations in temperature might influence growth data.

The lowest EE2 dose exposure (5ng/L) tested during the present study has been measured in the environment. For example, concentrations of EE2 in German wastewater effluents have been reported to range from 9ng/L (Kuch & Ballschmiter, 2001) to 15ng/L (Ternes et al., 1999). Similarly, levels ranging from 4-8ng/L EE2 were observed in effluent waters of France and the Netherlands (Belfroid et al., 1999; Cargouët et al., 2004), and EE2 concentrations in U.K. effluents have been recorded at concentrations of around 7ng/L (Desbrow et al., 1998). It therefore seems realistic that some aquatic organisms will experience the dual stressors of temperature change and high level estrogen exposure in combination.

We reported a significant main effect of incubation temperature alone on estrogen-induced GFP response in our zebrafish model in addition to a significant interaction between thermal regime and EE2. Being that zebrafish are frequently used as models of endocrine disruption in EDC evaluation, the affirmation that

thermal rearing conditions have the capacity to significantly alter responses to hormones means that water temperature should be carefully controlled during experiments to avoid potential misinterpretation of EDC action. When EDC-influenced teleost molecular endpoints are being considered in an environmental setting where temperature cannot be controlled, thermal conditions should be diligently recorded and taken into account when interpreting results.

Chapter 5

General Discussion



Chapter 5.

General Discussion

The objective of this thesis was to establish the optimal quantitative capability of a semi-automated, medium-throughput *in vivo* bioimaging assay using an estrogen-responsive transgenic (TG) zebrafish (*Danio rerio*) model (ERE:GFP:Casper) exposed to environmentally-relevant levels of a potent estrogenic endocrine disrupting chemical (EEDC), 17 α -ethynylestradiol (EE2). Parameters including controlled-breeding, accurate developmental staging, and orientation of the TG model were appraised in terms of their relative contribution to assay sensitivity and repeatability (Chapter 3.). The automated imaging system was also directly compared to a higher-content manual imaging modality in order to assess respective acquisition times, sensitivity and variation in quantified fluorescence responses. Test chemical preparation was highly standardised in an effort to achieve the best possible assay robustness, and a range of image analysis approaches applied with the aim of detecting EE2-induced fluorescence responses in the model under low (ng/L) exposure conditions. These established optimised assay parameters were then carried forward for examining the influence of an additional abiotic stressor (adverse temperature conditions) on EE2-induced fluorescence responses and growth in the larval TG model (Chapter 4.). Below, a synthesis of these results, their contributory value, and limitations will be discussed.

5.1 Optimised parameters for a semi-automated *in vivo* estrogenic screening assay

Despite endocrine disrupting chemicals representing a well-recognised health concern for humans and wildlife alike, there is currently a shortage of higher-throughput screens for quantifying estrogenic disruption *in vivo*. This is partially due to the need for transgenic animal models that are capable of responding sensitively and reliably to environmentally-relevant levels of estrogenic chemicals, and also because of a lack of affordable modalities that can

automatically quantify fluorescent responses in live animals arrayed in multiwell plates. In addition, there is an increasing emphasis on researchers to refine assays and reduce the number of animals used in research, while replacing vertebrate adult models with embryonic-stage animals incapable of independent feeding (<5 days post-fertilisation, dpf, for zebrafish) where possible.

Using the estrogen-responsive ERE:GFP:Casper model (developed by Green et al., 2016), parameters for obtaining the most sensitive dose-response data in 4dpf larvae were established. Embryos generated using a pair-spawn approach produced more sensitive data, with recorded green fluorescent protein (GFP) expression significantly elevated above that of chemically-unexposed larvae at 5ng/L EE2, and recorded response variation between individual animals was reduced compared to that of group-spawned larvae. This finding corroborates guidelines advocating the use of genetically-uniform models for minimising individual-level variation in response to toxicants (Barata et al., 2000; Nowack et al., 2007). More robust *in vivo* assays can reduce numbers of animal models required for statistically significant quantification of fluorescence responses. However, it has been suggested that such homogenisation of study populations may limit the reproducibility and external validity of results – an effect known as the ‘standardisation fallacy’ (Würbel, 2000; Würbel, 2002). This effect is thought to come about as a result of highly-standardised experimentation providing ‘direct information only with respect to the narrow range of conditions achieved by standardisation’ (Fisher, 1937). A number of simple precautions have been proposed for minimising standardisation fallacy, including testing animals in small batches across different days as opposed to using one large batch (Paylor, 2009), an approach adopted in Chapter 4.

Previous research using the ERE:GFP:Casper model recommended uniform lateral orientation of the model for improved fluorescence data acquisition (Green et al., 2016), and it was predicted that such standardisation would further reduce recorded individual-level fluorescence intensity variation. Contrary to this assumption, variably-orientated larvae generated fluorescence data variability comparable to that of uniform laterally-orientated animals. The most likely explanation for this negative finding is that the translucency of the ERE:GFP:Casper allowed for uninterrupted penetrance of the estrogen-induced fluorescence response, negating the need for specific orientation of the larval

body. This finding supported reports of an improved fluorescence signal in the ERE:GFP:Casper compared to the original pigmented ERE:GFP model (Green et al., 2016) and upheld the utility of the pigment-free 'Casper' phenotype for incorporation in further fluorescence reporter TG models. However, for higher-content qualification and quantification of fluorescence responses at the tissue-specific level, exposed larvae would need to be suitably orientated to best view and delineate the specific region of interest. The VAST Bioimager system represents a commercially-available platform capable of precisely orientating larvae for imaging of any desired tissue or organ system and would address this issue. It is also capable of loading, and subsequently expelling, larvae from wells of a 96-well plate, reducing time-consuming manual handling of animals and combining high-throughput and high-content capabilities. However, bearing in mind the high cost of the VAST platform, the ArrayScan system represents an affordable and highly user-friendly primary-screening approach for quantifying estrogenically-induced responses in an ERE-GFP:Casper model, capable of eliciting a detectable response at a 5ng/L EE2 exposure level widely reported as occurring in the environment (i.e. Belfroid et al., 1999; Cargouët et al., 2004; Desbrow et al., 1998; Kolpin et al., 2002).

A series of semi-automated image-masking approaches applied to the data were assessed for their relative capacity to extract sensitive and minimally variable (between individual larvae, within the same exposure condition) fluorescence data from the ArrayScan-generated images. A pixel thresholding approach which isolated and averaged the top 100 pixel values from within the delineated larval area was found to represent the most sensitive approach, indicating a significantly elevated GFP response compared to vehicle control larvae at 5ng/L EE2. Although the Top 300 thresholding approach detected an uptick in larval fluorescence at the same EE2 exposure concentration at the Top 100 approach, it incorporated higher variation between larvae exposed to the same dose condition. A possible explanation for this could be that, as the estrogen-induced GFP response was relatively weak at 5ng/L EE2, only small regions of the larvae were expressing GFP (probably estrogen receptors within liver cells – the first region reported to fluoresce during high-content analysis of EE2-exposed ERE:GFP:Caspers, Green et al., 2016). Thus, an image analysis approach that averaged pixel intensity data from a smaller area of the

responding larvae might incorporate less fluctuations in recorded fluorescence than an approach which covered a more expansive area.

It was expected that adoption of a manual imaging modality (Zeiss Axio Observer), which allowed for objective focussing to be manually fine-tuned and required larvae to be individually embedded before image acquisition, would generate more sensitive and repeatable data compared to the ArrayScan system. Larvae were also uniformly laterally arrayed (left side down) in an effort to incorporate the 'ideal' parameters predicted to generate the best image acquisition conditions possible at the same x1.25 level of magnification employed by the ArrayScan. Fluorescence intensity data was quantified using the same image analysis pipeline and, as anticipated, the optimised parameters assimilated using the Zeiss approach generated data with lowest significant response detected at a lower EE2 concentration compared to the ArrayScan approach. This finding was unsurprising as previous high-content analysis had shown that the ERE:GFP:Casper model was capable of eliciting significantly elevated GFP expression at exposure concentrations as low as 1ng/L EE2 using a confocal microscope (Nikon AIR) at a x4 level of magnification (Green et al., 2016).

However, compared to the robotised 1.5 hour acquisition time of the ArrayScan system, the manual approach was time-consuming, taking two personnel working constantly over 2 hours to embed and subsequently image the larvae. Furthermore, as a consequence of being embedded in agarose prior to imaging, the fragile larvae were subject to a higher degree of stressful handling and were less amenable to imaging over consecutive timepoints, limitations that the ArrayScan was able to circumnavigate.

This study elucidated the best possible approaches for quantifying larval-specific estrogen-induced fluorescence responses in the ERE:GFP:Casper model using the semi-automated ArrayScan platform. The results also illustrate the benefits of the model itself, which was capable of expressing a detectable GFP signal at a relatively low dose of EE2. The ERE:GFP:Casper estrogen-induced fluorescence response was strong enough that significant GFP elevation above baseline could be successfully detected in 96-well plates using a low level of magnification (x1.25) despite variable larval orientation at a

medium-throughput rate (56 'acceptable' images/hour). The system therefore represents a low-cost quantitative approach for the rapid screening of potential estrogenic activity in a compound in endogenously-feeding 4dpf larvae. Future work using the pipeline could take advantage of the system's capacity to repeatedly screen the same animal over time to monitor patterns of estrogen-induced responses in specific tissues. This research aim could potentially be achieved without the use of automated orientation systems and microfluidics if a custom-designed mould could be developed for rapidly positioning larvae within cavities formed in agarose without the need for embedding. Such orientation tools have been developed (i.e. Wittbrodt et al., 2014), but would potentially need further customisation in order to provide an imaging environment amenable to ArrayScan acquisition.

5.2 ArrayScan analysis reveals temperature modulation effects on ERE:GFP:Casper EE2-induced fluorescence responses and growth

This study set out to assess the potential for an abiotic stressor to impact on EE2-induced responses in an estrogen-responsive zebrafish model. Image analysis of ERE:GFP:Casper larvae exposed to EE2 and maintained under unfavourable temperature conditions revealed that thermal variation had an influence on both estrogen-induced fluorescence responses and larval growth. This study demonstrated that larval GFP responses to low-level EE2 exposure (5ng/L) were significantly (but transiently) elevated in animals raised at low ($24\pm 1^{\circ}\text{C}$) and high ($32\pm 1^{\circ}\text{C}$) water temperatures compared to EE2-exposed fish incubated at optimal spawning temperatures ($28\pm 1^{\circ}\text{C}$). We also observed amplified disruptions to normal growth under the combined influence of low-level EE2 and thermal stress, when compared to thermal stress in isolation.

These findings are consistent with previous research demonstrating an elevation in endocrine disrupting chemical (EDC)-induced deleterious effects in zebrafish larvae maintained at higher temperatures (i.e. Osterauer & Kohler, 2008; Brown et al., 2015). This is the first study, to our knowledge, to examine the effects of an EEDC on early-stage larval estrogen receptor signalling and growth-rate under the influence of thermal stress. Our findings also have some environmental relevance, being that 5ng/L levels of EE2 have been widely

reported in the aquatic environment and climate change is predicted to significantly alter global water temperatures over the course of this century.

This study has a number of possible limitations, one of the main being that we used only one parameter (body length) to measure growth. Further investigation could include a number of size characteristics including head size, body width and organ dimensions, with just a few reference individuals subject to higher-content imaging alongside the ArrayScan analysis to assess these growth metrics. In addition to additional sampling timepoints, this would provide an improved evaluation of larval growth under the combined influence of thermal stress and EE2. Contrary to our predictions, the rate of larval growth was not observed to be elevated in EE2-exposed larvae maintained at warmer temperatures compared with controls. It would appear that the combination of undesirable thermal regimes and exposure to a chemical stressor exacerbated larval growth retardation, particularly at higher temperatures.

We have demonstrated here the application of an optimised semi-automated imaging approach for the screening of an estrogen-responsive larval zebrafish model subject to both chemical and abiotic stressors over a series of timepoints. The system was capable of detecting significant elevations in EE2-induced fluorescence responses in 72hpf larvae maintained at unsatisfactory temperature conditions ($\pm 4^{\circ}\text{C}$ deviation from optimum thermal conditions), supplementing understanding of how variations in incubation temperature can influence the results of studies measuring responses to EEDCs. Furthermore, our system represents a useful screening tool for rapid evaluation of environmentally-relevant thermal effects on EEDC exposure. The amplified EE2-induced fluorescence responses that we observed in larvae kept at 24°C and 32°C water temperatures may have been indicative of a window of sensitivity to EEDC exposure and hinted at the potential for exacerbation of EE2-induced deleterious effects.

Due to an increasing emphasis on researchers to refine the use of animals in research, replacing vertebrate adult models with embryonic-stage animals where possible, there is an escalating need to understand how these animals respond to the parameters of their experimental environment. Temperature is a highly influential variable affecting early life-stage teleosts, and must therefore be

properly controlled and understood when interpreting data generated using such models, particularly with regards to responses involving the endocrine system. Our data serves to supplement understanding of how varying experimental temperature may effect early life-stage fish models and so contributes to more insightful interpretation of data generated.

Bibliography

- Abi Salloum, B., Steckler, T.L., Herkimer, C., Lee, J.S., Padmanabhan, V. (2013). Developmental programming: impact of prenatal exposure to bisphenol-A and methoxychlor on steroid feedbacks in sheep. *Toxicol. Appl. Pharmacol.*, **268**: 300–308.
- Al-Ansari, A.M., Saleem, A., Kimpe, L.E., Sherry, J.P., McMaster, M.E., Trudeau, V.L., Blais, J.M. (2010). Bioaccumulation of the pharmaceutical 17 α -ethinylestradiol in shorthead redhorse suckers (*Moxostoma macrolepidotum*) from the St. Clair River, Canada. *Environmental Pollution*, **158**: 2566-2571.
- Allanson, B.R. & Noble, R.G. (1964). The tolerance of *Tilapia mossambica* (Peters) to high temperature. *Transactions of the American Fisheries Society*, **93**: 323-332.
- Andersen, H.R., Andersson, A.M., Arnold, S.F., Autrup, H., Barfoed, M., Beresford, N.A., Bjerregaard, P., Christiansen, L.B., Gissel, B., Hummel, R. and Jørgensen, E.B. (1999). Comparison of short-term estrogenicity tests for identification of hormone-disrupting chemicals. *Environmental health perspectives*, **107**: 89.
- Anderson, P.D., Johnson, A.C., Pfeiffer, D., Caldwell, D.J., Hannah, R., Mastrocco, F., Sumpter, J.P., Williams, R.J. (2012). Endocrine disruption due to estrogens derived from humans predicted to be low in the majority of US surface waters. *Environmental Toxicology and Chemistry*, **31**: 1407-1415.
- Ankley, G.T. & Johnson, R.D. (2004). Small fish models for identifying and assessing the effects of endocrine-disrupting chemicals. *Ilar Journal*, **45**: 469-483.
- Aranda, A. & Pascual, A. (2001). Nuclear hormone receptors and gene expression. *Physiol. Rev.*, **81**: 1269–1304.
- Arditsoglou, A. & Voutsas, D. (2012). Occurrence and partitioning of endocrine-disrupting compounds in the marine environment of Thermaikos Gulf, Northern Aegean Sea, Greece. *Marine pollution bulletin*, **64**: 2443-2452.

- Aris, A.Z., Shamsuddin, A.S., Praveena, S.M. (2014). Occurrence of 17 α -ethynylestradiol (EE2) in the environment and effect on exposed biota: a review. *Environment international*, **69**: 104-119.
- Aryal, A., Li-C, G., Xu, W. (2007). *Influences of secondary metabolites on the performance of lepidopterous larvae*.
- Atkinson, D. (1994). Temperature and organism size: a biological law for ectotherms? *Advances in ecological research*, **25**: 1-1.
- Baker, V.A., Hepburn, P.A., Kennedy, S.J., Jones, P.A., Lea, L.J., Sumpter, J.P., Ashby, J. (1999). Safety evaluation of phytosterol esters. Part 1. Assessment of oestrogenicity using a combination of in vivo and in vitro assays. *Food and Chemical Toxicology*, **37**: 13-22.
- Bakos, K., Kovács, R., Staszny, Á., Sipos, D.K., Urbányi, B., Müller, F., Csenki, Z., Kovács, B. (2013). Developmental toxicity and estrogenic potency of zearalenone in zebrafish (*Danio rerio*). *Aquatic toxicology*, **136**: 13-21.
- Balak, K.J., Corwin, J.T., Jones, J.E. (1990). Regenerated hair cells can originate from supporting cell progeny: evidence from phototoxicity and laser ablation experiments in the lateral line system. *J. Neurosci.*, **10**: 2502–2512.
- Barata, C. & Baird, D.J. (2000). Determining the ecotoxicological mode of action of chemicals from measurements made on individuals: results from instar-based tests with *Daphnia magna* Straus. *Aquatic Toxicology*, **48**: 195-209.
- Bardet, P.L., Horard, B., Robinson-Rechavi, M., Laudet, V., Vanacker, J.M. (2002). Characterization of oestrogen receptors in zebrafish (*Danio rerio*). *J. Mol. Endocrinol.*, **28**: 153–163.
- Baronti, C., Curini, R., D'Ascenzo, G., Di Corcia, A., Gentili, A., Samperi, R. (2000). Monitoring natural and synthetic estrogens at activated sludge sewage treatment plants and in a receiving river water. *Environmental Science & Technology*, **34**: 5059-5066.

- Barrionuevo, W.R. & Burggren, W.W. (1999). O₂ consumption and heart rate in developing zebrafish (*Danio rerio*): influence of temperature and ambient O₂. *American Journal of Physiology-Regulatory, Integrative and Comparative Physiology*, **276**: R505-R513.
- Barton, B.A. (2002). Stress in fishes: a diversity of responses with particular reference to changes in circulating corticosteroids. *Integrative and comparative biology*, **42**: 517-525.
- Becerra, V. & Odermatt, J. (2012). Detection and quantification of traces of bisphenol A and bisphenol S in paper samples using analytical pyrolysis-GC/MS. *Analyst*, **137**: 2250-2259.
- Beekman, F.J & van der Have, F. (2007). The pinhole: gateway to ultra-high-resolution three-dimensional radionuclide imaging.
- Beekman, F.J., van der Have, F., Vastenhouw, B., van der Linden, A.J., van Rijk, P.P., Burbach, J.P.H., Smidt, M.P. (2005). U-SPECT-I: a novel system for submillimeter-resolution tomography with radiolabeled molecules in mice. *Journal of Nuclear Medicine*, **46**: 1194-1200.
- Behm, C.Z. & Lindner, J.R. (2006). Cellular and molecular imaging with targeted contrast ultrasound. *Ultrasound quarterly*, **22**: 67-72.
- Belfroid, A.C., Van der Horst, A., Vethaak, A.D., Schäfer, A.J., Rijs, G.B.J., Wegener, J., Cofino, W.P. (1999). Analysis and occurrence of estrogenic hormones and their glucuronides in surface water and waste water in The Netherlands. *Science of the Total Environment*, **225**: 101-108.
- Benoît, H.P., Pepin, P., Brown, J.A. (2000). Patterns of metamorphic age and length in marine fishes, from individuals to taxa. *Canadian Journal of Fisheries and Aquatic Sciences*, **57**: 856-869.

- Bérard, P., Bergeron, M., Pepin, C.M., Cadorette, J., Tétrault, M.A., Viscogliosi, N., Fontaine, R., Dautet, H., Davies, M., Deschamps, P., Lecomte, R. (2009). Development of a 64-channel APD detector module with individual pixel readout for submillimetre spatial resolution in PET. *Nuclear Instruments and Methods in Physics Research Section A: Accelerators, Spectrometers, Detectors and Associated Equipment*, **610**: 20-23.
- Beynen, A.C., Gärtner, K., van Zutphen, L.F.M. (2001). Standardization of Animal Experimentation. In: Van Zutphen LFM, Baumans V, Beynen AC, eds. *Principles of Laboratory Animal Science. Revised. Amsterdam: Elsevier*, 103–110
- Blanchfield, P.J., Kidd, K.A., Docker, M.F., Palace, V.P., Park, B.J., Postma, L.D. (2015). Recovery of a wild fish population from whole-lake additions of a synthetic estrogen. *Environmental science & technology*, **49**: 3136-3144.
- Blaxter, K.L. & Webster, A.J.F. (1991). Animal production and food: real problems and paranoia. *Animal Production*, **53**: 261-269.
- Blomley, M.J., Cooke, J.C., Unger, E.C., Monaghan, M.J. and Cosgrove, D.O. (2001). Microbubble contrast agents: a new era in ultrasound. *British Medical Journal*, **322**: 1222.
- Bodo, C. & Rissman, E.F. (2006). New roles for estrogen receptor beta in behavior and neuroendocrinology. *Front. Neuroendocrinol.*, **27**: 217–232.
- Bolz, U., Hagenmaier, H., Körner, W., (2001). Phenolic xenoestrogens in surface water, sediments, and sewage sludge from Baden-Württemberg, south-west Germany. *Environmental Pollution*, **115**: 291-301.
- Bonga, S.W. (1997). The stress response in fish. *Physiological reviews*, **77**: 591-625.
- Bonnet, C.S., Caillé, F., Pallier, A., Morfin, J.F., Petoud, S., Suzenet, F., Tóth, É. (2014). Mechanistic Studies of Gd³⁺-Based MRI Contrast Agents for Zn²⁺ Detection: Towards Rational Design. *Chemistry–A European Journal*, **20**: 10959-10969.
- Borden, M. (2009). Nanostructural features on stable microbubbles. *Soft Matter*, **5**: 716-720.

- Bradbury, S. & Evennett, P. J. (1995). *Contrast techniques in light microscopy*. Oxford: Bios Scientific Publishers.
- Brande-Lavridsen, N., Christensen-Dalsgaard, J., Korsgaard, B. (2008). Effects of prochloraz and ethinylestradiol on sexual development in *Rana temporaria*. *Journal of Experimental Zoology Part A: Ecological Genetics and Physiology*, **309**: 389-398.
- Brett, J.R. (1971). Energetic responses of salmon to temperature. A study of some thermal relations in the physiology and freshwater ecology of sockeye salmon (*Oncorhynchus nerka*). *American Zoologist*, 99-113.
- Brian, J.V., Harris, C.A., Runnalls, T.J., Fantinati, A., Pojana, G., Marcomini, A., Booy, P., Lamoree, M., Kortenkamp, A., Sumpter, J.P. (2008). Evidence of temperature-dependent effects on the estrogenic response of fish: Implications with regard to climate change. *Science of the Total Environment*, **397**: 72-81.
- Briciu, R.D., Kot-Wasik, A., Namiesnik, J. (2009). Analytical challenges and recent advances in the determination of estrogens in water environments. *Journal of chromatographic science*, **47**: 127-139.
- Brion, F., Le Page, Y., Piccini, B., Cardoso, O., Tong, S.K., Chung, B.C., Kah, O. (2012). Screening estrogenic activities of chemicals or mixtures in vivo using transgenic (cyp19a1b-GFP) zebrafish embryos. *PloS one*, **7**: p.e36069.
- Brion, F., Tyler, C.R., Palazzi, X., Laillet, B., Porcher, J.M., Garric, J., Flammarion, P. (2004). Impacts of 17 β -estradiol, including environmentally relevant concentrations, on reproduction after exposure during embryo-larval-, juvenile- and adult-life stages in zebrafish (*Danio rerio*). *Aquatic Toxicology*, **68**: 193-217.
- Brown, A.R., Owen, S.F., Peters, J., Zhang, Y., Soffker, M., Paull, G.C., Hosken, D.J., Wahab, M.A., Tyler, C.R. (2015). Climate change and pollution speed declines in zebrafish populations. *Proceedings of the National Academy of Sciences*, **112**: E1237-E1246.
- Brown, B.E., Darcy, G.H., Overholtz, W. (1987). Stock assessment/stock identification: an interactive process. In *Stock Identification Workshop, Panama City, Florida, USA, NOAA/NMFS*.

- Brown, N.P., Shields, R.J., Bromage, N.R. (2006). The influence of water temperature on spawning patterns and egg quality in the Atlantic halibut (*Hippoglossus hippoglossus* L.). *Aquaculture*, **261**: 993-1002.
- Brzozowski, A., Pike, A., Dauter, Z., Hubbard, R., Bonn, T., Engstrom, O., Ohman, L., Greene, G., Gustafsson, J., Carlquist, M. (1997). Molecular basis of agonism and antagonism in the oestrogen receptor. *Nature*, **389**: 753–758.
- Byerly, M.S., Al Salayta, M., Swanson, R.D., Kwon, K., Peterson, J.M., Wei, Z., Aja, S., Moran, T.H., Blackshaw, S., Wong, G.W. (2013). Estrogen-related receptor beta deletion modulates whole-body energy balance via estrogen-related receptor gamma and attenuates neuropeptide Y gene expression. *Eur. J. Neurosci.*, **37**: 1033-1047.
- Cabas, I., Liarte, S., García-Alcázar, A., Mesequer, J., Mulero, V., García-Ayala, A. (2012). 17α -Ethinylestradiol alters the immune response of the teleost gilthead seabream (*Sparus aurata* L.) both in vivo and in vitro. *Developmental & Comparative Immunology*, **36**: 547-556.
- Cano-Nicolau, J., Vaillant, C., Pellegrini, E., Charlier, T.D., Kah, O., Coumilleau, P. (2016). Estrogenic Effects of Several BPA Analogs in the Developing Zebrafish Brain. *Frontiers in neuroscience*, **10**.
- Cargouët, M., Perdiz, D., Levi, Y. (2007). Evaluation of the estrogenic potential of river and treated waters in the Paris area (France) using in vivo and in vitro assays. *Ecotoxicology and environmental safety*, **67**: 149-156.
- Carpenter, A.E., Jones, T.R., Lamprecht, M.R., Clarke, C., Kang, I.H., Friman, O., Guertin, D.A., Chang, J.H., Lindquist, R.A., Moffat, J., Golland, P. (2006). CellProfiler: image analysis software for identifying and quantifying cell phenotypes. *Genome biology*, **7**: p.R100.
- Cassen, B., Curtis, L., Reed, C., Libby, R. (1951). Instrumentation for I-131 use in medical studies. *Nucleonics*, **9**: 46-50.

- Cavallin, J.E., Durhan, E.J., Evans, N., Jensen, K.M., Kahl, M.D., Kolpin, D.W., Kolodziej, E.P., Foreman, W.T., LaLone, C.A., Makynen, E.A., Seidl, S.M., (2014). Integrated assessment of runoff from livestock farming operations: analytical chemistry, in vitro bioassays, and in vivo fish exposures. *Environmental toxicology and chemistry*, **33**: 1849-1857.
- Chang, S.H., Cheng, F.H., Hsu, W.H., Wu, G.Z. (1997). Fast algorithm for point pattern matching: invariant to translations, rotations and scale changes. *Pattern recognition*, **30**: 311-320.
- Chang, T.Y., Pardo-Martin, C., Allalou, A., Wählby, C., Yanik, M.F. (2012). Fully automated cellular-resolution vertebrate screening platform with parallel animal processing. *Lab on a Chip*, **12**: 711-716.
- Chen, C.Y., Wen, T.Y., Wang, G.S., Cheng, H.W., Lin, Y.H., Lien, G.W. (2007). Determining estrogenic steroids in Taipei waters and removal in drinking water treatment using high-flow solid-phase extraction and liquid chromatography/tandem mass spectrometry. *Science of the Total Environment*, **378**: 352-365.
- Chen, H., Hu, J., Yang, J., Wang, Y., Xu, H., Jiang, Q., Gong, Y., Gu, Y., Song, H. (2010). Generation of a fluorescent transgenic zebrafish for detection of environmental estrogens. *Aquatic Toxicology*, **96**: 53-61.
- Christiansen, S., Axelstad, M., Boberg, J., Vinggaard, A.M., Pedersen, G.A., Hass, U. (2014). Low-dose effects of bisphenol A on early sexual development in male and female rats. *Reproduction*, **147**: 477-487.
- Clark, J.H. & Gorski, J. (1970). Ontogeny of the estrogen receptor during early uterine development. *Science*, **169**: 76-78.
- Clark, J.H. & Peck, E.J. (1979) *Female Sex Steroids: Receptors and Function* (Springer, New York).
- Clarke, A. & Fraser, K.P.P. (2004). Why does metabolism scale with temperature? *Functional Ecology*, **18**: 243-251.

- Clotfelter, E.D., Lapidus, S.J.H., Brown, A.C. (2013). The effects of temperature and dissolved oxygen on antioxidant defences and oxidative damage in the fathead minnow *Pimephales promelas*. *Journal of fish biology*, **82**: 1086-1092.
- Coe, T.S. (2010). *The population-level impacts of endocrine disrupting chemicals in fish* (Doctoral dissertation, University of Exeter).
- Coe, T.S., Hamilton, P.B., Hodgson, D., Paull, G.C., Stevens, J.R., Sumner, K., Tyler, C.R. (2008). An environmental estrogen alters reproductive hierarchies, disrupting sexual selection in group-spawning fish. *Environmental science & technology*, **42**: 5020-5025.
- Colman, J.R., Baldwin, D., Johnson, L.L., Scholz, N.L. (2009). Effects of the synthetic estrogen, 17 α -ethinylestradiol, on aggression and courtship behavior in male zebrafish (*Danio rerio*). *Aquatic Toxicology*, **91**: 346-354.
- Conley, D.B., Tan, B., Bendok, B.R., Batjer, H.H., Chandra, R., Sidle, D., Rahme, R.J., Adel, J.G., Fishman, A.J. (2011). Comparison of intraoperative portable CT scanners in skull base and endoscopic sinus surgery: single center case series. *Skull Base*, **21**: 261-270.
- Coons, A.H. & Kaplan, M.H. (1950). Localization of antigen in tissue cells. *Journal of Experimental Medicine*, **91**: 1-13.
- Cortemeglia, C. & Beitinger, T.L. (2005). Temperature tolerances of wild-type and red transgenic zebra danios. *Transactions of the American Fisheries Society*, **134**: 1431-1437.
- Couse, J.F. & Korach, K.S. (1999). Estrogen receptor null mice: what have we learned and where will they lead us? *Endocr. Rev.*, **20**: 358-417.
- Cowley, S.M., Hoare, S., Mosselman, S., Parker, S.G. (1997). Estrogen receptors alpha and beta form heterodimers on DNA. *Journal of Biological Chemistry*, **272**: 19858–19862.
- Crisp, T.M., Clegg, E.D., Cooper, R.L., Wood, W.P., Anderson, D.G., Baetcke, K.P., Hoffmann, J.L., Morrow, M.S., Rodier, D.J., Schaeffer, J.E., Touart, L.W., Zeeman, M.G., Patel, Y.M. (1998). Environmental endocrine disruption: an effects assessment and analysis. *Environ. Health Perspect.*, **106**: 11–56.

- Csaba, G. (2011). The biological basis and clinical significance of hormonal imprinting, an epigenetic process. *Clin. Epigenetics*, **2**: 187–196.
- Cunningham, V.J. & Jones, T. (1993). Spectral analysis of dynamic PET studies. *Journal of Cerebral Blood Flow & Metabolism*, **13**: 15-23.
- Dalvi, R.S., Pal, A.K., Tiwari, L.R., Das, T., Baruah, K. (2009). Thermal tolerance and oxygen consumption rates of the catfish *Horabagrus brachysoma* (Günther) acclimated to different temperatures. *Aquaculture*, **295**: 116-119.
- Dang, H.M., Inagaki, Y., Yamauchi, Y., Kurihara, T., Vo, C.H., Sakakibara, Y. (2017). Acute Exposure to 17 α -Ethinylestradiol Alters Aggressive Behavior of Mosquitofish (*Gambusia affinis*) Toward Japanese Medaka (*Oryzias latipes*). *Bulletin of Environmental Contamination and Toxicology*, 1-6.
- Darzynkiewicz, Z., Bruno, S., Del Bino, G., Gorczyca, W., Hotz, M.A., Lassota, P., Traganos, F. (1992). Features of apoptotic cells measured by flow cytometry. *Cytometry*, **13**: 795-808.
- Daughton, C.G. & Ternes, T.A. (1999). Pharmaceuticals and personal care products in the environment: agents of subtle change? *Environmental health perspectives*, **107**: 907.
- Daughton, C.G. (2002). Environmental stewardship and drugs as pollutants. *The Lancet*, **360**: 1035-1036.
- De Chaumont, F., Dallongeville, S., Chenouard, N., Hervé, N., Pop, S., Provoost, T., Meas-Yedid, V., Pankajakshan, P., Lecomte, T., Le Montagner, Y., Lagache, T. (2012). Icy: an open bioimage informatics platform for extended reproducible research. *Nature methods*, **9**: 690-696.
- De Coster, S. & van Larebeke, N. (2012). Endocrine-disrupting chemicals: associated disorders and mechanisms of action. *J Environ. Public. Health.*, **2012**: 52.
- De Mes, T.Z.D., Kujawa-Roeleveld, K., Zeeman, G., Lettinga, G. (2008). Anaerobic biodegradation of estrogens—hard to digest. *Water Science and Technology*, **57**: 1177-1182.

- De Wit, M., Keil, D., van der Ven, K., Vandamme, S., Witters, E., De Coen, W. (2010). An integrated transcriptomic and proteomic approach characterizing estrogenic and metabolic effects of 17 α -ethinylestradiol in zebrafish (*Danio rerio*). *General and comparative endocrinology*, **167**: 190-201.
- Debbage, P. & Jaschke, W. (2008). Molecular imaging with nanoparticles: giant roles for dwarf actors. *Histochemistry and cell biology*, **130**: 845-875.
- Dekens, M.P., Pelegri, F.J., Maischein, H.M., Nüsslein-Volhard, C. (2003). The maternal-effect gene *futile* cycle is essential for pronuclear congression and mitotic spindle assembly in the zebrafish zygote. *Development*, **130**: 3907-3916.
- Derendorf, H., Lesko, L.J., Chaikin, P., Colburn, W.A., Lee, P., Miller, R., Powell, R., Rhodes, G., Stanski, D., Venitz, J. (2000). Pharmacokinetic/pharmacodynamic modeling in drug research and development. *The Journal of Clinical Pharmacology*, **40**: 1399-1418.
- Derouiche, L., Keller, M., Martini, M., Duittoz, A.H., Pillon, D. (2015). Developmental exposure to ethinylestradiol affects reproductive physiology, the GnRH neuroendocrine network and behaviors in female mouse. *Frontiers in neuroscience*, **9**: 463.
- Desbrow, C.E.J.R., Routledge, E.J., Brighty, G.C., Sumpter, J.P., Waldock, M. (1998). Identification of estrogenic chemicals in STW effluent. 1. Chemical fractionation and in vitro biological screening. *Environmental science & technology*, **32**: 1549-1558.
- Deshpande, N., Needles, A., Willmann, J.K. (2010). Molecular ultrasound imaging: current status and future directions. *Clinical radiology*, **65**: 567-581.
- Diamanti-Kandarakis, E., Bourguignon, J.P., Giudice, L.C., Hauser, R., Prins, G.S., Soto, A.M., Zoeller, R.T., Gore, A.C. (2009). Endocrine-disrupting chemicals: an Endocrine Society scientific statement. *Endocrine reviews*, **30**: 293-342.
- Doherty, L.F., Bromer, J.G., Zhou, Y., Aldad, T.S., Taylor, H.S. (2010). In utero exposure to diethylstilbestrol (DES) or bisphenol-A (BPA) increases EZH2 expression in the mammary gland: an epigenetic mechanism linking endocrine disruptors to breast cancer. *Horm. Cancer*, **1**: 146–155.

- Donaldson, M.R., Cooke, S.J., Patterson, D.A., Macdonald, J.S. (2008). Cold shock and fish. *Journal of Fish Biology*, **73**: 1491-1530.
- Doney, S.C., Ruckelshaus, M., Duffy, J.E., Barry, J.P., Chan, F., English, C.A., Galindo, H.M., Grebmeier, J.M., Hollowed, A.B., Knowlton, N., Polovina, J., (2011). *Climate change impacts on marine ecosystems*.
- Duffy, M.J. (2006). Estrogen receptors: role in breast cancer. *Crit. Rev. Clin. Lab. Sci.*, **43**: 325–347.
- Easterling, D.R., Horton, B., Jones, P.D., Peterson, T.C., Karl, T.R., Parker, D.E., Salinger, M.J., Razuvayev, V., Plummer, N., Jamason, P., Folland, C.K., (1997). Maximum and minimum temperature trends for the globe. *Science*, **277**: 364-367.
- Easterling, D.R., Meehl, G.A., Parmesan, C., Changnon, S.A., Karl, T.R., Mearns, L.O. (2000). Climate extremes: observations, modeling, and impacts. *Science*, **289**: 2068-2074.
- Eick, G.N. & Thornton, J.W. (2011). Evolution of steroid receptors from an estrogen-sensitive ancestral receptor. *Mol. Cell. Endocrinol.*, **334**: 31–38.
- Eladak, S., Grisin, T., Moison, D., Guerquin, M.J., N'Tumba-Byn, T., Pozzi-Gaudin, S., Benachi, A., Livera, G., Rouiller-Fabre, V., Habert, R. (2015). A new chapter in the bisphenol A story: bisphenol S and bisphenol F are not safe alternatives to this compound. *Fertility and sterility*, **103**: 11-21.
- Engeszer, R.E., Patterson, L.B., Rao, A.A., Parichy, D.M. (2007). Zebrafish in the wild: a review of natural history and new notes from the field. *Zebrafish*, **4**: 21-40.
- Erdfelder, E., Faul, F., Buchner, A. (1996). GPOWER: A general power analysis program. *Behavior research methods, instruments, & computers*, **28**: 1-11.
- Feng, Y., Yin, J., Jiao, Z., Shi, J., Li, M., Shao, B. (2012). Bisphenol AF may cause testosterone reduction by directly affecting testis function in adult male rats. *Toxicology letters*, **211**: 201-209.
- Fisher, R.A. (1937). *The design of experiments*. Oliver And Boyd; Edinburgh; London.

- Fisher, S.W. & Wadleigh, R.W. (1985). Effects of temperature on the acute toxicity and uptake of lindane by *Chironomus riparius* (Meigen)(Diptera: Chironomidae). *Journal of economic entomology*, **78**: 1222-1226.
- Förster, C., Makelä, S., Becker, D., Hultenby, K., Warner, M., Gustafsson, J.A. (2002). Involvement of Estrogen receptor beta in terminal differentiation of mammary epithelium. *Proc. Natl. Acad. Sci. USA*, **99**: 15578–15583.
- Foster, F.S., Mehi, J., Lukacs, M., Hirson, D., White, C., Chaggares, C., Needles, A. (2009). A new 15–50 MHz array-based micro-ultrasound scanner for preclinical imaging. *Ultrasound in medicine & biology*, **35**: 1700-1708.
- Fry, F.E.J. (1971). 1 The effect of environmental factors on the physiology of fish. *Fish physiology*, **6**: 1-98.
- Fujii, K., Kikuchi, S., Satomi, M., Ushio-Sata, N., Morita, N. (2002). Degradation of 17 β -estradiol by a gram-negative bacterium isolated from activated sludge in a sewage treatment plant in Tokyo, Japan. *Applied and Environmental Microbiology*, **68**: 2057-2060.
- Gadd, J.B., Northcott, G.L., Tremblay, L.A. (2010). Passive secondary biological treatment systems reduce estrogens in dairy shed effluent. *Environmental Science & Technology*, **44**: 7601-7606.
- Gagné, F., Bouchard, B., André, C., Farcy, E., Fournier, M. (2011). Evidence of feminization in wild *Elliptio complanata* mussels in the receiving waters downstream of a municipal effluent outfall. *Comparative Biochemistry and Physiology Part C: Toxicology & Pharmacology*, **153**: 99-106.
- Gallart-Ayala, H., Moyano, E., Galceran, M.T. (2011). Analysis of bisphenols in soft drinks by on-line solid phase extraction fast liquid chromatography–tandem mass spectrometry. *Analytica Chimica Acta*, **683**: 227-233.
- Giangrande, P.H., Pollio, G., McDonnell, D.P. (1997). Mapping and characterization of the functional domains responsible for the differential activity of the A and B isoforms of the human progesterone receptor. *J. Biol. Chem.*, **272**: 32889-32900.

- Gillet, C. & Quetin, P. (2006). Effect of temperature changes on the reproductive cycle of roach in Lake Geneva from 1983 to 2001. *Journal of fish biology*, **69**: 518-534.
- Gimeno, S., Komen, H., Jobling, S., Sumpter, J., Bowmer, T. (1998). Demasculinisation of sexually mature male common carp, *Cyprinus carpio*, exposed to 4-tert-pentylphenol during spermatogenesis. *Aquatic Toxicology*, **43**: 93-109.
- Glass, C.K. (1994). Differential recognition of target genes by nuclear receptor monomers, dimers, and heterodimers. *Endocrinol. Rev.*, **15**: 391–407.
- Godwin, J., Luckenbach, J.A., Borski, R.J. (2003). Ecology meets endocrinology: environmental sex determination in fishes. *Evolution & development*, **5**: 40-49.
- Goolish, E.M. & Okutake, K. (1999). Lack of gas bladder inflation by the larvae of zebrafish in the absence of an air-water interface. *Journal of fish biology*, **55**: 1054-1063.
- Gordon, C.J. (2003). Role of environmental stress in the physiological response to chemical toxicants. *Environmental research*, **92**: 1-7.
- Gordon, C.J. (2005). *Temperature and toxicology: an integrative, comparative, and environmental approach*. CRC press.
- Gorelick, D.A. & Halpern, M.E. (2011). Visualization of estrogen receptor transcriptional activation in zebrafish. *Endocrinology*, **152**: 2690-2703.
- Grebmeier, J.M., Moore, S.E., Overland, J.E., Frey, K.E., Gradinger, R. (2010). Biological response to recent Pacific Arctic sea ice retreats. *Eos, Transactions American Geophysical Union*, **91**: 161-162.
- Green, B.S. & Fisher, R. (2004). Temperature influences swimming speed, growth and larval duration in coral reef fish larvae. *Journal of Experimental Marine Biology and Ecology*, **299**: 115-132.
- Green, J.M., Metz, J., Lee, O., Trznadel, M., Takesono, A., Brown, A.R., Owen, S.F., Kudoh, T., Tyler, C.R. (2016). High-Content and Semi-Automated Quantification of Responses to Estrogenic Chemicals Using a Novel Translucent Transgenic Zebrafish. *Environmental Science & Technology*, **50**: 6536-6545.

- Green, S., Walter, P., Kumar, V., Krust, A., Bornert, J.M., Argos, P., Chambon, P. (1986). Human oestrogen receptor cDNA: sequence, expression and homology to v-erb-A. *Nature*, **320**: 134–139.
- Groot, C. (2010). *Physiological ecology of Pacific salmon*. UBC Press.
- Gruber, C.J., Tschugguel, W., Schneeberger, C., Huber, J.C. (2002). Production and actions of estrogens. *N. Engl. J. Med.*, **346**: 340-52.
- Gustafsson, J.A. (1999). Estrogen receptor β —a new dimension in estrogen mechanism of action. *J. Endocrinol.*, **163**: 379–383.
- Gustafsson, J.A. (2003). What pharmacologists can learn from recent advances in estrogen signalling. *Trends Pharmacol. Sci.*, **24**: 479–485.
- Haitinger, M. (1933). Erwiderung auf die vorstehenden Bemerkungen des Herrn Erich Tiede. *Mikrochemie*, **12**: 270-271.
- Hall, J.M. & McDonnell, D.P. (1999). The estrogen receptor beta-isoform (ERbeta) of the human estrogen receptor modulates ER alpha transcriptional activity and is a key regulator of the cellular response to estrogens and antiestrogens. *Endocrinology*, **140**: 5566–5578.
- Hallare, A.V., Schirling, M., Luckenbach, T., Köhler, H.R., Tribskorn, R. (2005). Combined effects of temperature and cadmium on developmental parameters and biomarker responses in zebrafish (*Danio rerio*) embryos. *Journal of Thermal Biology*, **30**: 7-17.
- Han, J., Qiu, W., Meng, S., Gao, W. (2012). Removal of ethinylestradiol (EE2) from water via adsorption on aliphatic polyamides. *Water research*, **46**: 5715-5724.
- Hansen, P.D., Dizer, H., Hock, B., Marx, A., Sherry, J., McMaster, M., Blaise, C. (1998). Vitellogenin—a biomarker for endocrine disruptors. *TrAC Trends in Analytical Chemistry*, **17**: 448-451.
- Hawkins, M.B., Thornton, J.W., Crews, D., Skipper, J.K., Dotte, A., Thomas, P. (2000). Identification of a third distinct estrogen receptor and reclassification of estrogen receptors in teleosts. *Proc. Natl. Acad. Sci. USA*, **97**: 10751–10756.

- Hayes, T., Haston, K., Tsui, M., Hoang, A., Haeffele, C., Vonk, A. (2003). Atrazine-induced hermaphroditism at 0.1 ppb in American leopard frogs (*Rana pipiens*): laboratory and field evidence. *Environmental health perspectives*, **111**: 568.
- Hayes, T.B., Khoury, V., Narayan, A., Nazir, M., Park, A., Brown, T., Adame, L., Chan, E., Buchholz, D., Stueve, T., Gallipeau, S. (2010). Atrazine induces robisncomplete feminization and chemical castration in male African clawed frogs (*Xenopus laevis*). *Proceedings of the National Academy of Sciences*, **107**: 4612-4617.
- Heldring, N., Pike, A., Andersson, S., Matthews, J., Cheng, G., Hartman, J., Tujague, M., Strom, A., Treuter, E., Warner, M., Gustafsson, J.A. (2007). Estrogen receptors: how do they signal and what are their targets, *Physiol. Rev.*, **87**: 905–931.
- Helguero, L.A., Faulds, M.H., Gustafsson, J.A., Haldosen, L.A. (2005). Estrogen receptors alfa (ERalpha) and beta (ERbeta) differentially regulate proliferation and apoptosis of the normal murine mammary epithelial cell line HC11. *Oncogene*, **24**: 6605–6616.
- Helmchen, F. & Denk, W. (2005). Deep tissue two-photon microscopy. *Nature methods*, **2**: 932-940.
- Henn, K. & Braunbeck, T. (2011). Dechoriation as a tool to improve the fish embryo toxicity test (FET) with the zebrafish (*Danio rerio*). *Comparative Biochemistry and Physiology Part C: Toxicology & Pharmacology*, **153**: 91-98.
- Heugens, E.H., Hendriks, A.J., Dekker, T., Straalen, N.M.V., Admiraal, W. (2001). A review of the effects of multiple stressors on aquatic organisms and analysis of uncertainty factors for use in risk assessment. *Critical reviews in toxicology*, **31**: 247-284.
- Hewitt, S.C. & Korach, K.S. (2002). Estrogen receptors: structure, mechanisms and function. *Rev. Endocr. Metab. Disord.*, **3**: 193-200.
- Hill, R.L. & Janz, D.M. (2003). Developmental estrogenic exposure in zebrafish (*Danio rerio*): I. Effects on sex ratio and breeding success. *Aquatic toxicology*, **63**: 417-429.

- Hinfray, N., Tebby, C., Garoche, C., Piccini, B., Bourguine, G., Aït-Aïssa, S., Kah, O., Pakdel, F., Brion, F. (2016). Additive effects of levonorgestrel and ethinylestradiol on brain aromatase (cyp19a1b) in zebrafish specific in vitro and in vivo bioassays. *Toxicology and applied pharmacology*, **307**: 08-114.
- Hirakawa, I., Miyagawa, S., Katsu, Y., Kagami, Y., Tatarazako, N., Kobayashi, T., Kusano, T., Mizutani, T., Ogino, Y., Takeuchi, T., Ohta, Y. (2012). Gene expression profiles in the testis associated with testis-ova in adult Japanese medaka (*Oryzias latipes*) exposed to 17 α -ethinylestradiol. *Chemosphere*, **87**: 668-674.
- Ho, S. M., Tang, W. Y., Belmonte de Frausto, J., Prins, G. S. (2011). Developmental exposure to estradiol and bisphenol A increases susceptibility to prostate carcinogenesis and epigenetically regulates phosphodiesterase type 4 variant 4. *Cancer Res.*, **66**: 5624–5632.
- Hornack, P.D. (2002). *JP The Basics of NMR*.
- Houde, E.D. (1989). Comparative growth, mortality, and energetics of marine fish larvae: temperature and implied latitudinal effects. *Fishery Bulletin*, **87**: 471-495.
- Huang, X., Gao, L., Wang, S., McManaman, J.L., Thor, A.D., Yang, X., Esteva, F.J., Liu, B. (2010). Heterotrimerization of the growth factor receptors erbB2, erbB3, and insulin-like growth factor-i receptor in breast cancer cells resistant to herceptin. *Cancer research*, **70**: 1204-1214.
- Hultcrantz, M., Simonoska, R., Stenberg, A.E. (2006). Estrogen and hearing: a summary of recent investigations. *Acta. Otolaryngol.*, **126**: 10–14.
- Hutchins, G.D., Miller, M.A., Soon, V.C., Receveur, T. (2008). Small animal PET imaging. *ILAR journal*, **49**: 54-65.
- Imamov, O., Morani, A., Shim, G.J., Omoto, Y., Thulin-Andersson, C., Warner, M., Gustafsson, J.A. (2001). Estrogen receptor beta regulates epithelial cellular differentiation in the mouse ventral prostate. *Proc. Natl. Acad. Sci. USA*, **101**: 9375–9380.
- IPCC, A. (2007). *Intergovernmental panel on climate change*. Geneva: IPCC Secretariat.

- Isidori, M., Cangiano, M., Palermo, F.A., Parrella, A. (2010). E-screen and vitellogenin assay for the detection of the estrogenic activity of alkylphenols and trace elements. *Comparative Biochemistry and Physiology Part C: Toxicology & Pharmacology*, **152**: 51-56.
- Itoh, K., Krupnik, V.E., Sokol, S.Y. (1998). Axis determination in *Xenopus* involves biochemical interactions of axin, glycogen synthase kinase 3 and beta-catenin. *Curr. Biol.*, **8**: 591–594.
- Jacobs, R.E. & Cherry, S.R. (2001). Complementary emerging techniques: high-resolution PET and MRI. *Current opinion in neurobiology*, **11**: 621-629.
- James, M.L. & Gambhir, S.S. (2012). A molecular imaging primer: modalities, imaging agents, and applications. *Physiological reviews*, **92**: 897-965.
- Janhunen, M., Piironen, J., Peuhkuri, N. (2010). Parental effects on embryonic viability and growth in Arctic charr *Salvelinus alpinus* at two incubation temperatures. *Journal of Fish Biology*, **76**: 2558-2570.
- Janz, D. M. & Weber, L. P. (2000). Endocrine system. In: *The laboratory fish*. Ostrander, G.K. Academic Press, London, UK, 415–439.
- Jarque, S., Fetter, E., Pípal, M., Smutná, M., Blaha, L., Scholz, S. Semi-automated detection of goitrogenic compounds using transgenic zebrafish embryos and the VAST Biolumager platform. Poster presented during SETAC Annual meeting 3-7 May 2015 in Barcelona.
- Jaszczak, R.J., Li, J., Wang, H., Zalutsky, M.R., Coleman, R.E. (1994). Pinhole collimation for ultra-high-resolution, small-field-of-view SPECT. *Physics in medicine and biology*, **39**: 425.
- Jedeon, K., De la Dure-Molla, M., Brookes, S.J., Liodice, S., Marciano, C., Kirkham, J., Canivenc-Lavier, M.C., Boudalia, S., Bergès, R., Harada, H., Berdal, A. (2013). Enamel defects reflect perinatal exposure to bisphenol A. *The American journal of pathology*, **183**: 108-118.
- Ji, C., Wei, L., Zhao, J., Wu, H. (2014). Metabolomic analysis revealed that female mussel *Mytilus galloprovincialis* was sensitive to bisphenol A exposures. *Environmental toxicology and pharmacology*, **37**: 844-849.

- Jin, M., Zhang, X., Wang, L., Huang, C., Zhang, Y., Zhao, M. (2009). Developmental toxicity of bifenthrin in embryo-larval stages of zebrafish. *Aquatic Toxicology*, **95**: 347-354.
- Jin, X., Jiang, G., Huang, G., Liu, J., Zhou, Q. (2004). Determination of 4-tert-octylphenol, 4-nonylphenol and bisphenol A in surface waters from the Haihe River in Tianjin by gas chromatography–mass spectrometry with selected ion monitoring. *Chemosphere*, **56**: 1113-1119.
- Jin, Y., Chen, R., Sun, L., Liu, W., Fu, Z. (2009). Photoperiod and temperature influence endocrine disruptive chemical-mediated effects in male adult zebrafish. *Aquatic toxicology (Amsterdam, Netherlands)*, **92**: 38.
- Jobling, S., Nolan, M., Tyler, C.R., Brighty, G., Sumpter, J.P. (1998). Widespread sexual disruption in wild fish. *Environmental science & technology*, **32**: 2498-2506.
- Johnson, A.C., Belfroid, A., Di Corcia, A. (2000). Estimating steroid oestrogen inputs into activated sludge treatment works and observations on their removal from the effluent. *Science of the Total Environment*, **256**: 163-173.
- Johnson, A.C., Williams, R.J., Matthiessen, P. (2006). The potential steroid hormone contribution of farm animals to freshwaters, the United Kingdom as a case study. *Science of the Total Environment*, **362**: 166-178.
- Judenhofer, M.S., Wehrl, H.F., Newport, D.F., Catana, C., Siegel, S.B., Becker, M., Thielscher, A., Kneilling, M., Lichy, M.P., Eichner, M., Klingel, K. (2008). Simultaneous PET-MRI: a new approach for functional and morphological imaging. *Nature medicine*, **14**: 459-465.
- Kajta, M. & Wójtowicz, A.K. (2013). Impact of endocrine-disrupting chemicals on neural development and the onset of neurological disorders. *Pharmacological Reports*, **65**: 1632-1639.
- Kang, J.H. & Chung, J.K. (2008). Molecular-genetic imaging based on reporter gene expression. *Journal of Nuclear Medicine*, **49**: 164S-179S.

- Keay, J. & Thornton, J.W. (2009). Hormone-activated estrogen receptors in annelid invertebrates: implications for evolution and endocrine disruption. *Endocrinology*, **150**: 1731-1738.
- Keyes, J.W., Leonard, P.F., Brody, S.L., Svetkoff, D.J., Rogers, W.L., Lucchesi, B.R. (1978). Myocardial infarct quantification in the dog by single photon emission computed tomography. *Circulation*, **58**: 227-232.
- Khayum, M.A., de Vries, E.F., Glaudemans, A.W., Dierckx, R.A., Doorduyn, J. (2014). In vivo imaging of brain estrogen receptors in rats: a 16α - ^{18}F -fluoro- 17β -estradiol PET study. *Journal of Nuclear Medicine*, **55**: 481-487.
- Kidd, K.A., Blanchfield, P.J., Mills, K.H., Palace, V.P., Evans, R.E., Lazorchak, J.M. and Flick, R.W. (2007). Collapse of a fish population after exposure to a synthetic estrogen. *Proceedings of the National Academy of Sciences*, **104**: 8897-8901.
- Kimbrel, E.A. & McDonnell, D.P. (2003). Function and mode of action of nuclear receptors: estrogen, progesterone, and vitamin D. *Pure and Applied Chemistry*, **75**: 1671–1683.
- Kimmel, C.B., Ballard, W.W., Kimmel, S.R., Ullmann, B., Schilling, T.F. (1995). Stages of embryonic development of the zebrafish. *Developmental dynamics*, **203**: 253-310.
- Klibanov, A.L. (2009). Preparation of targeted microbubbles: ultrasound contrast agents for molecular imaging. *Medical & biological engineering & computing*, **47**: 875-882.
- Klug, A., & Schwabe, J.W.R. (1995). Zinc fingers. *FASEB J.*, **9**: 597-604.
- Koehler, H.F., Helguero, L.A., Warner, M., Gustafsson, J.A. (2005). Reflections on the discovery and significance of oestrogen receptor beta. *Endocrine Reviews*, **26**: 465–478.
- Koide, A., Zhao, C., Naganuma, M., Abrams, J., Deighton-Collins, S., Skafar, D.F., Koide, S. (2007). Identification of regions within the F domain of the human estrogen receptor {alpha} that are important for modulating transactivation and protein–protein interactions. *Mol. Endocrinol.*, **21**: 829–842.

- Kolok, A.S. & Sellin, M.K. (2008). The environmental impact of growth-promoting compounds employed by the United States beef cattle industry: History, current knowledge, and future directions. In *Reviews of environmental contamination and toxicology*, 1-30. Springer New York.
- Kolpin, D.W., Furlong, E.T., Meyer, M.T., Thurman, E.M., Zaugg, S.D., Barber, L.B., Buxton, H.T. (2002). Pharmaceuticals, hormones, and other organic wastewater contaminants in US streams, 1999– 2000: A national reconnaissance. *Environmental science & technology*, **36**: 1202-1211.
- Körner, O., Kohno, S., Schönenberger, R., Suter, M.J.F., Knauer, K., Guillet, L.J., Burkhardt-Holm, P. (2008). Water temperature and concomitant waterborne ethinylestradiol exposure affects the vitellogenin expression in juvenile brown trout (*Salmo trutta*). *Aquatic toxicology*, **90**: 188-196.
- Kraitchman, D.L., Tatsumi, M., Gilson, W.D., Ishimori, T., Kedziorek, D., Walczak, P., Segars, W.P., Chen, H.H., Fritzges, D., Izbudak, I., Young, R.G. (2005). Dynamic imaging of allogeneic mesenchymal stem cells trafficking to myocardial infarction. *Circulation*, **112**: 1451-1461.
- Kuch, H.M. & Ballschmiter, K. (2001). Determination of endocrine-disrupting phenolic compounds and estrogens in surface and drinking water by HRGC–(NCI)– MS in the picogram per liter range. *Environmental science & technology*, **35**: 3201-3206.
- Kuiper, G.G.J.M., Carlsson, B., Grandien, K., Enmark, E., Häggblad, J., Nilsson, S., Gustafsson, J.A. (1997). Comparison of the ligand binding specificity and transcript tissue distribution of estrogen receptors α and β . *Endocrinology*, **138**: 863–870.
- Kuiper-Goodman, T., Scott, P. and Watanabe, H. (1987). Risk assessment of the mycotoxin zearalenone. *Regulatory toxicology and pharmacology*, **7**: 253-306.
- Kumar, V., Green, S., Stack, G., Berry, M., Jin, J.R., Chambon, P. (1987). Functional domains of the human estrogen receptor. *Cell*, **51**: 941–951.
- Kundakovic, M. & Champagne, F. A. (2011). Epigenetic perspective on the developmental effects of bisphenol A. *Brain Behav. Immun.* **25**: 1084–1093.

- Kurauchi, K., Hirata, T., Kinoshita, M. (2008). Characteristics of ChgH–GFP transgenic medaka lines, an in vivo estrogenic compound detection system. *Marine pollution bulletin*, **57**: 441-444.
- Kurauchi, K., Nakaguchi, Y., Tsutsumi, M., Hori, H., Kurihara, R., Hashimoto, S., Ohnuma, R., Yamamoto, Y., Matsuoka, S., Kawai, S.I., Hirata, T. (2005). In vivo visual reporter system for detection of estrogen-like substances by transgenic medaka. *Environmental science & technology*, **39**: 2762-2768.
- Kyme, A.Z., Zhou, V.W., Meikle, S.R., Fulton, R.R. (2008). Real-time 3D motion tracking for small animal brain PET. *Physics in medicine and biology*, **53**: 2651.
- Labadie, P. & Hill, E.M. (2007). Analysis of estrogens in river sediments by liquid chromatography–electrospray ionisation mass spectrometry: comparison of tandem mass spectrometry and time-of-flight mass spectrometry. *Journal of Chromatography A*, **1141**: 174-181.
- Lacy, R. C. (1997). Importance of genetic variation to the viability of mammalian populations. *Journal of Mammalogy*, **78**, 320-335.
- Laganà, A., Bacaloni, A., Fago, G., Marino, A. (2000). Trace analysis of estrogenic chemicals in sewage effluent using liquid chromatography combined with tandem mass spectrometry. *Rapid Communications in Mass Spectrometry*, **14**: 401-407.
- Lai, K.M., Johnson, K.L., Scrimshaw, M.D., Lester, J.N. (2000). Binding of waterborne steroid estrogens to solid phases in river and estuarine systems. *Environmental Science & Technology*, **34**: 3890-3894.
- Lammer, E., Carr, G.J., Wendler, K., Rawlings, J.M., Belanger, S.E., Braunbeck, T., (2009). Is the fish embryo toxicity test (FET) with the zebrafish (*Danio rerio*) a potential alternative for the fish acute toxicity test?. *Comparative Biochemistry and Physiology Part C: Toxicology & Pharmacology*, **149**: 196-209.
- Lange, A., Paull, G.C., Coe, T.S., Katsu, Y., Urushitani, H., Iguchi, T., Tyler, C.R. (2009). Sexual reprogramming and estrogenic sensitization in wild fish exposed to ethinylestradiol. *Environ. Sci. Technol.*, **43**: 1219–1225.

- Lange, I.G., Hartel, A., Meyer, H.D.D. (2002). Evolution of oestrogen functions in vertebrates. *J. Steroid Biochemistry and Molecular Biology*, **83**: 219–226.
- Länge, R., Hutchinson, T.H., Croudace, C.P., Siegmund, F., Schweinfurth, H., Hampe, P., Panter, G.H., Sumpter, J.P. (2001). Effects of the synthetic estrogen 17 α -ethinylestradiol on the life-cycle of the fathead minnow (*Pimephales promelas*). *Environmental Toxicology and Chemistry*, **20**: 1216-1227.
- Lanza, G.M. & Wickline, S.A. (2003). Targeted ultrasonic contrast agents for molecular imaging and therapy. *Current problems in cardiology*, **28**: 625-653.
- Larsen, M.G., Hansen, K.B., Henriksen, P.G., Baatrup, E. (2008). Male zebrafish (*Danio rerio*) courtship behaviour resists the feminising effects of 17 α -ethinyloestradiol—morphological sexual characteristics do not. *Aquatic Toxicology*, **87**: 234-244.
- Larsson, D.G.J., Adolfsson-Erici, M., Parkkonen, J., Pettersson, M., Berg, A.H., Olsson, P.E., Förlin, L. (1999). Ethinyloestradiol—an undesired fish contraceptive? *Aquatic toxicology*, **45**: 91-97.
- Lassiter, C.S., Kelley, B., Linney, E. (2002). Genomic structure and embryonic expression of estrogen receptor beta a (ERbeta a) in zebrafish (*Danio rerio*). *Gene*, **299**: 141–151.
- Lee, H.C., Lu, P.N., Huang, H.L., Chu, C., Li, H.P., Tsai, H.J. (2014). Zebrafish transgenic line huORFZ is an effective living bioindicator for detecting environmental toxicants. *PloS one*, **9**: p.e90160.
- Lee, O., Green, J.M. and Tyler, C.R. (2015). Transgenic fish systems and their application in ecotoxicology. *Critical reviews in toxicology*, **45**: 124-141.
- Lee, O., Takesono, A., Tada, M., Tyler, C.R., Kudoh, T. (2012a). Biosensor zebrafish provide new insights into potential health effects of environmental estrogens. *Environmental health perspectives*, **120**: 990.
- Lemaire, G., Mnif, W., Mauvais, P., Balaguer, P., Rahmani, R. (2006). Activation of α - and β -estrogen receptors by persistent pesticides in reporter cell lines. *Life sciences*, **79**: 1160-1169.

- Lemmen, J.G., Broekhof, J.L.M., Kuiper, G.G.J.M., Gustafsson, J.A., Van der Saag, P.T., Van der Burg, B. (1999). Expression of estrogen receptor alpha and beta during mouse embryogenesis. *Mech. Dev.*, **81**: 163-167.
- Li, L., Bonneton, F., Tohme, M., Bernard, L., Chen, X.Y., Laudet, V. (2016). In Vivo Screening Using Transgenic Zebrafish Embryos Reveals New Effects of HDAC Inhibitors Trichostatin A and Valproic Acid on Organogenesis. *PLoS one*, **11**: p.e0149497.
- Li, Z.B., Chen, K. and Chen, X. (2008). 68Ga-labeled multimeric RGD peptides for microPET imaging of integrin $\alpha\beta3$ expression. *European journal of nuclear medicine and molecular imaging*, **35**: 1100-1108.
- Liao, C., Liu, F., Kannan, K. (2012). Bisphenol S, a new bisphenol analogue, in paper products and currency bills and its association with bisphenol A residues. *Environmental science & technology*, **46**: 6515-6522.
- Lima, D.L., Schneider, R.J., Esteves, V.I. (2012). Sorption behavior of EE2 on soils subjected to different long-term organic amendments. *Science of the total environment*, **423**: 120-124.
- Lindberg, M.K., Moverare, S., Skrtic, S., Gao, H., Dahlman-Wright, K., Gustafsson, J.-Å., Ohlsson, C. (2003). Estrogen receptor (ER)- β reduces ER α -regulated gene transcription, supporting a “Ying Yang” relationship between ER α and ER β in mice. *Mol. Endocrinol.*, **17**: 203–208.
- Liu, J., Wang, R., Huang, B., Lin, C., Zhou, J. and Pan, X. (2012c). Biological effects and bioaccumulation of steroidal and phenolic endocrine disrupting chemicals in high-back crucian carp exposed to wastewater treatment plant effluents. *Environmental pollution*, **162**: 325-331.
- Liu, S., Ying, G.G., Zhang, R.Q., Zhou, L.J., Lai, H.J., Chen, Z.F. (2012). Fate and occurrence of steroids in swine and dairy cattle farms with different farming scales and wastes disposal systems. *Environmental pollution*, **170**: 190-201.
- Long, Y., Li, L., Li, Q., He, X., Cui, Z. (2012). Transcriptomic characterization of temperature stress responses in larval zebrafish. *PLoS one*, **7**: p.e37209.

- Lu, Q.L., Liang, H.D., Partridge, T., Blomley, M.J.K. (2003). Microbubble ultrasound improves the efficiency of gene transduction in skeletal muscle in vivo with reduced tissue damage. *Gene therapy*, **10**: 396-405.
- Lubahn, D.B., Moyer, J.S., Golding, T.S., Couse, J.F., Korach, K.S., Smithies, O. (1993). Alteration of reproductive function but not prenatal sexual development after insertional disruption of the mouse estrogen receptor gene. *Proc. Natl. Acad. Sci. USA*, **90**: 11162–11166.
- Luine, V.N., Jacome, L.F., MacLusky, N.J. (2003). Rapid enhancement of visual and place memory by estrogens in rats. *Endocrinology*, **144**: 2836 –2844.
- Ma, C.H., Dong, K.W., Yu, K.L. (2000). cDNA cloning and expression of a novel estrogen receptor beta-subtype in goldfish (*Carassius auratus*). *Biochim.Biophys. Acta.*, **1490**: 145–152.
- Massoud, T.F. & Gambhir, S.S. (2003). Molecular imaging in living subjects: seeing fundamental biological processes in a new light. *Genes & development*, **17**: 545-580.
- Matthews, J. & Gustafsson, J.A. (2003). Estrogen signaling: a subtle balance between ER alpha and ER beta. *Mol. Interv.*, **3**: 281–292.
- Matthews, M., Trevarrow, B., Matthews, J. (2002). A virtual tour of the guide for zebrafish users. *Resource*, **31**: 34-40.
- Mazellier, P., Méité, L., De Laat, J. (2008). Photodegradation of the steroid hormones 17 β -estradiol (E2) and 17 α -ethinylestradiol (EE2) in dilute aqueous solution. *Chemosphere*, **73**: 1216-1223.
- McCormick, M.I. & Molony, B.W. (1995). Influence of water temperature during the larval stage on size, age and body condition of a tropical reef fish at settlement. *Marine ecology progress series. Oldendorf*, **118**: 59-68.
- McDonnell, D. P. & Norris, J. D. (2002). Connections and regulation of the human estrogen receptor. *Science*, **296**: 1642–1644.
- McEwen, B.S. & Alves, S.E. (1999). Estrogen actions in the central nervous system. *Endocrinol. Rev.*, **20**: 279–307.

- McGee, M.R., Julius, M.L., Vajda, A.M., Norris, D.O., Barber, L.B., Schoenfuss, H.L. (2009). Predator avoidance performance of larval fathead minnows (*Pimephales promelas*) following short-term exposure to estrogen mixtures. *Aquatic toxicology*, **91**: 355-361.
- McKenna, N.J, Lanz, R.B, O'Malley BW. (1999). Nuclear receptor coregulators: cellular and molecular biology. *Endocr. Rev.*, **20**: 321–344.
- Meekan, M.G., Carleton, J.H., McKinnon, A.D., Flynn, K., Furnas, M. (2003). What determines the growth of tropical reef fish larvae in the plankton: food or temperature? *Marine Ecology Progress Series*, **256**: 193-204.
- Meltser, I., Tahera, Y., Simpson, E., Hultcrantz, M., Charitidi, K., Gustafsson, J.A., Canlon, B. (2008). Estrogen receptor beta protects against acoustic trauma in mice. *J. Clin. Invest.*, **118**: 1563–1570.
- Menuet, A., Pellegrini, E., Anglade, I., Blaise, O., Laudet, V., Kah, O., Pakdel, F. (2002). Molecular characterization of three estrogen receptor forms in zebrafish: binding characteristics, transactivation properties, and tissue distributions. *Biol. Reprod.*, **66**, 1881–1892.
- Metcalfe, C.D., Metcalfe, T.L., Kiparissis, Y., Koenig, B.G., Khan, C., Hughes, R.J., Croley, T.R., March, R.E., Potter, T. (2001). Estrogenic potency of chemicals detected in sewage treatment plant effluents as determined by in vivo assays with Japanese medaka (*Oryzias latipes*). *Environmental Toxicology and Chemistry*, **20**: 297-308.
- Meyer, F.P. (1991). Aquaculture disease and health management. *Journal of animal science*, **69**: 4201-4208.
- Miller, T.J. (2007). Contribution of individual-based coupled physical–biological models to understanding recruitment in marine fish populations. *Marine Ecology Progress Series*, **347**: 127-138.
- Mills, L.J. & Chichester, C. (2005). Review of evidence: are endocrine-disrupting chemicals in the aquatic environment impacting fish populations? *Science of the Total Environment*, **343**: 1-34.

- Milstein, A., Zoran, M., Peretz, Y. and Joseph, D., 2000. Low temperature tolerance of pacu, *Piaractus mesopotamicus*. *Environmental biology of fishes*, **58**: 455-460.
- Mittendorf, R. (1995). Teratogen update: carcinogenesis and teratogenesis associated with exposure to diethylstilbestrol (DES) in utero. *Teratology*, **51**: 435-445.
- Mok, G.S., Wang, Y. & Tsui, B.M. (2009). Quantification of the multiplexing effects in multi-pinhole small animal SPECT: a simulation study. *IEEE transactions on nuclear science*, **56**: 2636-2643.
- Montano, M.M., Muller, V., Trobaugh, A., Katzenellenbogen, B.S. (1995). The carboxy-terminal F domain of the human estrogen receptor: role in the transcriptional activity of the receptor and the effectiveness of antiestrogens as estrogen antagonists. *Mol. Endocrinol.*, **9**: 814–825.
- Morani, A., Barros, R.P.A., Imamov, O., Hultenby, K., Arner, A., Warner, M., Gustafsson, J.A. (2006). Lung dysfunction causes systemic hypoxia in estrogen receptor beta knockout (ER^{-/-}) mice. *Proc. Natl. Acad. Sci. USA*, **103**: 7165–7169.
- Mortensen, A.S. & Arukwe, A. (2007). Effects of 17 α -ethynylestradiol on hormonal responses and xenobiotic biotransformation system of Atlantic salmon (*Salmo salar*). *Aquatic Toxicology*, **85**: 113-123.
- Mortimer, J.A., Collie, J., Jupiter, T., Chapman, R., Liljevik, A., Betsy, B. (2003). Growth rates of immature hawksbills (*Eretmochelys imbricata*) at Aldabra Atoll, Seychelles (Western Indian Ocean). In *Seminoff JA (compiler) Proceedings of the twenty-second annual symposium on sea turtle biology and conservation. NOAA Technical Memorandum NMFS-SEFSC-503 (247-248)*.
- Naderi, M., Wong, M.Y., Gholami, F. (2014). Developmental exposure of zebrafish (*Danio rerio*) to bisphenol-S impairs subsequent reproduction potential and hormonal balance in adults. *Aquatic toxicology*, **148**: 195-203.
- Nagler, J.J., Cavileer, T., Sullivan, J., Cyr, D.G., Rexroad III, C. (2007). The complete nuclear estrogen receptor family in the rainbow trout: discovery of the novel ER α 2 and both ER β isoforms. *Gene*, **392**: 164–173.

- Nasu, M., Sugimoto, T., Kaji, H., Chihara, K. (2000). Estrogen modulates osteoblast proliferation and function regulated by parathyroid hormone in osteoblastic SaOS-2 cells: role of insulin-like growth factor (IGF)-I and IGF-binding protein-5. *Journal of endocrinology*, **167**: 305-313.
- Negri-Cesi, P. (2015). Bisphenol A interaction with brain development and functions. *Dose-Response*, **13**: p.1559325815590394.
- Nezafatian, E., Zadmajid, V., Cleveland, B.M. (2017). Short-term Effects of Genistein on the Reproductive Characteristics of Male Gibel Carp, *Carassius auratus gibelio*. *Journal of the World Aquaculture Society*.
- Nilsson, S., Mäkelä, S., Treuter, E., Tujague, M., Thomsen, J., Andersson, G., Enmark, E., Pettersson, K., Warner, M., Gustafsson, J.A. (2001). Mechanisms of estrogen action. *Physiological Reviews*, **81**: 1535-1565.
- Norris, D. O., & Carr, J. A. (2013). *Vertebrate endocrinology*. Academic Press.
- Nowak, C., Jost, D., Vogt, C., Oetken, M., Schwenk, K., Oehlmann, J. (2007). Consequences of inbreeding and reduced genetic variation on tolerance to cadmium stress in the midge *Chironomus riparius*. *Aquatic Toxicology*, **85**: 278-284.
- Nowicki, J.P., Miller, G.M., Munday, P.L. (2012). Interactive effects of elevated temperature and CO₂ on foraging behavior of juvenile coral reef fish. *Journal of Experimental Marine Biology and Ecology*, **412**: 46-51.
- Oakley, R.H., Sar, M., Cidlowski, J.A. (1996). The human glucocorticoid receptor β isoform. *J. Biol. Chem.*, **271**: 9550–9559.
- OECD. (2003). Draft summary report of the sixth meeting of the task force on endocrine disrupters testing and assessment (EDTA 6). Draft as of March 12, 2003.
- O'Reilly, C.M., Sharma, S., Gray, D.K., Hampton, S.E., Read, J.S., Rowley, R.J., Schneider, P., Lenters, J.D., McIntyre, P.B., Kraemer, B.M., Weyhenmeyer, G.A. (2015). Rapid and highly variable warming of lake surface waters around the globe. *Geophysical Research Letters*, **42**.

- Örn, S., Holbech, H., Madsen, T.H., Norrgren, L., Petersen, G.I. (2003). Gonad development and vitellogenin production in zebrafish (*Danio rerio*) exposed to ethinylestradiol and methyltestosterone. *Aquatic Toxicology*, **65**: 397-411.
- Ospina-Alvarez, N. & Piferrer, F. (2008). Temperature-dependent sex determination in fish revisited: prevalence, a single sex ratio response pattern, and possible effects of climate change. *PLoS One*, **3**: p.e2837.
- Osterauer, R. & Köhler, H.R. (2008). Temperature-dependent effects of the pesticides thiacloprid and diazinon on the embryonic development of zebrafish (*Danio rerio*). *Aquatic Toxicology*, **86**: 485-494.
- Paaijmans, K.P., Heinig, R.L., Seliga, R.A., Blanford, J.I., Blanford, S., Murdock, C.C., Thomas, M.B. (2013). Temperature variation makes ectotherms more sensitive to climate change. *Global change biology*, **19**: 2373-2380.
- Packard M.G. & Teather, L.A. (1997a). Posttraining estradiol injections enhance memory in ovariectomized rats: cholinergic blockade and synergism. *Neurobiol. Learn. Mem.*, **68**: 172–188.
- Pais, A., Gunanathan, C., Margalit, R., Eti, B.I., Yosepovich, A., Milstein, D., Degani, H. (2011). In vivo magnetic resonance imaging of the estrogen receptor in an orthotopic model of human breast cancer. *Cancer research*, **71**: 7387-7397.
- Palermo, F.A., Mosconi, G., Angeletti, M., Polzonetti-Magni, A.M. (2008). Assessment of water pollution in the Tronto River (Italy) by applying useful biomarkers in the fish model *Carassius auratus*. *Archives of environmental contamination and toxicology*, **55**: 295-304.
- Pankhurst, N.W. & Munday, P.L. (2011). Effects of climate change on fish reproduction and early life history stages. *Marine and Freshwater Research*, **62**: 1015-1026.
- Pankhurst, N.W. & Thomas, P.M. (1998). Maintenance at elevated temperature delays the steroidogenic and ovulatory responsiveness of rainbow trout *Oncorhynchus mykiss* to luteinizing hormone releasing hormone analogue. *Aquaculture*, **166**: 163-177.

- Panter, G.H., Hutchinson, T.H., Länge, R., Lye, C.M., Sumpter, J.P., Zerulla, M., Tyler, C.R. (2002). Utility of a juvenile fathead minnow screening assay for detecting (anti-) estrogenic substances. *Environmental Toxicology and Chemistry*, **21**: 319-326.
- Pardo-Martin, C., Chang, T.Y., Koo, B.K., Gilleland, C.L., Wasserman, S.C., Yanik, M.F. (2010). High-throughput in vivo vertebrate screening. *Nature methods*, **7**: 634-636.
- Paris, M., Brunet, F., Markov, G.V., Schubert, M., Laudet, V. (2008). The amphioxus genome enlightens the evolution of the thyroid hormone signaling pathway. *Dev. Genes Evol.*, **218**: 667–680.
- Parng, C., Anderson, N., Ton, C., McGrath, P. (2004). Zebrafish apoptosis assays for drug discovery. *Methods in cell biology*, **76**: 75-85.
- Parrella, A., Lavoragna, M., Criscuolo, E., Russo, C., Isidori, M. (2014). Estrogenic activity and cytotoxicity of six anticancer drugs detected in water systems. *Science of The Total Environment*, **485**: 216-222.
- Parrott, J.L. & Blunt, B.R. (2005). Life-cycle exposure of fathead minnows (*Pimephales promelas*) to an ethinylestradiol concentration below 1 ng/L reduces egg fertilization success and demasculinizes males. *Environmental toxicology*, **20**: 131-141.
- Parrott, J.L. & Wood, C.S. (2002). Fathead minnow lifecycle tests for detection of endocrine-disrupting substances in effluents. *Water quality research journal of Canada*, **37**: 651-667.
- Partridge, C., Boettcher, A., Jones, A.G. (2010). Short-term exposure to a synthetic estrogen disrupts mating dynamics in a pipefish. *Hormones and Behavior*, **58**: 800-807.
- Patel, A., Panter, G.H., Trollope, H.T., Glennon, Y.C., Owen, S.F., Sumpter, J.P., Rand-Weaver, M. (2016). Testing the “read-across hypothesis” by investigating the effects of ibuprofen on fish. *Chemosphere*, **163**: 592-600.

- Pawlowski, S., Van Aerle, R., Tyler, C.R., Braunbeck, T. (2004). Effects of 17 α -ethynylestradiol in a fathead minnow (*Pimephales promelas*) gonadal recrudescence assay. *Ecotoxicology and environmental safety*, **57**: 330-345.
- Paylor, R. (2009). Questioning standardization in science: some scientists suggest that environmental standardization may lead to spurious findings. The implication from this hypothesis will likely be controversial. *Nature methods*, **6**: 253-255.
- Penman, D.J. & Piferrer, F. (2008). Fish gonadogenesis. Part I: genetic and environmental mechanisms of sex determination. *Reviews in Fisheries Science*, **16**: 16-34.
- Penza, M., Jeremic, M., Marrazzo, E., Maggi, A., Ciana, P., Rando, G., Grigolato, P.G., Di Lorenzo, D. (2011). The environmental chemical tributyltin chloride (TBT) shows both estrogenic and adipogenic activities in mice which might depend on the exposure dose. *Toxicology and applied pharmacology*, **255**: 65-75.
- Persoone, G., Van de Vel, A., Van Steertegem, M., De Nayer, B. (1989). Predictive value of laboratory tests with aquatic invertebrates: influence of experimental conditions. *Aquatic Toxicology*, **14**: 149-167.
- Peters, R.E., Courtenay, S.C., Hewitt, L.M., MacLatchy, D.L. (2010). Effects of 17 α -ethynylestradiol on early-life development, sex differentiation and vitellogenin induction in mummichog (*Fundulus heteroclitus*). *Marine environmental research*, **69**: 178-186.
- Petit, F., Valotaire, Y., Pakdel, F. (1995). Differential functional activities of rainbow trout and human estrogen receptors expressed in the yeast *Saccharomyces cerevisiae*. *Eur. J. Biochem.*, **233**: 584-592.
- Pettersson, K., Grandien, K., Kuiper, G.G., Gustafsson, J.A. (1997). Mouse estrogen receptor β forms estrogen response element binding heterodimers with estrogen receptor α . *Molecular Endocrinology*. **11**: 1486–1496.
- Phelps, M.E. (2000). PET: the merging of biology and imaging into molecular imaging. *The Journal of Nuclear Medicine*, **41**: 661.

- Pojana, G., Gomiero, A., Jonkers, N., Marcomini, A. (2007). Natural and synthetic endocrine disrupting compounds (EDCs) in water, sediment and biota of a coastal lagoon. *Environment International*, **33**: 929-936.
- Prins, G.S. & Birch, L. (1995). The developmental pattern of androgen receptor expression in rat prostate lobes is altered after neonatal exposure to estrogen. *Endocrinology*, **136**: 1303–1314.
- Prins, G.S. (1992). Neonatal estrogen exposure induces lobe-specific alterations in adult rat prostate androgen receptor expression. *Endocrinology*, **130**: 2401–2412.
- Prins, G.S., Marmer, M., Woodham, C., Chang, W., Kuiper, G., Gustafsson, J.A., Birch, L. (1998). Estrogen receptor-beta messenger ribonucleic acid ontogeny in the prostate of normal and neonatally estrogenized rats. *Endocrinology*, **139**: 874–883.
- Pulak, R. (2016). Tools for automating the imaging of zebrafish larvae. *Methods*, **96**: 118-126.
- Purdom, C.E., Hardiman, P.A., Bye, V.V.J., Eno, N.C., Tyler, C.R., Sumpter, J.P. (1994). Estrogenic effects of effluents from sewage treatment works. *Chemistry and Ecology*, **8**: 275-285.
- Reel, J.R., Lamb, J.C., Neal, B.H. (1996). Survey and assessment of mammalian estrogen biological assays for hazard characterization. *Toxicological Sciences*, **34**: 288-305.
- Reigner, B.G., Williams, P.E., Patel, I.H., Steimer, J.L., Peck, C., van Brummelen, P., (1997). An evaluation of the integration of pharmacokinetic and pharmacodynamic principles in clinical drug development. *Clinical pharmacokinetics*, **33**: 142-152.
- Rempel, M.A. & Schlenk, D. (2008). Effects of environmental estrogens and antiandrogens on endocrine function, gene regulation, and health in fish. *Int. Rev. Cell Mol. Biol.*, **267**: 207–252.

- Reyhani, N., Volkova, K., Hallgren, S., Bollner, T., Olsson, P.E., Olsén, H., Hällström, I.P. (2011). 17 α -Ethinyl estradiol affects anxiety and shoaling behavior in adult male zebra fish (*Danio rerio*). *Aquatic toxicology*, **105**: 41-48.
- Richter, S.H., Garner, J.P., Würbel, H. (2009). Environmental standardization: cure or cause of poor reproducibility in animal experiments? *Nature methods*, **6**: 257-261.
- Rijnsdorp, A.D., Peck, M.A., Engelhard, G.H., Möllmann, C., Pinnegar, J.K. (2009). Resolving the effect of climate change on fish populations. *ICES Journal of Marine Science: Journal du Conseil*, p.fsp056.
- Rittscher, J. (2010). Characterization of biological processes through automated image analysis. *Annual Review of Biomedical Engineering*, **12**: 315-344.
- Robinson, B.J. & Hellou, J. (2009). Biodegradation of endocrine disrupting compounds in harbour seawater and sediments. *Science of the total environment*, **407**: 5713-5718.
- Roessig, J.M., Woodley, C.M., Cech, J.J., Hansen, L.J. (2004). Effects of global climate change on marine and estuarine fishes and fisheries. *Reviews in Fish Biology and Fisheries*, **14**: .251-275.
- Roh, H. & Chu, K.H. (2010). A 17 β -estradiol-utilizing bacterium, *Sphingomonas* strain KC8: Part I-Characterization and abundance in wastewater treatment plants. *Environmental science & technology*, **44**: 4943-4950.
- Roman-Blas, J.A., Castañeda, S., Largo, R., Herrero-Beaumont, G. (2009). Osteoarthritis associated with estrogen deficiency. *Arthritis. Res. Ther.*, **11**: 241.
- Rombough, P.J. & Garside, E.T. (1982). Cadmium toxicity and accumulation in eggs and alevins of Atlantic salmon *Salmo salar*. *Canadian Journal of Zoology*, **60**: 2006-2014.
- Rombough, P.J. (1997), January. *The effects of temperature on embryonic and larval development. In Seminar Series-Society For Experimental Biology* (Vol. **61**: 177-224). Cambridge University Press.

- Rountrey, A.N., Coulson, P.G., Meeuwig, J.J., Meekan, M. (2014). Water temperature and fish growth: otoliths predict growth patterns of a marine fish in a changing climate. *Global change biology*, **20**: 2450-2458.
- Routledge, E.J., Sheahan, D., Desbrow, C., Brighty, G.C., Waldock, M., Sumpter, J.P. (1998). Identification of estrogenic chemicals in STW effluent. 2. In vivo responses in trout and roach. *Environmental Science & Technology*, **32**: 1559-1565.
- Rouze, N.C., Schmand, M., Siegel, S., Hutchins, G.D. (2004). Design of a small animal PET imaging system with 1 microliter volume resolution. *IEEE Transactions on nuclear science*, **51**: 757-763.
- Saaristo, M., Craft, J.A., Lehtonen, K.K., Lindström, K. (2009). Sand goby (*Pomatoschistus minutus*) males exposed to an endocrine disrupting chemical fail in nest and mate competition. *Hormones and Behavior*, **56**: 315-321.
- Saha, G.B. (2015). *Basics of PET imaging: physics, chemistry, and regulations*. Springer.
- Salam, M.A., Sawada, T., Ohya, T., Ninomiya, K., Hayashi, S. (2008). Detection of environmental estrogenicity using transgenic medaka hatchlings (*Oryzias latipes*) expressing the GFP-tagged choriogenin L gene. *Journal of Environmental Science and Health, Part A*, **43**: 272-277.
- Sassi-Messai, S., Gibert, Y., Bernard, L., Nishio, S.I., Lagneau, K.F.F., Molina, J., Andersson-Lendahl, M., Benoit, G., Balaguer, P., Laudet, V. (2009). The phytoestrogen genistein affects zebrafish development through two different pathways. *PLoS One*, **4**: p.e4935.
- Schaefer, J. & Ryan, A. (2006). Developmental plasticity in the thermal tolerance of zebrafish *Danio rerio*. *Journal of Fish Biology*, **69**: 722-734.
- Schindelin, J., Arganda-Carreras, I., Frise, E., Kaynig, V., Longair, M., Pietzsch, T., Preibisch, S., Rueden, C., Saalfeld, S., Schmid, B., Tinevez, J.Y. (2012). Fiji: an open-source platform for biological-image analysis. *Nature methods*, **9**: 676-682.

- Schmidt, K. & Starck, J.M. (2010). Developmental plasticity, modularity, and heterochrony during the phylotypic stage of the zebra fish, *Danio rerio*. *Journal of Experimental Zoology Part B: Molecular and Developmental Evolution*, **314**: 166-178.
- Schnurr, M.E., Yin, Y., Scott, G.R. (2014). Temperature during embryonic development has persistent effects on metabolic enzymes in the muscle of zebrafish. *Journal of Experimental Biology*, **217**: 1370-1380.
- Schofield, O., Ducklow, H.W., Martinson, D.G., Meredith, M.P., Moline, M.A., Fraser, W.R. (2010). How do polar marine ecosystems respond to rapid climate change? *Science*, **328**: 1520-1523.
- Scholz, S. & Gutzeit, H.O. (2000). 17- α -ethinylestradiol affects reproduction, sexual differentiation and aromatase gene expression of the medaka (*Oryzias latipes*). *Aquatic toxicology*, **50**: 363-373.
- Scholz, S. & Klüver, N. (2009). Effects of endocrine disrupters on sexual, gonadal development in fish. *Sexual development*, **3**: 136-151.
- Schramm, N.U., Ebel, G., Engeland, U., Schurrat, T., Behe, M., Behr, T.M. (2003). High-resolution SPECT using multipinhole collimation. *IEEE Transactions on Nuclear Science*, **50**: 315-320.
- Schreck, C.B. (1982). Stress and rearing of salmonids. *Aquaculture*, **28**: 241-249.
- Schröter, C., Herrgen, L., Cardona, A., Brouhard, G.J., Feldman, B., Oates, A.C., (2008). Dynamics of zebrafish somitogenesis. *Developmental Dynamics*, **237**: 545-553.
- Schubert, M., Escriva H, Xavier-Neto J, Laudet V. (2006). Amphioxus and tunicates as evolutionary model systems. *Trends in ecology & evolution* (Personal edition), **21**: 269-277.
- Schulz, V., Torres-Espallardo, I., Renisch, S., Hu, Z., Ojha, N., Börnert, P., Perkuhn, M., Niendorf, T., Schäfer, W.M., Brockmann, H., Krohn, T. (2011). Automatic, three-segment, MR-based attenuation correction for whole-body PET/MR data. *European journal of nuclear medicine and molecular imaging*, **38**: 138-152.

- Schwindt, A.R., Winkelman, D.L., Keteles, K., Murphy, M., Vajda, A.M. (2014). An environmental oestrogen disrupts fish population dynamics through direct and transgenerational effects on survival and fecundity. *Journal of applied ecology*, **51**: 582-591.
- Segner, H., Carroll, K., Fenske, M., Janssen, C.R., Maack, G., Pascoe, D., Schäfers, C., Vandenberg, G.F., Watts, M., Wenzel, A. (2003). Identification of endocrine-disrupting effects in aquatic vertebrates and invertebrates: report from the European IDEA project. *Ecotoxicology and environmental safety*, **54**: 302-314.
- Shaner, N.C., Steinbach, P.A., Tsien, R.Y. (2005). A guide to choosing fluorescent proteins. *Nature methods*, **2**: 905-909.
- Sheiner, L.B. & Steimer, J.L. (2000). Pharmacokinetic/pharmacodynamic modeling in drug development. *Annual review of pharmacology and toxicology*, **40**: 67-95.
- Shelby, M.D., Newbold, R.R., Tully, D.B., Chae, K., Davis, V.L. (1996). Assessing environmental chemicals for estrogenicity using a combination of in vitro and in vivo assays. *Environmental health perspectives*, **104**: 1296.
- Shi, X.Y., Sheng, G.P., Li, X.Y., Yu, H.Q. (2010). Operation of a sequencing batch reactor for cultivating autotrophic nitrifying granules. *Bioresour Technol*, **101**: 2960-2964.
- Shughrue, P., Lane, M., Merchenthaler, I. (1997). Comparative distribution of estrogen receptor-alpha and -beta mRNA in the rat central nervous system. *J Comp Neurol*, **388**: 507-525.
- Shughrue, P.J., Lane, M.V., Scrimo, P.J., Merchenthaler, I. (1998). Comparative distribution of estrogen receptor-alpha (ER-alpha) and -beta (ER-beta) mRNA in the rat pituitary, gonad, and reproductive tract. *Steroids*, **63**: 498-504.
- Shyu, C., Cavileer, T.D., Nagler, J.J., Ytreberg, F.M. (2011). Computational estimation of rainbow trout estrogen receptor binding affinities for environmental estrogens. *Toxicology and applied pharmacology*, **250**: 322-326.
- Sibly, R.M. & Atkinson, D. (1994). How rearing temperature affects optimal adult size in ectotherms. *Functional Ecology*, 486-493.

- Skelly, D.K., Bolden, S.R., Dion, K.B. (2010). Intersex frogs concentrated in suburban and urban landscapes. *EcoHealth*, **7**: 374-379.
- Smith, C.L. & O'Malley, B.W. (2004). Coregulator function: a key to understanding tissue specificity of selective receptor modulators. *Endocr. Rev.*, **25**: 45–71.
- Smits, A.P., Skelly, D.K., Bolden, S.R. (2014). Amphibian intersex in suburban landscapes. *Ecosphere*, **5**: 1-9.
- Sodré, F.F., Locatelli, M.A.F., Jardim, W.F. (2010). Occurrence of emerging contaminants in Brazilian drinking waters: a sewage-to-tap issue. *Water, Air, and Soil Pollution*, **206**: 57-67.
- Sokolova, I.M. & Lannig, G. (2008). Interactive effects of metal pollution and temperature on metabolism in aquatic ectotherms: implications of global climate change. *Climate Research*, **37**: 181-201.
- Somero, G.N. (2010). The physiology of climate change: how potentials for acclimatization and genetic adaptation will determine 'winners' and 'losers'. *Journal of Experimental Biology*, **213**: 912-920.
- Somjen, D., Katzburg, S., Sharon, O., Grafi-Cohen, M., Knoll, E., Stern, N. (2011). The effects of estrogen receptors alpha- and beta-specific agonists and antagonists on cell proliferation and energy metabolism in human bone cell line. *J. Cell. Biochem.*, **112**: 625–632.
- Song, S.K., Sun, S.W., Ramsbottom, M.J., Chang, C., Russell, J., Cross, A.H. (2002). Dysmyelination revealed through MRI as increased radial (but unchanged axial) diffusion of water. *Neuroimage*, **17**: 1429-1436.
- Song, T.Y., Wu, H., Komarov, S., Siegel, S.B., Tai, Y.C. (2010). A sub-millimeter resolution PET detector module using a multi-pixel photon counter array. *Physics in medicine and biology*, **55**: 2573.
- Speirs, V., Skliris, G.P., Burdall, S.E., Carder, P.J. (2002). Distinct expression patterns of ER α and ER β in normal human mammary gland. *J. Clin. Pathol.*, **255**: 371–374.

- Spence, R., Fatema, M.K., Reichard, M., Huq, K.A., Wahab, M.A., Ahmed, Z.F., Smith, C. (2006). The distribution and habitat preferences of the zebrafish in Bangladesh. *Journal of Fish Biology*, **69**: 1435-1448.
- Spence, R., Gerlach, G., Lawrence, C., Smith, C. (2008). The behaviour and ecology of the zebrafish, *Danio rerio*. *Biological Reviews*, **83**: 13-34.
- Sponaugle, S. & Cowen, R.K. (1996). Larval Supply and Patterns of Recruitment for Two Caribbean Reef fishes *Stegastes partitus*. *Marine and Freshwater Research*, **47**: 433-447.
- Stachel, B., Ehrhorn, U., Heemken, O.P., Lepom, P., Reincke, H., Sawal, G., Theobald, N., (2003). Xenoestrogens in the River Elbe and its tributaries. *Environmental pollution*, **124**: 497-507.
- Stoker, C., Rey, F., Rodriguez, H., Ramos, J.G., Sirosky, P., Larriera, A., Luque, E.H., Muñoz-de-Toro, M. (2003). Sex reversal effects on *Caiman latirostris* exposed to environmentally relevant doses of the xenoestrogen bisphenol A. *General and comparative endocrinology*, **133**: 287-296.
- Subasinghe, R.P. & Sommerville, C. (1992). Effects of temperature on hatchability, development and growth of eggs and yolk sac fry of *Oreochromis mossambicus* (Peters) under artificial incubation. *Aquaculture Research*, **23**: 31-39.
- Suzuki, T., Matsuzaki, T., Hagiwara, H., Aoki, T., Takata, K. (2007). Recent advances in fluorescent labeling techniques for fluorescence microscopy. *Acta histochemica et cytochemica*, **40**: 131-137.
- Svenson, A., Allard, A.S., Ek, M. (2003). Removal of estrogenicity in Swedish municipal sewage treatment plants. *Water Research*, **37**: 4433-4443.
- Tai, Y.C., Chatziioannou, A.F., Yang, Y., Silverman, R.W., Meadors, K., Siegel, S., Newport, D.F., Stickel, J.R., Cherry, S.R. (2003). MicroPET II: design, development and initial performance of an improved microPET scanner for small-animal imaging. *Physics in medicine and biology*, **48**: 1519.
- Takahashi, H. (1977). Juvenile hermaphroditism in the zebrafish, *Brachydanio rerio*. *北海道大學水産學部研究彙報= BULLETIN OF THE FACULTY OF FISHERIES HOKKAIDO UNIVERSITY*, **28**: 57-65.

- Tang, X., Hashmi, M.Z., Zhang, H., Qian, M., Yu, C., Shen, C., Qin, Z., Huang, R., Qiao, J., Chen, Y. (2013). A preliminary study on the occurrence and dissipation of estrogen in livestock wastewater. *Bulletin of environmental contamination and toxicology*, **90**: 391-396.
- Taylor, M.R. & Harrison, P.T.C. (1999). Ecological effects of endocrine disruption: current evidence and research priorities. *Chemosphere*, **39**: 1237-1248.
- Ternes, T.A., Stumpf, M., Mueller, J., Haberer, K., Wilken, R.D., Servos, M. (1999a). Behavior and occurrence of estrogens in municipal sewage treatment plants—I. Investigations in Germany, Canada and Brazil. *Science of the Total Environment*, **225**: 81-90.
- Thornton, J.W. (2001). Evolution of vertebrate steroid receptors from an ancestral estrogen receptor by ligand exploitation and serial genome expansions. *Proc. Natl. Acad. Sci. USA*, **98**: 5671–5676.
- Thornton, J.W., Need, E., Crewes, D. (2003). Resurrecting the ancestral steroid receptor: ancient origin of estrogen signaling. *Science*, **301**: 1714–1717.
- Thorpe, K.L., Cummings, R.I., Hutchinson, T.H., Scholze, M., Brighty, G., Sumpter, J.P., Tyler, C.R. (2003). Relative potencies and combination effects of steroidal estrogens in fish. *Environmental science & technology*, **37**: 1142-1149.
- Tingaud-Sequeira, A., Andre, M., Fogue, J., Barthe, C., Babin, P.J. (2004). Expression patterns of three estrogen receptor genes during zebrafish (*Danio rerio*) development: evidence for high expression in neuromasts. *Gene Expr. Patterns*, **4**: 561–568.
- Tingaud-Sequeira, A., Ouadah, N. and Babin, P.J. (2011). Zebrafish obesogenic test: a tool for screening molecules that target adiposity. *Journal of lipid research*, **52**: 1765-1772.
- Tomšíková, H., Aufartová, J., Solich, P., Nováková, L., Sosa-Ferrera, Z., Santana-Rodríguez, J.J. (2012). High-sensitivity analysis of female-steroid hormones in environmental samples. *TrAC Trends in Analytical Chemistry*, **34**: 35-58.

- Tremblay, A., Tremblay, G.B., Labrie, F., Giguère, V. (1999). Ligand-independent recruitment of SRC-1 to estrogen receptor β through phosphorylation of activation function AF-1. *Mol. Cell*, **3**: 513–519.
- Tsai, M.J. & O'Malley, B.W. (1994). Molecular mechanisms of action of steroid/thyroid receptor superfamily members. *Annu. Rev. Biochem.*, **63**: 451–486.
- Tsien, R.Y. (1998). The green fluorescent protein. *Annual review of biochemistry*, **67**: 509-544.
- Tucker, B. & Lardelli, M. (2007). A rapid apoptosis assay measuring relative acridine orange fluorescence in zebrafish embryos. *Zebrafish*, **4**: 113-116.
- Tuomainen, U. & Candolin, U. (2011). Behavioural responses to human-induced environmental change. *Biological Reviews*, **86**: 640-657.
- Tyler, C., Jobling, S., Sumpter, J.P. (1998). Endocrine disruption in wildlife: a critical review of the evidence. *Critical reviews in toxicology*, **28**: 319-361.
- Uchida, D., Yamashita, M., Kitano, T., Iguchi, T. (2002). Oocyte apoptosis during the transition from ovary-like tissue to testes during sex differentiation of juvenile zebrafish. *Journal of Experimental Biology*, **205**: 711-718.
- Uchida, D., Yamashita, M., Kitano, T., Iguchi, T. (2004). An aromatase inhibitor or high water temperature induce oocyte apoptosis and depletion of P450 aromatase activity in the gonads of genetic female zebrafish during sex-reversal. *Comparative Biochemistry and Physiology Part A: Molecular & Integrative Physiology*, **137**: 11-20.
- USEPA, U., *Environmental Protection Agency. (2002b). Short-term methods for estimating the chronic toxicity of effluents and receiving waters to freshwater organisms.* EPA-821-R-02-013.
- USEPA, U., *Environmental Protection Agency. (2002a) Methods for measuring the acute toxicity of effluents and receiving waters to freshwater and marine organisms.* EPA-821-R-02-012.
- Vader, J.S., Van Ginkel, C.G., Sperling, F.M.G.M., De Jong, J., De Boer, W., De Graaf, J.S., Van Der Most, M., Stokman, P.G.W. (2000). Degradation of ethinyl estradiol by nitrifying activated sludge. *Chemosphere*, **41**: 1239-1243.

- Vaiserman, A. (2014). Early-life exposure to endocrine disrupting chemicals and later-life health outcomes: an epigenetic bridge? *Aging Dis.*, **5**: 419–429.
- Van Aerle, R., Pounds, N., Hutchinson, T.H., Maddix, S., Tyler, C.R. (2002). Window of sensitivity for the estrogenic effects of ethinylestradiol in early life-stages of fathead minnow, *Pimephales promelas*. *Ecotoxicology*, **11**: 423-434.
- Van den Belt, K., Verheyen, R., Witters, H. (2003). Comparison of vitellogenin responses in zebrafish and rainbow trout following exposure to environmental estrogens. *Ecotoxicology and environmental safety*, **56**: 271-281.
- Van Vliet, M.T., Franssen, W.H., Yearsley, J.R., Ludwig, F., Haddeland, I., Lettenmaier, D.P., Kabat, P. (2013). Global river discharge and water temperature under climate change. *Global Environmental Change*, **23**: 450-464.
- Van Wezel, A.P. & Jonker, M.T. (1998). Use of the lethal body burden in the risk quantification of field sediments; influence of temperature and salinity. *Aquatic toxicology*, **42**: 287-300.
- Van Zuiden, T.M., Chen, M.M., Stefanoff, S., Lopez, L., Sharma, S. (2016). Projected impacts of climate change on three freshwater fishes and potential novel competitive interactions. *Diversity and Distributions*.
- Vaska, P., Woody, C.L., Schlyer, D.J., Shokouhi, S., Stoll, S.P., Pratte, J.F., O'Connor, P., Junnarkar, S.S., Rescia, S., Yu, B., Purschke, M. (2004). RatCAP: miniaturized head-mounted PET for conscious rodent brain imaging. *IEEE Transactions on Nuclear Science*, **51**: 2718-2722.
- Vegeto, E., Shahbaz, M.M., Wen, D.X., Goldman, M.E., O'Malley, B.W., McDonnell, D.P. (1993). Human progesterone receptor A form is a cell- and promoter-specific repressor of human progesterone receptor B function. *Mol Endocrinol.*, **7**: 1244–1255.
- Veiga-Lopez, A., Luense, L.J., Christenson, L.K., Padmanabhan, V. (2013). Developmental programming: gestational bisphenol-A treatment alters trajectory of fetal ovarian gene expression. *Endocrinology*, **154**: 1873-1884.
- Versonnen, B.J. & Janssen, C.R. (2004). Xenoestrogenic effects of ethinylestradiol in zebrafish (*Danio rerio*). *Environmental toxicology*, **19**: 198-206.

- Vicentini, C.A., Franceschini-Vicentini, I.B., Bombonato, M.T.S., Bertolucci, B., Lima, S.G., Santos, A.S. (2005). Morphological study of the liver in the teleost *Oreochromis niloticus*. *Int. j. morphol*, **23**: 211-216.
- Viñas, P., Campillo, N., Martínez-Castillo, N., Hernández-Córdoba, M. (2010). Comparison of two derivatization-based methods for solid-phase microextraction–gas chromatography–mass spectrometric determination of bisphenol A, bisphenol S and biphenol migrated from food cans. *Analytical and bioanalytical chemistry*, **397**: 115-125.
- Vinggaard, A.M., Nellemann, C., Dalgaard, M., Jørgensen, E.B., Andersen, H.R. (2002). Antiandrogenic effects in vitro and in vivo of the fungicide prochloraz. *Toxicological Sciences*, **69**: 344-353.
- Vonesch, C., Aguet, F., Vonesch, J.L. and Unser, M. (2006). The colored revolution of bioimaging. *IEEE signal processing magazine*, **23**: 20-31.
- Vos, J.G., Dybing, E., Greim, H.A., Ladefoged, O., Lambré, C., Tarazona, J.V., Brandt, I., Vethaak, A.D. (2000). Health effects of endocrine-disrupting chemicals on wildlife, with special reference to the European situation. *Critical reviews in toxicology*, **30**: 71-133.
- Vosges, M., Le Page, Y., Chung, B.C., Combarous, Y., Porcher, J.M., Kah, O., Brion, F. (2010). 17 α -Ethinylestradiol disrupts the ontogeny of the forebrain GnRH system and the expression of brain aromatase during early development of zebrafish. *Aquatic toxicology*, **99**: 479-491.
- Wada-Hiraike, O., Warner, M., Gustafsson, J. A. (2006). New developments in oestrogen signalling in colonic epithelium. *Biochem. Soc. Trans.*, **34**: 1114-1116.
- Walker, S.L., Ariga, J., Mathias, J.R., Coothankandaswamy, V., Xie, X., Distel, M., Köster, R.W., Parsons, M.J., Bhalla, K.N., Saxena, M.T., Mumm, J.S. (2012). Automated reporter quantification in vivo: high-throughput screening method for reporter-based assays in zebrafish. *PloS one*, **7**: p.e29916.
- Walker, V.R. & Korach, K.S. (2004). Estrogen receptor knockout mice as a model for endocrine research. *ILAR Journal*, **45**: 455–461.

- Wang, H., Huang, Z.Q., Xia, L., Feng, Q., Erdjument-Bromage, H., Strahl, B.D., Briggs, S.D., Allis, C.D., Wong, J., Tempst, P., Zhang, Y. (2001). Methylation of histone H4 at arginine 3 facilitating transcriptional activation by nuclear hormone receptor. *Science*, **293**: 853–857.
- Watanabe, T., Inoue, S., Ogawa, S., Ishii, Y., Hiroi, H., Ikeda, K., Orimo, A., Muramatsu, M. (1997). Agonistic effect of tamoxifen is dependent on cell type, ERE-promoter context, and estrogen receptor subtype: functional difference between estrogen receptors alpha and beta. *Biochem. Biophys. Res. Commun.*, **236**: 140–145.
- Watson, C.S., Alyea, R.A., Jeng, Y.J., Kochukov, M.Y. (2007). Nongenomic actions of low concentration estrogens and xenoestrogens on multiple tissues. *Molecular and cellular endocrinology*, **274**: 1-7.
- Watson, C.S., Bulayeva, N.N., Wozniak, A.L., Finnerty, C.C. (2005). Signaling from the membrane via membrane estrogen receptor- α : estrogens, xenoestrogens, and phytoestrogens. *Steroids*, **70**: 364-371.
- Weber, D.A. & Ivanovic, M. (1995). Pinhole SPECT: ultra-high resolution imaging for small animal studies.
- Weber, S., Leuschner, P., Kämpfer, P., Dott, W., Hollender, J. (2005). Degradation of estradiol and ethinyl estradiol by activated sludge and by a defined mixed culture. *Applied Microbiology and Biotechnology*, **67**: 106-112.
- Weihua, Z., Lathe, R., Warner, R., Gustafsson, J.A. (2002). An endocrine pathway in prostate, ERbeta, AR, 5alpha-androstane-3beta, 17betadiol, and CYP7B1, prostate growth. *Proc. Natl. Acad. Sci. USA*, **99**: 13589–13594.
- Weissleder, R. & Mahmood, U. (2001). Molecular imaging 1. *Radiology*, **219**: 316-333.
- Westerfield, M. (1995). *The Zebrafish Book*. Eugene: University of Oregon Press.
- White, R.M., Sessa, A., Burke, C., Bowman, T., LeBlanc, J., Ceol, C., Bourque, C., Dovey, M., Goessling, W., Burns, C.E., Zon, L.I. (2008). Transparent adult zebrafish as a tool for in vivo transplantation analysis. *Cell stem cell*, **2**: 183-189.

- Wilkins, B.J. & Pack, M. (2013). Zebrafish models of human liver development and disease. *Comprehensive Physiology*.
- Williams, L.E. (2008). Anniversary paper: nuclear medicine: fifty years and still counting. *Medical physics*, **35**: 3020-3029.
- Willmann, J.K., Van Bruggen, N., Dinkelborg, L.M., Gambhir, S.S. (2008). Molecular imaging in drug development. *Nature reviews Drug discovery*, **7**: 591-607.
- Wilson, C. (2012). Aspects of larval rearing. *ILAR Journal*, **53**: 169-178.
- Winata, C.L., Korzh, S., Kondrychyn, I., Zheng, W., Korzh, V., Gong, Z. (2009). Development of zebrafish swimbladder: The requirement of Hedgehog signaling in specification and organization of the three tissue layers. *Developmental biology*, **331**: 222-236.
- Wittbrodt, J.N., Liebel, U., Gehrig, J. (2014). Generation of orientation tools for automated zebrafish screening assays using desktop 3D printing. *BMC biotechnology*, **14**: 36.
- Woodham, C., Birch, L., Prins, G.S. (2003). Neonatal estrogens down regulate prostatic androgen receptor levels through a proteasome-mediated protein degradation pathway. *Endocrinology*. **144**: 4841–4850.
- Würbel, H. (2000). Behaviour and the standardization fallacy. *Nature genetics*, **26**: 263-263.
- Würbel, H. (2002). Behavioral phenotyping enhanced–beyond (environmental) standardization. *Genes, Brain and Behavior*, **1**: 3-8.
- Wurtz, J.M., Bourguet, W., Renaud, J.P., Vivat, V., Chambon, P., Moras, D., Gronemeyer, H. (1996). A canonical structure for the ligand-binding domain of nuclear receptors. *Nat. Struct. Biol.*, **3**: 87–94.
- Xia, X., Feng, H., Li, C., Qin, C., Song, Y., Zhang, Y., Lan, X. (2016). ^{99m}Tc-labeled estradiol as an estrogen receptor probe: Preparation and preclinical evaluation. *Nuclear medicine and biology*, **43**: 89-96.

- Xie, H.G., Kim, R.B., Wood, A.J., Stein, C.M. (2001). Molecular basis of ethnic differences in drug disposition and response. *Annual review of pharmacology and toxicology*, **41**: 815-850.
- Xu, H., Yang, J., Wang, Y., Jiang, Q., Chen, H., Song, H. (2008). Exposure to 17 α -ethynylestradiol impairs reproductive functions of both male and female zebrafish (*Danio rerio*). *Aquatic Toxicology*, **88**: 1-8.
- Yang, J., Singleton, D.W., Shaughnessy, E.A., Khan, S.A. (2008). The F-domain of estrogen receptor-alpha inhibits ligand induced receptor dimerization. *Mol. Cell. Endocrinol.*, **295** :94–100.
- Yang, Y., Guan, J., Yin, J., Shao, B., Li, H. (2014). Urinary levels of bisphenol analogues in residents living near a manufacturing plant in south China. *Chemosphere*, **112**: 481-486.
- Yang, Y., Yin, J., Yang, Y., Zhou, N., Zhang, J., Shao, B., Wu, Y. (2012). Determination of bisphenol AF (BPAF) in tissues, serum, urine and feces of orally dosed rats by ultra-high-pressure liquid chromatography–electrospray tandem mass spectrometry. *Journal of Chromatography B*, **901**: 93-97.
- Yang, Z. (2000). *Phylogenetic analysis by maximum likelihood (PAML)*.
- Yokota, H., Seki, M., Maeda, M., Oshima, Y., Tadokoro, H., Honjo, T., Kobayashi, K., 2001. Life-cycle toxicity of 4-nonylphenol to medaka (*Oryzias latipes*). *Environmental Toxicology and Chemistry*, **20**: 2552-2560.
- Yoshimoto, T., Nagai, F., Fujimoto, J., Watanabe, K., Mizukoshi, H., Makino, T., Kimura, K., Saino, H., Sawada, H., Omura, H. (2004). Degradation of estrogens by *Rhodococcus zopfii* and *Rhodococcus equi* isolates from activated sludge in wastewater treatment plants. *Applied and environmental microbiology*, **70**: 5283-5289.
- Yu, Y., Huang, Q., Cui, J., Zhang, K., Tang, C. and Peng, X. (2011). Determination of pharmaceuticals, steroid hormones, and endocrine-disrupting personal care products in sewage sludge by ultra-high-performance liquid chromatography–tandem mass spectrometry. *Analytical and bioanalytical chemistry*, **399**: 891-902.

- Zagzebski, J.A. (1996). *Essentials of ultrasound physics*. Mosby.
- Zanzonico, P. (2004). April. Positron emission tomography: a review of basic principles, scanner design and performance, and current systems. In *Seminars in nuclear medicine* (Vol. 34, No. 2, pp. 87-111). WB Saunders.
- Zaragoza, C., Gomez-Guerrero, C., Martin-Ventura, J.L., Blanco-Colio, L., Lavin, B., Mallavia, B., Tarin, C., Mas, S., Ortiz, A., Egido, J. (2011). Animal models of cardiovascular diseases. *BioMed Research International*.
- Zeddies, D.G. & Fay, R.R. (2005). Development of the acoustically evoked behavioral response in zebrafish to pure tones. *Journal of Experimental Biology*, **208**: 1363-1372.
- Zeng, Z., Liu, X., Seebah, S., Gong, Z. (2005). Faithful expression of living color reporter genes in transgenic medaka under two tissue-specific zebrafish promoters. *Developmental dynamics*, **234**: 387-392.
- Zeng, Z., Shan, T., Tong, Y., Lam, S.H., Gong, Z. (2005). Development of estrogen-responsive transgenic medaka for environmental monitoring of endocrine disrupters. *Environmental science & technology*, **39**: 9001-9008.
- Zha, J., Sun, L., Zhou, Y., Spear, P.A., Ma, M., Wang, Z. (2008). Assessment of 17 α -ethinylestradiol effects and underlying mechanisms in a continuous, multigeneration exposure of the Chinese rare minnow (*Gobiocypris rarus*). *Toxicology and applied pharmacology*, **226**: 298-308.
- Zhang, X. & Gong, Z. (2013). Fluorescent transgenic zebrafish Tg (nkx2. 2a: mEGFP) provides a highly sensitive monitoring tool for neurotoxins. *PloS one*, **8**: p.e55474.
- Zhang, Y. & Fox, G.B. (2012). PET imaging for receptor occupancy: meditations on calculation and simplification. *Journal of biomedical research*, **26**: 69-76.
- Zhang, Y., Yuan, C., Hu, G., Li, M., Zheng, Y., Gao, J., Yang, Y., Zhou, Y., Wang, Z., (2013). Characterization of four nr5a genes and gene expression profiling for testicular steroidogenesis-related genes and their regulatory factors in response to bisphenol A in rare minnow *Gobiocypris rarus*. *General and comparative endocrinology*, **194**: 31-44.

- Zhang, Y., Zhang, S., Zhou, W., Ye, X., Ge, W., Cheng, C.H., Lin, H., Zhang, W. and Zhang, L. (2012). Androgen rather than estrogen up-regulates brain-type cytochrome P450 aromatase (cyp19a1b) gene via tissue-specific promoters in the hermaphrodite teleost ricefield eel *Monopterus albus*. *Molecular and cellular endocrinology*, **350**: 125-135.
- Zhou, Y., Zha, J., Wang, Z. (2012). Occurrence and fate of steroid estrogens in the largest wastewater treatment plant in Beijing, China. *Environmental monitoring and assessment*, **184**: 6799-6813.
- Zhou, Y., Zha, J., Xu, Y., Lei, B., Wang, Z. (2012). Occurrences of six steroid estrogens from different effluents in Beijing, China. *Environmental monitoring and assessment*, **184**: 1719-1729.
- Ziegler, S.I. (2005). Positron emission tomography: principles, technology, and recent developments. *Nuclear Physics A*, **752**: 679-687.
- Zoeller, R.T, Brown, T.R., Doan, L.L., Gore, A.C., Skakebaek, N.E., Soto, A.M., Woodruff, T.J., vom Saal, F.S. (2012). Endocrine-disrupting chemicals and public health protection: a statement of principles from the endocrine society. *Endocrinology*, **153**: 4097–4110.
- Zum Winkel, K., Scheer, K.E., Schenck, P., Gelinsky, P., Prpic, B., Adam, W.E. (1965). Die funktionell-morphologische Diagnostik von Nierenkrankheiten mit der Kamera-Szintigraphie und der Isotopen-Nephrographie. *DMW-Deutsche Medizinische Wochenschrift*, **90**: 2229-2238.
- Zwart, W., de Leeuw, R., Rondaij, M., Neefjes, J., Mancini, M.A., Michalides, R. (2010). The hinge region of the human estrogen receptor determines functional synergy between AF-1 and AF-2 in the quantitative response to estradiol and tamoxifen. *J. Cell Sci.*, **123**: 1253–1261.